Neglected Infrastructures for 6G–Underwater Communications: How Mature are They?

Nhu-Ngoc Dao[a], Ngo Hoang Tu[b,c], Tran Thien Thanh[c], Vo Nguyen Quoc Bao[d], Woongsoo Na[e], Sungrae Cho[f]

[a]*Department of Computer Science and Engineering, Sejong University, Seoul 05006, South Korea*
[b]*Department of Electrical and Information Engineering, Seoul National University of Science and Technology, Seoul 01811, South Korea*
[c]*Department of Computer Engineering, Ho Chi Minh City University of Transport, Ho Chi Minh City 710372, Vietnam*
[d]*Posts and Telecommunications Institute of Technology, Ho Chi Minh City 710372, Vietnam*
[e]*Department of Computer Science and Engineering, Kongju National University, Cheonan 31080, South Korea*
[f]*School of Computer Science and Engineering, Chung-Ang University, Seoul 06974, South Korea*

Abstract

In recent years, we have witnessed a major expansion of wireless communications, extending from terrestrial to aerial spaces to facilitate novel user services. While aerial access infrastructure is widely accepted to be an essential part of a comprehensive sixth-generation (6G) network, underwater wireless communications (UWC), unfortunately, are neglected. This observation questions us about the maturity of UWC technologies and its potentials for 6G. First, we describe an overview of 6G access infrastructures, revealing the gaps concerning underserved spaces and services. Next, we investigate current developments of cutting-edge technologies that enable heterogeneous multiaccess UWCs. Furthermore, we introduce UWC-enabled application scenarios that possibly improve the popularity of 6G in aquatic environments. Then, we analyze a feasible approach for a UWC integration to complement the 6G infrastructures, achieving a fully comprehensive framework. Finally, open challenges are discussed to drive future studies toward the maturation of UWC. This study is expected to facilitate interested researchers and engineers with a systematical reference framework of state-of-the-art UWC knowledge and information.

Keywords: 6G network, underwater communication, underwater sensor network, wireless communication

1. Introduction

Following the successful commercialization of fifth-generation (5G) networks worldwide, the interest of academia and industry is now focused on sixth-generation (6G) networks. Recently, a large number of 6G proposals have been investigated to define the 6G network from many aspects, such as system requirements, network architecture, foundational technologies, envisioned services, and open challenges. As the international central body in charge of network standardization, the International Telecommunication Union-Telecommunication Standardization Sector (ITU-T) has started a focus group *Network-2030* to identify potential technologies and innovations for the architectural design and determine the scope of services of 6G networks. In particular, the four key characteristics include (*i*) time engineered communications, (*ii*) multi-sense systems, (*iii*) coexistence of heterogeneous access infrastructures, and (*iv*) complex and constrained environment [1, 2, 3]. These characteristics drive the development of 6G infrastructures, making them more comprehensive and universal to facilitate emerging horizontal and vertical services.

Email addresses: nndao@sejong.ac.kr (Nhu-Ngoc Dao), tu.ngo@ut.edu.vn (Ngo Hoang Tu), thanh.tran@ut.edu.vn (Tran Thien Thanh), baovnq@ptithcm.edu.vn (Vo Nguyen Quoc Bao), wsna@kongju.ac.kr (Woongsoo Na), srcho@cau.ac.kr (Sungrae Cho)

As a response, an extensive literature review in [12] demonstrated that the aerial access infrastructure has been accepted as a native component complementing the 6G network. Hence, airborne platforms at various altitudes and satellites may function as mobile access points to provide wireless connectivity to underserved areas, both on the ground and in aerial spaces [13]. A reference model of aerial access network integration into the 6G infrastructure adopts the following two standards: the 3rd Generation Partnership Project (3GPP) technical specification 3GPP TS 23.501 [14] for mobile architecture frameworks; and the European Telecommunications Standards Institute (ETSI) technical report ETSI TR 103 611 [15] for possible interconnection models of satellites/airborne platforms and mobile systems. This unified air-ground access infrastructure enables various emerging user services such as inflight infotainment, aerial information harvesting, remote and distributed Internet of things (IoT) systems, and regular Internet connectivity in isolated areas. These services significantly promote diverse horizontal business sectors, e.g., intelligent transportation, smart agriculture, search and rescue, and aerial surveillance.

While the aerial space continues to be captured by the increasing number of mobile devices and services as part of the Internet of Everything (IoE) revolution, underwater wireless communication (UWC) appears to be an external network that minimally interacts with the emerging 6G ecosystem. Most ex-

Table 1: Comparison between our study and other related studies.

Reference	Research scope	Contributions
[4]	Magnetic induction communications	This study provided a comprehensive review on underwater magnetic induction communications from several perspectives such as channel models, transmission distance, communication reliability, and performance improvement along with the respective constraints.
[5]	Optical wireless communications	This study reviewed UWOCs to shed light on the challenges, advancements, and visions of the technology. The relevant specifications at each network layer are evaluated, from the bottom physical layers to the top application layers.
[6]	Secure acoustic networks	This study discussed major vulnerabilities and security threats at the physical and transport layers in underwater acoustic communications (UAC). In addition, existing countermeasure mechanisms, security protocols, and trustful network architectures are analyzed to evaluate the resistance capability of the networks against security attacks.
[7]	Communication reliability	This study reviewed underwater communication technologies and network models that provide high reliability in underwater communications. In particular, routing protocols at the data link and network layers are investigated in underwater multimodal networks.
[8]	Localization protocols	This study taxonomized existing localization algorithms in underwater communication networks. The taxonomy is developed based on various system parameters, with considerations of node mobility and network architecture models.
[9]	Formation controls	This study focused on formation control problems associated with AUV operations. A classification framework is proposed to compare existing methods of joint automation engineering and network architecture in terms of vehicle performance and communication capabilities.
[10]	Data gathering and mobility	This study provided an analysis of existing studies on data gathering techniques and solutions in underwater wireless sensor networks. Simulations are conducted to evaluate related approaches in various static and mobility models by adjusting the communication metrics such as transmit power, latency, and drop rate.
[11]	Routing protocols	This study classified existing underwater communications routing protocols into three categories: energy-aware, data-aware, and geographic-aware protocols. Communication efficiencies as well as the advantages and disadvantages of existing protocols are summarized systematically.
Our paper	UWC integration into 6G networks	Our study analyzes the feasibility of UWC integration into 6G access infrastructure. In particular, we investigated state-of-the-art technologies and solutions in UWC and suggested an integration model to seamlessly interconnect air, ground, and underwater systems in a fully comprehensive access framework.

isting 6G proposals and studies did not address UWC in their envisioned technologies and applications. This may be because of a number of barriers between airborne and underwater communication environments. First, the longstanding challenge of continuous wireless transmission through water-air surfaces is difficult to resolve efficiently owing to signal reflection problems. Second, the uncertainty, instability, and high absorbency of underwater environments are considered unfriendly to wireless network infrastructure deployments. Third, human activities are limited with exceptional services in the aquatic space [16]. Although these obstacles are significant, we continue attempting to overcome any challenges for the development of UWC. This situation prompted us to investigate state-of-the-art UWC technologies and determine whether the UWC is sufficiently mature for possible integration into the emerging 6G systems toward a fully comprehensive access infrastructure interconnecting three pillars: air, ground, and underwater communications.

To support the aforementioned approach, we first reviewed relevant surveys and tutorials in the field. Table 1 presents a comparison of the present and related studies. A number of studies have been performed, each focusing on specific areas of UWC research. For instance, Li *et al.* provided a comprehensive survey on underwater magnetic induction communications, in which fundamental aspects of the wireless channels are investigated [4] and Saeed *et al.* studied underwater wireless optical communications (UWOCs) to obtain a better understanding of current statements of the technology [5]. From another perspective, Jiang *et al.* discussed security problems in an underwater acoustic networking environment [6] while communication reliability and localization issues were clarified by the studies of Li *et al.* [7] and Islam *et al.* [8], respectively. In addition, the formation control of a single autonomous underwater vehicle (AUV) and AUV swarms [9], the data gathering mechanisms in static and mobile networking models [10], and routing protocols at multiple network operation layers [11] are also thoroughly examined. Although these literature reviews attracted attention among researchers working toward the development of UWC, we have not found any existing study devoted to studying UWC connectivity in a 6G context.

Hence, the aim of this study is to address the aforementioned gap. To this end, we designed the survey scope and methodology to conduct the study as shown in Fig. 1. The survey comprised the following steps:

- First, we start with the widely accepted 6G access network, with aerial infrastructure as its natural integral component. Here, the network architecture and access interface are analyzed to evaluate the interconnectivity of the entire network. Thus, underserved services and areas, particularly in underwater environments, are justified. More details are provided in Section 2.

- Second, we analyzed current developments of heterogeneous multi-access UWCs by reviewing their enabled networking, communication, and computing technologies. Existing solutions are classified based on their goals toward realizing critical operations such as transmission distance, data rate, communication reliability, formation con-

Table 2: Nomenclature

Abbreviation	Description	Abbreviation	Description
3D	Three-dimensional	MIMO	Multiple-input multiple-output
3GPP	Third Generation Partnership Project	ML	Machine learning
ABS	Aerial base station	MMSE	Minimum mean square error
AILSOMP	Adaptive iterative local searching OMP	MPL	Movement prediction location
ANS	Acoustic navigation system	MSA	Maritime situational awareness
ASV	Autonomous surface vehicle	MRC	Maximum ratio combining
ATR	Automatic Target Recognition	NOMA	Non-orthogonal multiple access
aUE	Arial user equipment	NRZ-OOK	Non-return-to-zero on-off keying
AUV	Autonomous underwater vehicle	OFDM	Orthogonal frequency division multiplexing
BER	Bit error rate	OMP	Orthogonal matching pursuit
BPSK	Binary phase shift keying	OWF	Offshore wind farm
CCS	Carbon capture and storage	PAM	Pulse amplitude modulation
CE	Channel estimation	PID	Proportional–integral–derivative
CNN	Convolutional neural network	PNE	Post nonlinear equalization
CRLB	Cramer-Rao lower bound	QAM	Quadrature amplitude modulation
DFE	Decision feedback equalizer	QoS	Quality of service
DMT	Discrete multi-tone	QPSK	Quadrature phase shift keying
DRL	Deep reinforcement learning	RAN	Radio access network
DVL	Doppler velocity logger	RF	Radio-frequency
ETSI	European Telecommunications Standards Institute	RIS	Reconfigurable intelligent surface
GNS	Geophysical navigation system	RMSE	Root-mean-square-error
GPS	Global positioning system	ROV	Remotely operated vehicle
gUE	Ground user equipment	RSS	Received signal strength
HIS	Hierarchical identity-based signcryption	SBL	Short baseline
IDMA	Interleave division multiple access	SDD-CS	Static-dynamic discriminative compressed sensing
IMU	Inertial measurement unit	SiPM	Silicon-photomultiplier
INS	Inertial navigation system	SNR	Signal-to-noise ratio
IoE	Internet of Everything	TMF	Trust management framework
IoT	Internet of Things	ToA	Time-of-arrival
ITSWLS	Improved three-stage weighted least squares	TDoA	Time-difference-of-arrival
LBL	Long baseline	UAAV	unmanned aerial-aquatic vehicle
LCRLA	Logarithmic cost recursive least absolutes	UAC	Underwater acoustic communication
LCRLS	Logarithmic cost recursive least squares	ULES	Underwater localization evaluation scheme
LCLMA	Logarithmic cost least mean absolute	USBL	Ultra-short baseline
LCLMS	Logarithmic cost least mean squares	USV	Unmanned surface vehicle
LDPC	Low-density parity check	UWC	Underwater wireless communication
LED	Light-emitting-diode	UWOC	Underwater wireless optical communication
LSMSE	Least square mean square error	UWSN	Underwater wireless sensor network
MCM	Mine countermeasures	wUE	Water user equipment
MEMS	Microelectromechanical system		

trol, localization and navigation, as well as security and privacy protection. Finally, we drew conclusions from these analyses, see Section 3 for further details. In addition, we envisioned potential underwater application scenarios that would benefit from UWC infrastructure (Sections 4).

- Third, we investigate a feasible UWC integration into the 6G network. In particular, on-shore interconnections with air and ground systems provide backhaul links to the Internet, whereas off-shore access networks provide fronthaul connections to underwater user devices. Section 5 analyzes this model in detail. Then, open challenges are presented to drive future research toward UWC maturation in the context of 6G in Section 6.

The contributions of this paper are as follows. The survey provides potential readers with a systematical reference framework, where they may find state-of-the-art knowledge and innovations in the field. UWC systems are used in the context of 6G networks, demonstrating their ability to complement the network toward achieving a fully comprehensive access infrastructure, where air, ground, and underwater communications are seamlessly integrated. From the UWC perspective, on-shore and off-shore components and interfaces are anatomized thoroughly. In addition, supporting technologies and algorithms for heterogeneous multiaccess UWCs are being investigated to concretely justify the feasibility of the proposed architecture. Finally, potential applications and open challenges in UWCs are highlighted. Table 2 summarizes common acronyms used in this paper.

2. 6G Access Infrastructures Analysis

A thorough investigation in [12] revealed that potential 6G access networks include aerial vehicle platforms (e.g., satellites, aircraft, and drones), which function as additional base stations in air, along with typical terrestrial base stations, as shown in Fig. 2. Thus, this section is dedicated to studying state-of-the-art advances in such 6G access infrastructures as well as their limitations in supporting underwater services.

Section II. 6G Access Infrastructure Analysis
- 2.1. Terrestrial access networks
- 2.2. Aerial access networks
- 2.3. Underserved services

Section III. Current UWC Development
- 3.1. Cable-assisted communications
- 3.2. Transmission distance
- 3.3. Data rate
- 3.4. Communication reliability
- 3.5. Formation control
- 3.6. Localization and navigation
- 3.7. Security and privacy protection

Section IV. Underwater Application Scenarios
- 4.1. Military applications
- 4.2. Science applications
- 4.3. Industry applications

Section V. Feasible UWC-Integrated 6G Access Networks
- 5.1. On-shore interconnections
- 5.2. Off-shore access networks

Section VI. Open Challenges

Figure 1: The survey scope and methodology.

2.1. Terrestrial Access Networks

Since the first generation, terrestrial access networks have been considered the basic infrastructure that constitutes any mobile network. Many terrestrial access components, technologies, and architectures retained from the five predecessors play important roles in 6G networks [17, 18]. In particular, hierarchical and heterogeneous access networks involve macrocells for wide coverage to simultaneously serve a large number of user devices, smallcells (e.g., microcells and picocells) for data rate boosting in specific local areas, and portable cells for dynamic coverage and data rate enhancements. In 6G networks, such components would be upgraded by embedding emerging technologies such as beamforming to align transmission directions, ultra-massive multiple-input multiple-output (umMIMO), and novel multiplexing and scheduling schemes for better spectrum efficiency (e.g., orthogonal/non-orthogonal multiple access and rate splitting multiple access) [19, 20, 21, 22, 23, 24, 25, 26, 27, 28]. To optimize spectrum efficiency, antenna arrays would be deployed at remote locations, rather than being centrally located at base station towers, forming new concepts of remote radio heads within cell-free models. In addition, new designs of antenna elements have been proposed, such as intelligent reflecting surfaces and backscatter communications, which leverage multipath effects of wireless signals to improve channel gains after being reflected and/or amplified at antenna elements in the surfaces [29, 30]. Moreover, 6G encourages several public and private technologies to function as additional gateways and alternative paths for users accessing the networks such as Wi-Fi-assisted hotpots, low-power Bluetooth gateways, and peer-to-peer communications. All the aforementioned technologies enable a comprehensive terrestrial 6G access infrastructure.

From a spectrum allocation perspective, 6G involves a broad range of frequencies to support the new radio (NR) access interfaces for on-the-ground devices, i.e., ground user equipment (gUE). In particular, the macrocells generally utilize sub-6 GHz bands for long transmissions to provide conventional wireless connections in indoor and outdoor environments, whereas the small cells utilize high frequencies such as mmWave and THz bands for robust data rates over short distances. As a result, a variety of user services are enabled such as mobile broadband Internet access for rich media content (e.g., videos on-demand, social media, multiplayer interactive online gaming, distance learning) [31], Internet of things (IoT) services [32], industrial IoT networks [33, 34], smart home/buildings applications [35], precision agriculture applications [36], and vehicular ad-hoc network [37, 38]. Moreover, low-latency remote services benefit from diverse access technologies for stable connections, such as telehealthcare (i.e., e-Health and m-Health) services (e.g., telemedicine, medical transportation services, Internet of medical things, online training sessions for healthcare professionals) [39, 40, 41, 42, 43], and disease detection using in-body nano-sensor communication [44, 45, 46, 47]. With THz bands, heavy-traffic services that request ultra-high data rate can be efficiently facilitated [48] including high-definition live video streaming [49], holographic teleportation [50, 51], and metaverse [52].

Additionally, terrestrial base stations need an effective resource management mechanism for radio, computing, and storage resource optimization locally and globally in the entire networks [53, 54, 55, 56, 57, 58, 59, 60]. As a response, a new air interface driven by artificial intelligence (AI) technology (referred to as intelligent radio [61]) has been proposed for efficiently optimizing communication schemes for any hardware, radio environment, and application in the context of 6G operation [62, 63, 64]. Although the aforementioned technologies enable the terrestrial access networks to supply Terabit-per-second links, some applications are hardly deployed by using only terrestrial base stations. With fixed-location characteristics, these types of base stations (e.g., terrestrial cellular and WLAN systems) cannot provide efficient wireless coverage for ground users living in rugged mountain terrains and off-shore areas as well as for aerial/space users while they are traveling by planes or spaceships. Consequently, flying base stations belonging to aerial access infrastructures function as dynamic networks to provide communication links for such kinds of users [65, 66].

2.2. Aerial Access Networks

In the aerial access networks, there are three tiers called low-altitude platforms (LAPs), high-altitude platforms (HAPs), and low Earth orbit (LEO) satellite constellations. Airborne objects such as drones, aircraft, unmanned aerial vehicles (UAVs), balloons, and airplanes equipped with wireless transceiver antennas function as an aerial base station (ABS) to supply wireless communication services. These ABSs are located at different altitudes of 0–10 km (LAPs) and 20–50 km (HAPs) relative to sea level. In the network, ABSs connect directly to end users via radio fronthaul links, whereas they connect to the core network via the backhaul links, which may be served by satellites or terrestrial base stations [67]. The LAP/HAP networks can

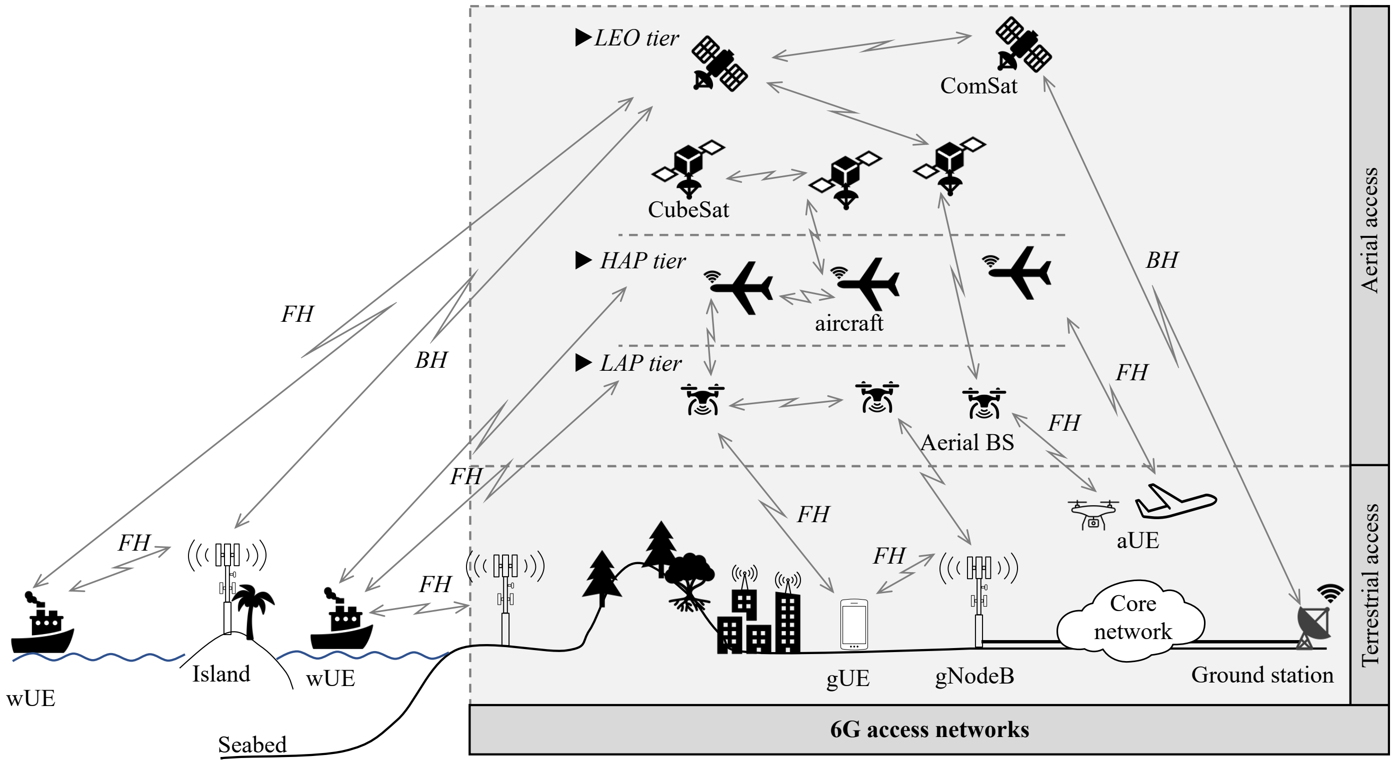

Figure 2: 6G wireless access networks involving terrestrial and aerial infrastructures (FH–fronthaul and BH–backhaul).

be the most appropriate candidate for providing temporary access networks in some situations, such as disasters (e.g., large-scale or urban) [68, 69], public healthcare surveillance and rescue services [70, 71], disaster relief [72], maritime search and rescue [73, 74], maritime wireless communication among vessels [75], precision agriculture [76, 77], intelligent transport systems [78, 79, 80, 81], and in unusually crowded places (e.g., shopping centers, airports, and hospitals in rush hours) [82].

In the LEO range of 500—1500 km, there are two kinds of spaceborne satellites: CubeSats and ComSats. The function of CubeSats is to provide high-speed Internet services, whereas the function of ComSats is to assure service availability [83]. These satellites connect to terrestrial core networks through ground stations via satellite links operating at Ku, Ka, V, and THz bands [84], whereas inter-satellite links between LEO satellites can be either free space optical or THz-band communication links [85]. In particular, with regenerative payload configuration, satellites can communicate directly with terrestrial base stations or ABSs (LAP/HAP) [86, 87]. Furthermore, LEO satellites potentially provide traffic offloading or backhauling for both LAPs/HAPs and terrestrial networks [88, 89]. In this case, a UE can reach the core network for data access, optionally through a 6G terrestrial base station or an ABS, and then be delivered on the backhaul links via LEO satellite constellations. By contrast, terrestrial base stations and/or ABSs can be presented at backhaul links of satellites for enhancing the network performance [90], as shown in Fig. 2.

Typical end users using satellite communication links can be shipborne objects, people devices on ships traveling on the seas, generally called water user equipment (wUE), or gUE in rural areas or isolated areas, or aUEs utilizing space travel services or on a flight. Generally, the main function of LEO systems is to provide permanent and cost-effective Internet connectivity worldwide, which can be classified into fixed, broadcast, and mobile satellite services [91, 92, 93]. Prime examples can be maritime services used by wUEs such as maritime broadband, maritime safety, and maritime navigation [94, 95, 96]). For aUEs, LEO communications provide high-speed THz fronthaul connectivity for a vast number of airplanes [97, 98]. Particularly, with LEO satellite communications, enormous novel services can be promoted in the near future, such as aeronautical services (e.g., space travel or space exploration), space industry, deep space telescope, earth observation (e.g., prediction of crop yields at rural sites [99, 100] or urban monitoring), earth remote sensing, and learning from outer space (e.g., training astronauts on space facilities). With conjunction between terrestrial and aerial access infrastructures, 6G promisingly provides a complete heterogeneous service solution (e.g., super-smart society) for jointed and diverse ecosystems with immense ultra-smart electronic IoT elements involved, such as eEducation, eCity [101, 102, 103], eIndustry, eCommerce, eAgriculture, and eGovernment [104, 105, 106].

2.3. *Underserved Services*

Although the aforementioned 6G multi-tier space-air-ground access infrastructure can provide global Internet connectivity, the quality of services in numerous usage scenarios may not meet the users' expectations. For instance, the latency of satellite communication links is not always assured in several cases, including, emerging applications for wUEs in which a low latency requirement is mandatory. Additionally, swarms of UAVs as ABSs can efficiently function in on-shore areas but not off-shore owing to a lack of long-lasting power for operation or difficulties in maintenance, or even cannot be deployed in underwater environments (e.g., Internet services for broad-sea and deep-sea activities such as underwater surveillance, exploration, and photography). Recently, a new concept of a network formed by a swarm of floating objects, e.g., floating cellular towers or unmanned surface vehicles, to provide Internet connectivity for both off-shore marine and maritime IoTs to perform professional applications such as marine monitoring and sensing of vast ocean [107, 108] was introduced. In addition, these floating networks assist the communication between the terrestrial base stations and ships [109]. These proposed architectures focused mainly on the sea-surface networks and neglected underwater communications, which provide emerging underwater use cases such as holographic imaging of real-time underwater observation and on-land real-time tracking systems for tourists' safety while participating in deep-sea tourism. Consequently, the 6G access architecture is expected to require a novel complement underwater platform integrated into the aforementioned parts, including terrestrial and aerial access networks to form a comprehensive wireless access network around the globe.

3. Current UWC Development

To achieve the prospective UWC integration into 6G networks, we devote this section to discussing several key pillar aspects of heterogeneous multi-access UWCs, such as cable-assisted communications, transmission distance, data rate, communication reliability, formation control, localization and navigation, and security and privacy protection.

3.1. Cable-Assisted Communications

In emerging 6G scenarios, fulfilling communication requirements among the aerial, terrestrial, and underwater infrastructures has become very important and challenging. Because of the high attenuation characteristics of water environments, direct wireless transmissions among network terminals seem intractable. For example, water-aerial and water-terrestrial communications are challenging owing to high bottom and surface reflection losses, whereas UWCs suffer from high path-loss, absorption, scattering, geometric diffusion, and outward energy radiation [7]. Submarine cable is known as an effective traditional solution with the potential to provide certainty, stability, and reliability for cable-based sink nodes because of its superior performance in terms of ultra-reliability, low-latency, high data rate transmission, and long distance propagation [110, 111, 112, 113, 114]. In particular, [110] provided a comprehensive overview and summary of the authors' practical experience over decades in submarine optical fiber cable engineering, structures, features, installation, maintenance, operation safety, information management, and some on-working

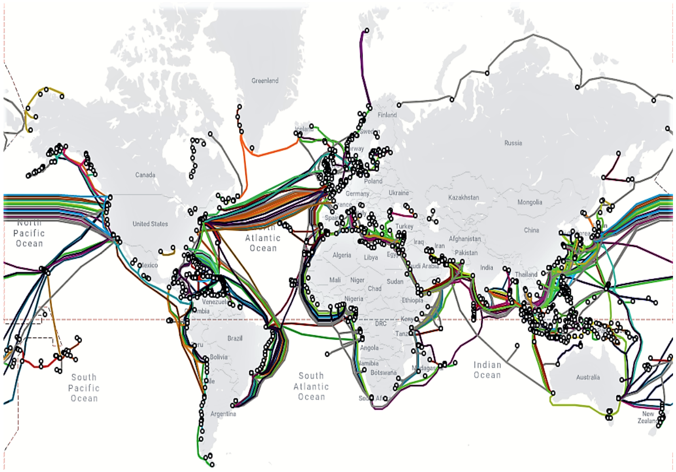

Figure 3: State-of-the-art schematic map of the submarine cable network around the world [115].

projects. In [111], the technologies for optical submarine cables used in the past, present, and future to improve the capacity have been reviewed. Furthermore, [112] provides an underwater cable route design using an AUV, where the described method of using an AUV with an automatic decision-making algorithm has been demonstrated to provide an efficient route for the designed underwater model. In addition, [113] characterized the nonlinearity of submarine cables, where the fiber effective area has been accurately estimated in long-distance experiments. Furthermore, Eid *et al.* [114] measured and compared signal gains among various optimization methods for optic fiber systems, including hybrid optical amplifiers, gain-flattened filters, glass composition, and fiber Bragg grating. These optimization algorithms can be performed individually or simultaneously to improve the data rates for the fiber optic systems significantly.

A state-of-the-art schematic submarine cable map around the world is illustrated in Fig. 3. In this figure, we can observe that submarine cables are widely employed today, which yields a promising figure for the hybrid cable-assisted and UWCs toward a fully comprehensive access 6G infrastructure. However, because of the expensive cost of implementation and maintenance for submarine cables in water environments as well as the particularity of underwater applications, dense configurations should be adopted only in some sensitive areas, e.g., attractive and commercial islands and straits, whereas sparse installations should be established in others. In academic studies for cost savings, Downie *et al.* [116] compared overall costs and capacity performance among various configurations for underwater systems, including single-core fiber full C-band, single-core fiber C+L-band, and multiple-core fiber full C-band. Their numerical results have revealed that single-core fiber full C-band offers not only the lowest overall cost but also the greatest capacity. Unlike [116], the authors in [117] investigated an overall system cost/bit metric for submarine cable systems using a massive space-division multiplexing technique, which was a more techno-economically conclusive optimization metric than the capacity. Some key findings in [117] include reducing consumed system bandwidths, 40% cost/bit savings compared to the state-of-the-art approaches, improving cable capacity by threefold, and indicating the tradeoff between power efficiency of optical amplifiers and noise figure in a cost-optimized system. Furthermore, an automatic inspection system has been studied in [118], where localization, path planning, and inspection missions for submarine cables are conducted by an AUV. When a submarine optical cable's life span could be shortened by changes in underwater environments (e.g., human activities and natural disasters), [118] contributed not only to substantial cost savings for routine inspection and maintenance, but also to reducing potential risks for maintenance tasks performed by people in aquatic environments.

Based on cable-assisted communications, wireless links among cable-based sink nodes and mobile underwater devices/vehicles are within a short distance range. In such a scenario, underwater acoustic waves and wireless blue-green lights can be utilized in each cell, leading to a significant improvement in UWC performance, which promises to meet demands for high-performance and broadband underwater information in 6G networks. An applicable network integration of UWCs into 6G infrastructures is shown in Fig. 10, where a hybrid infrastructure between cable-assisted communications and UWCs can be observed. In [119], a hybrid platform of acoustic, optical, and fiber optic underwater communications has been proposed, where experiment results have demonstrated high achievable performance in terms of ultra-reliability, high data rate, low power consumption, and long distance propagation. Furthermore, Cossu *et al.* [120] designed optical ethernet modems for UWCs, which were tested in seawater at the La Spezia harbor. Their testbed prototypes have demonstrated fully compatible and practical characteristics with 10Base-T Ethernet support for UWCs. Although open-sea and deep-water transmissions were not examined in [120], laboratory calibrations based on tested turbidity and extinction coefficient estimations allowed prediction of an achievable transmission range of a minimum of 40 m in deep waters. In addition, [121] and [122] proposed hybrid underwater fiber and wireless communications with a fully passive optical lens installed at the front-end of fiber optic cables, where an underwater laser beam from a front-end extender has been experimentally demonstrated to provide an effective increment in UWC transmission distance.

3.2. Transmission Distance

To transmit over long distances in aquatic environments, the conception of UACs has been adopted owing to their low attenuation characteristic. The overall attenuation for an UAC over distance d (m) at frequency f (kHz) can be modeled in dB as [123]

$$A(d, f) = \xi_0 + 10k \log_{10} \frac{d}{d_0} + (d - d_0)\,\alpha(f), \quad (1)$$

where ξ_0 (dB) is a loss strength in reference distance d_0 (m), k denotes a spreading factor that equals to 1 for cylindrical spreading (i.e., shallow waters), 2 for spherical spreading (i.e., deep waters), and 1.5 for the practical spreading. In (1), $\alpha(f)$ represents an absorption loss of an acoustic wave, which can be expressed in dB/km at f (kHz) as follows [124]:

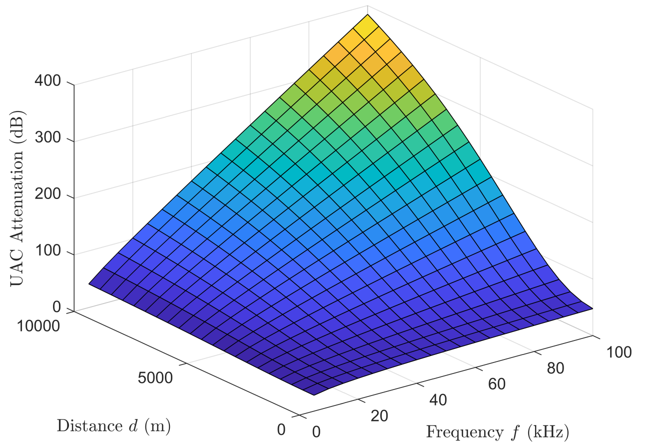

Figure 4: Illustration of the UAC attenuation, where $k = 1.5$, $\xi_0 = 17.56$ dB, and $d_0 = 100$ m.

$$\alpha(f) = \frac{0.1 f^2}{1 + f^2} + \frac{44 f^2}{4100 + f^2} + 2.75 \times 10^{-4} f^2 + 0.003. \quad (2)$$

Fig. 4 shows the numerical results of UAC attenuations with different distances and frequencies, assuming $k = 1.5$, $\xi_0 = 17.56$ dB, and $d_0 = 100$ m. The results in Fig. 4 reveal that it is possible to transmit within several kilometers in aquatic mediums by using acoustic waves. In addition, we recognize that in the low frequency range, the attenuation of UAC does not change substantially over various distances, whereas the corresponding attenuation varies dramatically in the high frequency regime. Therefore, transmitting over a long distance and at a high frequency is a considerable challenge to combating the UAC attenuation. Zhou *et al.* [125] conducted an experiment for the UAC performance at the frequency of 85 KHz in the Gulf of Mexico, where a channel estimation (CE) based on decision feedback equalizer (DFE) and quadrature phase shift keying (QPSK) was designed to process communication measurements and modulations, respectively. Their preliminary results demonstrated the capability to transmit over 1.5 km and achieved a 34 Kbps data rate. In [126], a similar experiment for UWC characteristics was deployed in the roadstead of Brest in France. The testbed model in [126] involved a least square mean square error (LSMSE)-based CE and a QPSK modulation for multiple-input multiple-output (MIMO) UWC systems that transmitted via 0.5 km at the frequency of 23 KHz and achieved a data rate of 20.17 Kbps. Furthermore, [127] compared the performance of massive MIMO systems for IoT UWCs using acoustic, RF, and optical technologies, where a linear minimum mean square error (MMSE)-based CE and a maximum ratio combining (MRC) technique were leveraged. The results revealed that at 180 KHz, the transmission range of an acoustic channel can be achieved up to 3 km with an achievable 96.7 Kbps data rate, whereas propagation distances for RF and optical technologies are only 100 m but achieve higher data rates, e.g., 70.6 Mbps and 85.7 Mbps for RF and optical channels, respectively. It is worth noting that the research in [125, 126, 127] mainly focus on long distance propagation using acoustic waves, despite the fact that they suffer from very low achievable data rates.

In addition to the contributions of [125, 126, 127], there are some recent studies related to a long propagation distance for UACs, including novel throughput analysis, CE, adaptive modulation, machine learning, and real-time video transmission, which potentially promote 6G integrated applications. In particular, [128] provided a comprehensive throughput analysis for UAC channel models, where a space-time inconsistency interference, a binary phase shift keying (BPSK) modulation, and a MMSE-based CE were considered. The results have shown that a propagation range was achieved within up to $2-7$ km at the frequency of 10 KHz by assuming a raw data rate of 1 Kbps. Furthermore, Kari *et al.* [129] proposed robust adaptive algorithms to enhance the CE efficiency for UACs, including those based on logarithmic cost least mean absolute (LCLMA), logarithmic cost least mean squares (LCLMS), logarithmic cost recursive least absolutes (LCRLA), and logarithmic cost recursive least squares (LCRLS). The realistic experiment results in [129] have demonstrated the capability to communicate over a 1 km propagation range in an underwater medium operating at 15 KHz, and they still provide efficient CE via the proposed estimators. Subsequently, [130] proposed a novel estimation method, named static-dynamic discriminative compressed sensing (SDD-CS), which achieved better UACs' performance than those based on classic estimators (e.g., least square QR-factorization, individual/simultaneous orthogonal matching pursuit (OMP), compressed sensing Kalman filter, and LCRLS). The working system in [130] was operating at 16 KHz with a 1 km transmission range. Furthermore, in [131], a deep learning-based receiver was proposed to predict the performance of UAC channels, where the model was performed in the South China Sea. Experimental results demonstrated that the proposed deep learning scheme achieves better performance with lower training overhead than the traditional DFE-based CE. For example, at the 12 KHz operating frequency, it can transmit with a communication range of 8 km and an average data rate of 2.4 Mbps. Unlike [131], the authors in [132] proposed machine-learning-based adaptive modulation schemes promoting an extremely long propagation distance for UACs, where (*i*) the experiment was conducted in the sea trial of Northern Israel within a 100 km communication range at the frequencies of $0.9-1.5$ KHz, and (*ii*) a BPSK/QPSK modulation and a DFE-based CE were also utilized to perform communication measurements. Even for mismatched environmental information, the machine-learning-based algorithms proposed in [132] still provided a performance improvement in realistic channels, leading to an accurate prediction of the best modulation scheme. In addition, Bocus *et al.* [133] investigated a Turbo-coded massive MIMO system to boost the throughput of a 1 km UAC channel operating at the frequency of 32.5 KHz. This allowed an achievable higher data rate that promoted real-time video transmission over long distance acoustic underwater links, resulting in an acceptable real-time video quality.

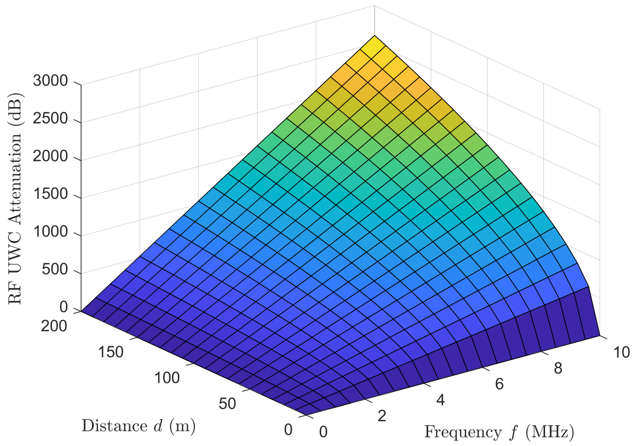

Figure 5: Impact of propagation distance and frequency on the RF UWC attenuation, where $\sigma = 4.3$ S/m.

3.3. Data Rate

Owing to the higher attenuation of RF UWCs and UWOCs than that of UACs, RF and optical technologies cannot be leveraged to transmit over long propagation distances. Nevertheless, they can provide a significantly higher data rate in short-range communications. We can appropriately adopt each kind of technology for specific purposes. This part pays more attention to the achievable high data rate for UWCs. Therefore, RF and optical communications dominate as the most efficient candidates.

The channel attenuation for a RF UWC over distance d (m) at frequency f (Hz) is typically modeled in dB as [134]

$$A(d, f) = \sqrt{\pi\sigma\mu_0}\sqrt{d^2 f}, \tag{3}$$

where $\mu_0 = 4\pi\times10^{-7}$ (H/m) denotes a vacuum permeability and σ (S/m) denotes a water conductivity. We note that σ is a function of temperature and salinity, being approximately 4.3 S/m and $0.001-0.01$ S/m for seawater and fresh water, respectively. Fig. 5 illustrates channel attenuation properties for RF UWCs. The influence behaviors of d and f on channel properties in Fig. 5 are similar to the characteristics in Fig. 4. However, in the typical range of RF operating frequencies, shorter distances are beneficial for a low attenuation as compared to UAC propagation distances, owing to the aforementioned tradeoffs. Inspired by this, Pavan *et al.* [135] conducted experiments using RF signals at frequency 6.78 MHz for multihop UWCs and their models were performed in a shallow water of the Arabian Sea and Bay of Bengal. It is revealed that 2 Mbps of a data rate can be achieved over 200 m of a propagation distance. Subsequently, in [136], Pavan *et al.* also investigated experiments for characterizing properties of RF UWCs in the same locations as in [135]; however, they further considered multihop multiple-cluster networks. Unfortunately, the achievable data rate in [136] is only 1 Mbps for a distance of 100 m. Recently, [127] employed a massive MIMO system to boost a system data rate for RF UWCs. As expected, the results in [127] have demonstrated that at 180 KHz and 100 m, up to 70.6 Mbps for RF UWC channels can be achieved. In addition, [127] also showed that at the same frequency and propagation distance, the achievable data transmission rate of 85.7 Mbps was determined for UWOCs. It is noted that, by considering shorter propagation distances, RF UWCs do not offer substantial gains in achievable data rate, whereas UWOCs can provide significant data rate improvements. In other words, for some UWC links that require shorter propagation distances, using optical communications is more appropriate than using RF communications.

The attenuation of a UWOC signal over distance d (m) can be defined as [137]

$$A(d) = 10dc(\lambda)\log_{10}(e), \tag{4}$$

where $c(\lambda)$ represents a beam attenuation coefficient that characterizes absorptions and scattering losses. The typical values of $c(\lambda)$ in pure seawater, clear ocean, coastal ocean, and turbid harbor underwater mediums are 0.056, 0.150, 0.305, and 2.170, respectively. Fig. 6(a) depicts the attenuation property versus the propagation distance d with various typical aquatic environments. The main difference between RF UWCs and UWOCs is propagation medium characteristics [138]. In particular, a water medium is handled as a dielectric for optical channels, whereas it is observed as a conductor for RF channels. Because an electromagnetic wave in a dielectric medium suffers from lower attenuation than in a conductor medium, UWCs using optical technology can provide higher data rates than those using RF for a propagation range limited to tens of meters. Furthermore, Fig. 6(b) shows that the visible light wavelengths provide the lowest attenuation, particularly for the blue-green region. Inspired by these advantages, many scientists around the world have recently paid more attention to research into blue-green transparent windows for light aquatic communications, which not only improves the data rate but also enhances the transmit range for UWOCs. Specifically, Khalighi *et al.* [139] introduced the utilization of pulse amplitude modulation (PAM) with silicon-photomultipliers (SiPMs) for clear-UWOCs using a blue wavelength, where a data rate of 50 Mbps was achieved at a maximum distance range of 20 m. In [140], an over 100 Mbps full-duplex UWOC using the green light with a photodiode module and a high-speed pin detector was experimentally demonstrated, where the propagation distances of 16 m, 4.8 m, 3.2 m, and 1.6 m were the maximum ranges to achieve 100 Mbps for the pure seawater, clear ocean, coastal ocean, and turbid harbor mediums, respectively. Furthermore, in [141], a data rate of 500 Mbps was achieved by using the blue-green-based laser diode and pin detector for coded clear-UWOCs that were transmitted over 7 m. [142] proposed a novel SiPM and utilized attenuation length indicator for green-laser-diode-based turbid-UWOCs to enhance the data rate with up to 1 Gbps at a 32 m transmission distance. Subsequently, 2 Gbps has been a further improved data rate in [143], through leveraging an autoencoder for clear-UWOCs that were transmitted over 20 m, whereas up to 2.175 Gbps within 1.2 m was achieved by utilizing multi-pin MRC reception and quadrature amplitude modulation (QAM) for green light-emitting-diode (LED)-based pure-UWOCs in [144]. In addition, for clear-UWOCs using the blue-green-based laser diode, the works in [145] and [146] experimentally demonstrated that the use of non-return-to-zero on-off keying (NRZ-OOK) modulation can achieve 2.2 Gbps within 12 m and 2.7 Gbps within 34.5 m, respectively. Liu *et al.* [147] proposed an OOK modulation-based clear-UWOC system utilizing the white light, generated by mixing the green, blue, and red laser diodes, where an allowable peak real-time data rate of 3.4 Gbps was obtained at 2.3 m. In addition, [148] provided a clear-UWOC proposal using series-connected Gallium Nitride micro-LED arrays operating at the blue wavelength with QAM loaded into the orthogonal frequency division multiplexing (OFDM) subcarriers. The experimental results in [148] have demonstrated the achievable rates of up to 4.92 Gbps, 3.22 Gbps, and 3.4 Gbps at the 1.5 m, 3 m, and 4.5 m transmission distances, respectively. In addition to improving the data transmission rate and enhancing the communication distance for clear-UWOC systems, Fei *et al.* [149] leveraged discrete multi-tone (DMT) and post nonlinear equalization (PNE) technologies at the blue wavelength. Specifically, the rates of 16.6 Gbps, 13.2 Gbps, and 6.6 Gbps have been experimentally achieved corresponding to the transmission distances at 5 m, 35 m, and 55 m, respectively.

3.4. Communication Reliability

Communication reliability represents the probability that the destination can successfully receive the signals sent from transmitter(s), which is typically evaluated through the bit error rate (BER) performance. We note that the lower value of BER is expected to achieve higher communication reliability. Nevertheless, this issue becomes more challenging in UWC networks because of the aforementioned underwater characteristics. This part describes related works on the high communication reliability purpose for UWCs. For example, in [150], two coding schemes, including Turbo code and low density parity check (LDPC), integrated with the MMSE-based CE and OFDM scheme, were investigated for UWOCs to achieve a 10^{-3} BER with the transmit range of 12 m. It is also shown that, at BER $= 10^{-3}$, the Turbo code can achieve a power gain of $2-4$ dB for three types of water (i.e., pure seawater, coastal ocean, and turbid harbor) compared to the LDPC coding scheme. Jain *et al.* [151] examined the non-orthogonal multiple access (NOMA), OOK modulation, and maximum likelihood detection assisted turbid-UWOCs using visible light wavelengths, where a 4.2×10^{-3} BER was obtained at a signal-to-noise ratio (SNR) of 50 dB. However, we note that the SNR value of 50 dB is considerably large for communication systems because it can cause the interference to other systems or channels. Furthermore, [152] proposed a hybrid chaotic system that can be integrated into arbitrary transducers for high reliability UACs. The results in [152] showed that, at a frequency of 50 KHz and a fixed data rate of 1 Kbps, a 4.5×10^{-3} BER was achieved at SNR = 18 dB over a 1 km communication link. Huang *et al.* [153] proposed a novel convert UAC system based on chaos signal and mimic ship-radiated noise. Based on the sea testbed environment in [153], at operating frequency and data rate assumptions of 44.1 KHz and 50 bps, respectively, the proposed scheme can reliably transmit with

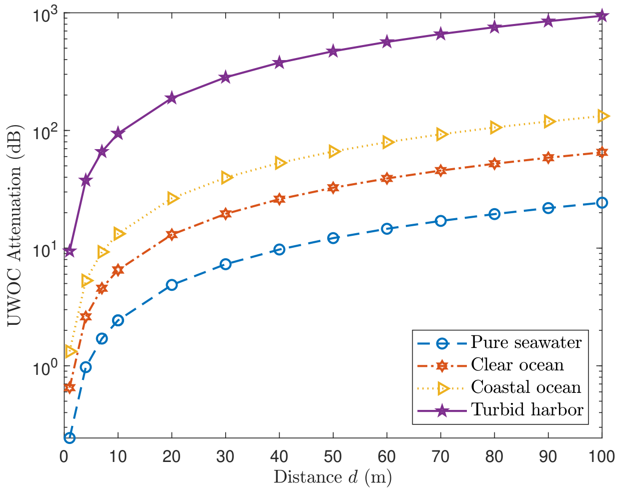

(a) UWOC attenuation for some typical aquatic environments.

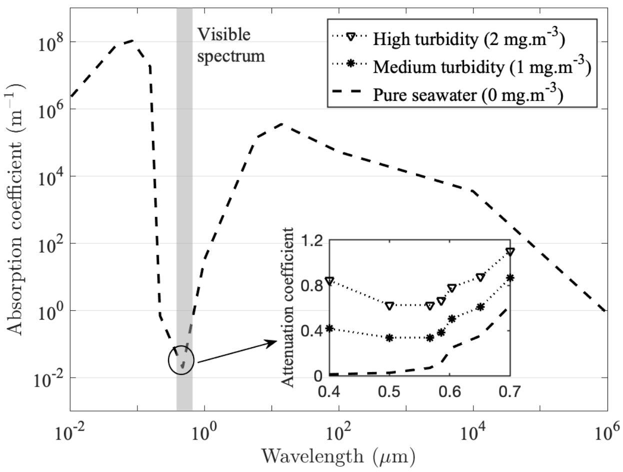

(b) Absorption and attenuation coefficients of underwater environments vs. different turbidity and wavelengths.

Figure 6: Channel properties for UWOCs and transparent window for light aquatic attenuation.

$10^{-3} \sim 10^{-4}$ in the order of BER over 10 km of the communication distance. In addition, the use of a software-defined UAC was studied in [154] with real-time physical-layer adaptation mechanisms that enable either joint adaptation of channel coding rate and modulation constellation or seamless switching between OFDM and direct sequence spread spectrum. The experimental results in [154] have revealed a tradeoff between BER and data rate such that BER $= 2 \times 10^{-5}$ with 104 Kbps and BER $= 10^{-3}$ with 208 Kbps are obtained in real time over a 200 m communication link. In [155], Ramavath *et al.* proposed a MIMO turbid-UWOC system using OOK modulation and Reed-Solomon code to achieve a 10^{-5} BER at SNR $= 1.2$ dB with the assumption of a 30 m distance link and a 500 Mbps data rate, where the proposed system offered the transmit power gain of a minimum of 35 dB compared to the uncoded single-input single-output system.

In addition to the long distance propagation and high data rate purposes, [128, 126, 133, 143, 135, 146, 139, 147, 148, 149] contributed the high communication reliability. Specifically, a 10^{-4} BER was achieved with the proposed systems in [128, 126, 133]. The multihop RF UWC relaying network in [135] offered BER $= 4.3\times10^{-3}$ over a 200 m distance link. Furthermore, the proposed DMT and PNE mechanisms for clear-UWOCs in [149] provided a 3.8×10^{-3} BER at maximum data rate and propagation distance. In the same manner as the BER observation at maximum data rate and propagation distance for clear-UWOC systems, the works of [147], [148], and [139] offered BER $= 3.5\times10^{-3}$, BER $= 1.5\times10^{-3}$, and BER $= 10^{-5}$, respectively. Subsequently, the NRZ-OOK-based clear-UWOCs proposed in [146] can provide a 2×10^{-6} BER at 90.7 m but with only a 0.15 Gbps data rate. In addition, [143] considered the tradeoffs among long distance propagation, high data rate, and high communication reliability. At a fixed 20 m link, the proposed autoencoder for clear-UWOCs obtained a 9×10^{-3} BER with a 2 Gbps data rate, whereas only a 10^{-3} BER was achieved but with 1.5 Gbps.

In summary, the state-of-the-art studies on the tradeoffs among long distance propagation, high data rate, and high communication reliability for UWCs are provided in Table 3. In this table, we denote P-UWOC, C-UWOC, CT-UWOC, and T-UWOC as the pure, clear, coastal, and turbid water types for UWOCs, respectively. In addition, the columns entitled "A" and "E" indicate the model being investigated by either the analysis or experiment measurements.

3.5. Formation Control

Because AUVs have widely emerged as one of the essential tools for UWCs, AUV operations in the hostile underwater environment are worth considering. As a result of the UWC integration with 6G infrastructures, the deployment density of AUVs can be very high, which would lead to unexpected collisions in the network if the AUV trajectories and formation are not investigated. In addition, mystery thermals and some potential threats from the unknown ocean floor and sea can cause trouble for the AUV operation. Formation control in heterogeneous UWCs is the cooperative control for AUVs to follow a predetermined trajectory while maintaining a desired relative network architecture, which is beneficial to fulfilling UAV tasks with better scalability, flexibility, and adaptability [9]. This subsection provides details on the classification of formation architectures and control strategies.

3.5.1. Formation Architectures

Based on the decision-making process, the formation architectures can be categorized into three pillar classifications: centralized, distributed, and hierarchical.

Centralized Architecture. In the centralized formation architecture, a centralized controller plays a main role in the action decision-making for AUV swarms in the whole network,

Table 3: Summary of state-of-the-art UWC studies on the tradeoffs among distance, data rate, and reliability.

Ref.	Year	Network	A	E	Frequency/ Wavelength	Distance	Data rate	Reliability	Techniques/Remarks
[125]	2017	UAC		✓	85 KHz	1.5 km	34 Kbps		DFE-based CE, QPSK
[126]	2020	UAC		✓	23 KHz	0.5 km	20.17 Kbps	0.9999	LSMSE-based CE, MIMO, QPSK
[127]	2021	UAC	✓		180 KHz	3 km	96.7 Kbps		Linear MMSE-based CE, MRC receiver, massive MIMO
		RF UWC			180 KHz	100 m	70.6 Mbps		
		UWOC			Blue-green	100 m	85.7 Mbps		
[128]	2020	UAC	✓		10 KHz	2 – 7 km	fixed 1 Kbps	0.9999	Throughput analysis for a new interference UWC model, MMSE-based CE, BPSK
[129]	2017	UAC	✓		15 KHz	1 km		0.999	Adaptive CE with LCLMA, LCLMS, LCRLA, and LCRLS
[130]	2020	UAC	✓		16 KHz	1 km	fixed 4 Kbps	0.9 – 0.999	SDD-CS-based CE, QPSK modulation
[131]	2019	UAC		✓	12 KHz	8 km	2.4 Mbps	0.99	DFE-based CE, deep learning-based CE, BPSK
[132]	2020	UAC		✓	0.9 – 1.5 KHz	100 km	BPSK: 234 bps QPSK: 466 bps		Machine-learning-based adaptive modulation, DFE-based CE, BPSK/QPSK
[133]	2018	UAC	✓		32.5 KHz	1 km	224 Kbps	0.9999	Turbo code, massive MIMO, real-time video transmission
[135]	2019	RF UWC		✓	6.78 MHz	200 m	2 Mbps	0.9957	Multihop relaying network
[136]	2020	RF UWC		✓	6.78 MHz	100 m	1 Mbps		Multihop multiple-cluster network
[139]	2020	C-UWOC	✓		Blue	20 m	50 Mbps	0.99999	PAM, SiPMs
[140]	2018	P-UWOC		✓	Green	16 m	100 Mbps	0.9998	Full-duplex communication, photodiode module, high-speed pin detector
		C-UWOC				4.8 m		0.99978	
		CT-UWOC				3.2 m		0.999983	
		T-UWOC				1.6 m		≈ 1	
[141]	2020	C-UWOC	✓			7 m	500 Mbps		Channel coding, laser diode, pin detector
[142]	2020	T-UWOC		✓	Green	32 m	1 Gbps		A novel SiPM, attenuation length indicator, laser diode
[143]	2021	C-UWOC	✓		Green	20 m	2 Gbps	0.991	Autoencoder
							1.5 Gbps	0.999	
[144]	2018	P-UWOC	✓		Green	1.2 m	2.175 Gbps		QAM, LED, multi-pin MRC reception
[145]	2017	C-UWOC		✓	Blue-green	12 m	2.2 Gbps		NRZ-OOK, laser diode
[146]	2017	C-UWOC		✓	Blue-green	34.5 m	2.7 Gbps	0.9966	NRZ-OOK, laser diode
						90.7 m	0.15 Gbps	0.999998	
[147]	2018	C-UWOC		✓	White light	2.3 m	3.4 Gbps	0.9965	OOK, laser diode
							3.2 Gbps	0.9964	
							3.1 Gbps	0.9963	
[148]	2020	C-UWOC		✓	Blue	1.5 m	4.92 Gbps	< 0.9985	Series-connected Gallium Nitride micro-LED arrays, QAM, OFDM
						3 m	3.22 Gbps		
						4.5 m	3.4 Gbps		
[149]	2018	C-UWOC		✓	Blue	5 m	16.6 Gbps	< 0.9962	DMT, PNE
						35 m	13.2 Gbps		
						55 m	6.6 Gbps		
[150]	2017	P/CT/T-UWOC	✓		Blue-green	12 m		0.999	LDPC, Turbo code, OFDM, MMSE-based CE
[151]	2020	T-UWOC	✓		Visible light	Normalize		0.9958	NOMA, OOK, maximum likelihood
[152]	2018	UAC	✓		50 KHz	1 km	fixed 1 Kbps	0.9955	Hybrid chaotic system
[153]	2020	UAC		✓	44.1 KHz	10 km	fixed 50 bps	0.999 – 0.9999	A novel convert UAC with chaos signal and mimic ship-radiated noise
[154]	2018	UAC		✓	100 KHz	200 m	104 Kbps	0.99998	Software-defined architecture, real-time physical-layer adaptation mechanisms
							208 Kbps	0.999	
[155]	2020	T-UWOC	✓		Blue	30 m	500 Mbps	0.99999	OOK, Reed-Solomon code, MIMO

as shown in Fig. 7(a). With this architecture, the global information of all AUVs and environments (e.g., locations, speeds, and obstacles) is gathered at a central controller based on the help of network sensors, from which the actions (e.g., avoiding obstacles, moving to destination, maintaining formation) are decided [156, 157]. Here, the communication between a centralized controller and each AUV is regarded as the transmit-feedback relationship. Rehman *et al.* [156] investigated a centralized approach for the formation control where proportional–integral–derivative (PID) controllers were utilized as centralized controllers for the motion control in each direction to follow the desired trajectory of two hovering AUVs. In addition, the nonlinear coupled dynamic model was developed for transportation by considering the effects of hydrostatic, hydrodynamic, and thrust factors. The numerical results in [156] have revealed that, although the system cannot compromise the stability requirement because of the characteristics of a rigid structure in the nonlinear coupled dynamic model, the transportation tasks for desired motion in the horizontal plane, overcoming uncertainties, maintaining the desired formation, and a tolerance

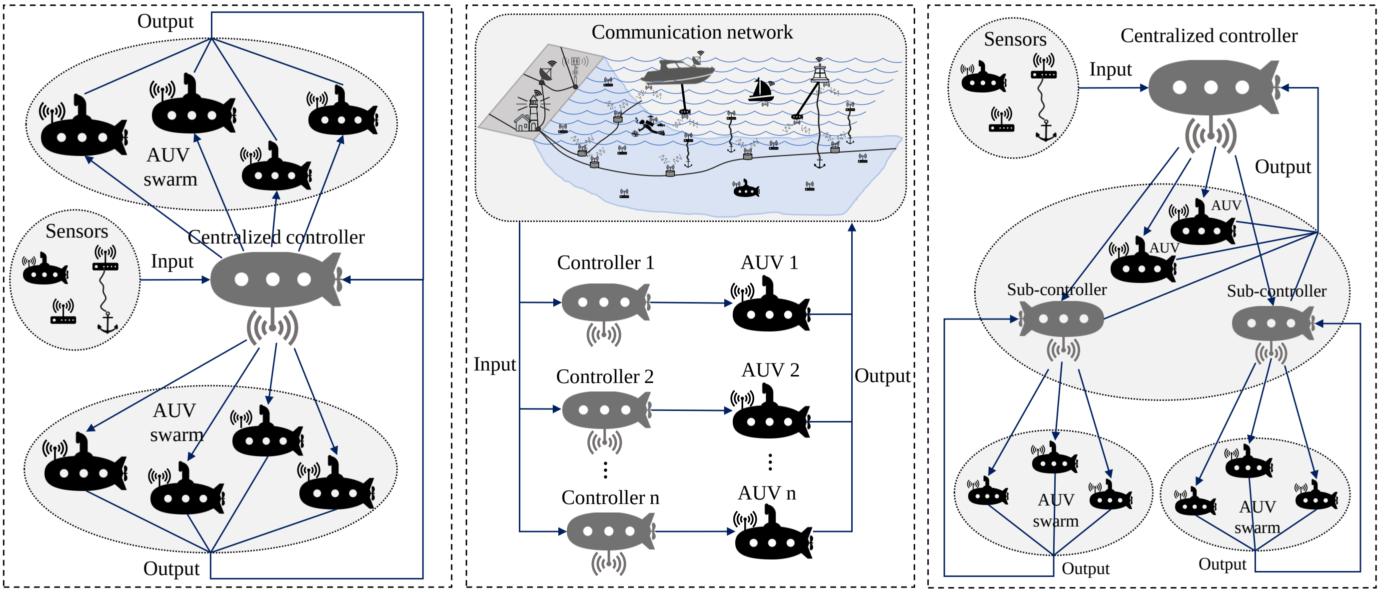

(a) Centralized formation (b) Distributed formation (c) Hierarchical formation

Figure 7: Formation architectures for AUVs in the underwater infrastructure.

tracking of ±5% are satisfied. In [157], the authors designed a centralized formation control system that leverages centralized controllers for an AUV swarm while maximizing range-related information for target localization and tracking missions. By computing the control actions for each agent from the supervisor and utilizing a discrete event law, the trajectories of AUVs were well scheduled with a low collision probability.

Distributed Architecture. Fig. 7(b) illustrates the distributed formation classification, where each AUV has a controller to share the computing and communication burden. In this architecture, both controllers and AUVs can exchange information with network environments, and each AUV can share its information with a subset of AUVs in the network. Accordingly, based on local information about the AUV swarm, each controller can decide independently, and an AUV can maintain the desired speed and distance with neighbors. Therefore, maintaining formation requires synchronization among related AUVs [158]. From the theoretical and experimental perspectives, [159] studied a robust distributed formation controller for an AUV swarm, where a position control loop and an attitude control loop are designed to effectively control the translational motion and rotational motion of multiple AUVs, respectively. In addition, they considered the dynamic factors (e.g., nonlinearity, external disturbances, and parametric uncertainties) for more practical scenarios. The strong robustness of the proposed distributed formation control method has been validated by the numerical simulation results. Furthermore, Yuan *et al.* [160] introduced a novel concept of formation learning control for multi-agent AUVs with heterogeneous nonlinear uncertain dynamics, which consists of two layers: a decentralized deterministic learning controller at the lower layer and a distributed adaptive observer at the upper layer. In a lower layer, they leveraged radial basis function neural networks to train data and perform the formation control protocol for each local AUV agent, where a fully distributed fashion was considered without utilizing any global information. In an upper layer, based on graph theory and multi-agent consensus, a distributed adaptive observer was constructed. The simulation and experimental results in [160] have demonstrated the effectiveness of the proposed system.

Hierarchical Architecture. Because a centralized cluster formation requires too much overhead from the centralized controller to perform a network and a distributed cluster formation brings huge challenges to collaborative communications, the hierarchical formation architecture has been inspirationally utilized [161, 162]. As shown in Fig. 7(c), the hierarchical architecture can be regarded as an extension of the centralized classification, which includes a centralized controller and one or multiple sub-controllers that organize AUV swarms into clusters. A centralized controller can decide based on the global information of all AUVs, sub-controllers, and environments and then send commands to sub-controllers. Sub-controllers process and transmit the commands to their own cluster. Subsequently, AUVs in each cluster perform the received commands. Eventually, they send feedback in the inverse direction sequentially. In [161], Haghighi *et al.* presented a hierarchical framework for multiple UAVs to perform formation maneuvers that are determined by some agile and time-independent trajectories led by virtual leaders. Based on the path-following guidance method and inherent collision avoidance pattern, they showed the admissible performance of the proposed system with low computational complexity. Similar to [161], [162] also contributed to a hierarchical architecture for AUV cluster formation to perform task allocation strategies. The employed strategies dealt with local hierarchical cluster information and utilized a priority sampling method to sample and store them in the experience pool. The actor-critic dual network was subsequently leveraged to derive optimal strategies for evaluation, which yielded the fast convergence speed with a small number of iterations.

Each architecture has its own set of benefits and drawbacks that are listed in Table 4. We note that the aforementioned drawbacks in Table 4 are relative and can be remedied with appropriate designs.

3.5.2. Formation Control Strategies

To offer a robust formation with its own purpose, different formation control strategies have been proposed to meet various missions [163], which can be roughly categorized into the following:

- Leader-follower strategies: A single or multiple AUVs play the leader role, whereas others act as followers that track the locations and orientations of the leader(s) to perform formation [162, 164, 165]. In addition, a virtual leader strategy is further proposed [161], which can be regarded as a moving reference node with a predefined trajectory of the whole formation.

- Behavior-based strategies: Each AUV is oriented to adopt several desired behaviors with their own purpose, including maintaining formation, moving to a destination, and avoiding collision. [166, 167].

- Virtual structure strategies: AUVs maintain a geometric shape with a rigidly virtual structure (i.e., fixed relative distances and bearing) [168].

- Graph theory-based strategies: Each node in a graph is represented as an AUV. If any AUV has an influence on another AUV (e.g., interdependence on their states), it is categorized into a directed graph classification, in which there exists a directional edge between AUVs [160, 159]. Alternatively, it belongs to an undirected graph classification, in which the length of an edge is measured by the distance between two AUVs.

- Artificial potential function strategies: These strategies depend on attractive and repulsive potential functions that represent the potential energies of desired locations and obstacles, respectively [169]. In addition, the movements of AUVs in these strategies depend on a potential force. If a potential force moves AUVs, their potential energy will be reduced. We note that desired locations offer an attractive potential force to orientate AUVs toward their desired locations, whereas obstacles offer a repulsive potential force to move AUVs away from these.

- Lyapynov function-based strategies: Each AUV has its own auxiliary functions that are generated by utilizing the Lyapynov method (i.e., converting a formation control problem into a stabilization problem) [170, 171]. In these strategies, the entire formation can be determined by identifying an equilibrium point that is regarded as a solution of the Lyapynov function.

Each kind of strategy has different benefits and drawbacks, as summarized in Table 4. To satisfy multiple missions flexibly, the aforementioned strategies can also be simultaneously combined together. Specifically, Chen *et al.* [172] introduced an integrated approach involving the virtual structure and leader-follower formation control strategies, which significantly improved the stability, rapidity, and accuracy of multiple AUVs. Here, the proposed framework [172] utilizes a fusion control method with a redistribution algorithm and two path updating methods with a hybrid bio-inspired self-organizing map mechanism to achieve the feasibility of real-time formations in three-dimensional UWC environments. In [156], the behavior-based and virtual structure formation control strategies were mixed together to perform multiple tasks for multiple AUVs. Furthermore, [157] leveraged the benefits of both the leader-follower and behavior-based strategies for multiple AUV missions. The obtained achievements in [156] and [157] were mentioned in the centralized formation architecture classification. Subsequently, [166] investigated a novel joint formation control strategy for multiple AUVs in which a triangular structure comprised of a leader and two followers was established based on graph theory. Moreover, the formation task for moving to the destination was decomposed into different subtasks with different priorities, where the obstacle avoidance subtask was designed as the highest priority. In [167], a rigid virtual structure with triangles of nodes in UWC networks was constructed for high formation control performance in terms of reliability and efficiency, which was referred to as TRiForm. The results in [167] have revealed that TRiForm can successfully control multiple AUVs in the network to reach the predefined destination and perfectly maintain the formations under motion and distance measurement errors. Gao *et al.* [173] adopted the formation tracking control for multiple AUVs with graph theory utilization, where the follower AUV can track all the leader AUV states that are globally stabilized within a given settling time. In [169], the artificial potential and a novel formation control algorithm for an AUV swarm were designed, which were suitable for both followers and leaders to perform the trajectory and velocity tracking missions as well as maintain the predefined formation. Moreover, it has been demonstrated that the proposed algorithm in [169] can improve the network performance in terms of scalability, adaptability, and communication consumption. Furthermore, a Lyapunov function-based stability analysis for multiple AUVs with leader-follower relationships was proposed in [170], where the multi-layer neural network, sliding mode control, and adaptive robust techniques were designed to establish the network controller. Some advantages of the proposed framework [170] could be highlighted as follows: (*i*) prior knowledge of hydrodynamic damping and external disturbances was not required, leading to easy practical implementation, (*ii*) the system greatly reduced the inherent chattering of the sliding mode controller, and (*iii*) only the line-of-sight and angle sensor information of the leader AUV were required. Similar to [170], [171] also handled two of the same aspects (i.e., leader-follower and Lyapunov function-based formation control strategies). However, in [171], a three-dimensional coordination controller was further employed by integrating back-

Table 4: Summary of advantages and disadvantages of UWC formation control classifications.

Aspect	Classification	Advantages	Disadvantages
Architecture	Centralized	Convenient and straightforward to deploy, low-cost implementation	Weak robustness in the face of centralized controller failures, lack of scalability owing to restricted communication range, required global information
	Distributed	Better robustness and scalability than centralized architecture, sharing computing and communication burden with each AUV, not required global information	High-cost implementation from the required number of controllers corresponding to the AUV density, it requires synchronization among related AUVs
	Hierarchical	High scalability, sharing computing, and communication burden with sub-controllers	Weak robustness with respect to centralized controller failures, required global information
Strategy	Leader-follower	Designs in formation control functions are only required for leaders, resulting in a low complexity of controller configurations	Weakness in robustness because followers do not communicate with one another, if a leader fails, the entire formation led by this leader also fails
	Behavior-based	Minimum information exchange is required among AUVs	Low stability, difficulty in designing basic behaviors and local control planning
	Virtual structure	Easy description for coordinated behaviors of AUVs, well-maintaining formation based on the rigid structure	Poor adaptability and flexibility because of the characteristics of the rigid structure
	Graph theory-based	Sufficient theoretical support for formation control with well-developed graph theory	High complexity in designing and solving a graph theory-based implementation
	Artificial potential function	Low complexity and easy implementation of real-time controls without considering the minimum value	Difficulty in finding the local minimum value because of the complex designed function
	Lyapunov function-based	High stability and controllability	High computational complexity because of the conversion of stabilization problems with auxiliary functions

stepping technique and sliding mode control into the leader-follower AUV approach with a triangular prism formation. The simulation results in [171] have demonstrated that the designed controllers can perform well in the desired formation and the coordination control mechanism is effective.

3.6. Localization and Navigation

Localization and navigation are two of the most crucial challenges for UAVs to perform collaborative missions. It is evident that the localization and control mechanisms using the global positioning system (GPS) are not efficient in the medium and deep underwater regions because of the UWC characteristics. Even if GPS is utilized, it only applies to the shallow water application scenarios or surface buyos that are integrated into the whole network. In this subsection, we primarily focus on the design capability of location estimation and navigation strategies in the general UWC networks. The survey framework and major topic organization for localization and navigation are depicted in Fig. 8.

3.6.1. Localization

Because most of the underwater applications require the sensed data along with location information of network nodes (or even obstacles), the design of localization algorithms has become one of the emerging and essential key pillars for UWCs. According to the computational design, the localization algorithms for UWC networks can be categorized into centralized and distributed [8].

Centralized Localization. In the case of centralized localization designs, a positioning algorithm for location estimates is computed at a central location (e.g., sink node, AUV centralized controller) through the globally collected information. In [174], a received signal strength (RSS)-based localization algorithm was investigated to estimate the positions of static nodes in UWOC networks, where the Cramer-Rao lower bound (CRLB) was also investigated to determine the best achievable expectation of the estimator. The results in [174] have shown that the root-mean-square-error (RMSE) of the positioning estimate is significantly lower than the baseline and manifold regularization. Lin *et al.* [175] proposed compressive sensing-based self-localization using RSS indicators for mobile nodes in UAC networks, where the random way-point and layered-scan models were considered to tackle the distance problem of the moving path. The objectives in [175] were to achieve high localization accuracy while reducing the network cost and energy loss. In [176], the authors proposed a virtual node assisted localization method for UACs, where (*i*) the algorithm was conducted via the static and dynamic virtual node classifications, (*ii*) an auxiliary node was leveraged for virtual node setup, RSS indicator ranging, and error measurement, and (*iii*) an on-board GPS was equipped in each network node that utilizes virtual node and geometry. The proposed scheme in [176] has demonstrated high localization coverage, small localization errors, and low communication overhead. Furthermore, [177] studied an RSS-based localization framework for energy-harvesting UWOC networks. The sensor nodes begin communicating only when they have accumulated enough energy harvested from the ambiance. The network localization was performed by measuring the RSSs of network nodes and then computing block kernel matrices. Extensive simulations in [177] have revealed that the proposed framework reduces the estimation error of the shortest path of each block kernel matrix, leading to an achievement very close to CRLB. Subsequently, Saeed *et al.* [178] proposed a robust three-dimensional (3D) localization algorithm based on low-rank matrix completion and outlier removal methods for UWOCs. Additionally, the optimal anchor placement was investigated in [178]. In [179], the authors first designed a consensus-based unscented Kalman filtering algorithm for asynchronous passive localization in UAC networks. To elimi-

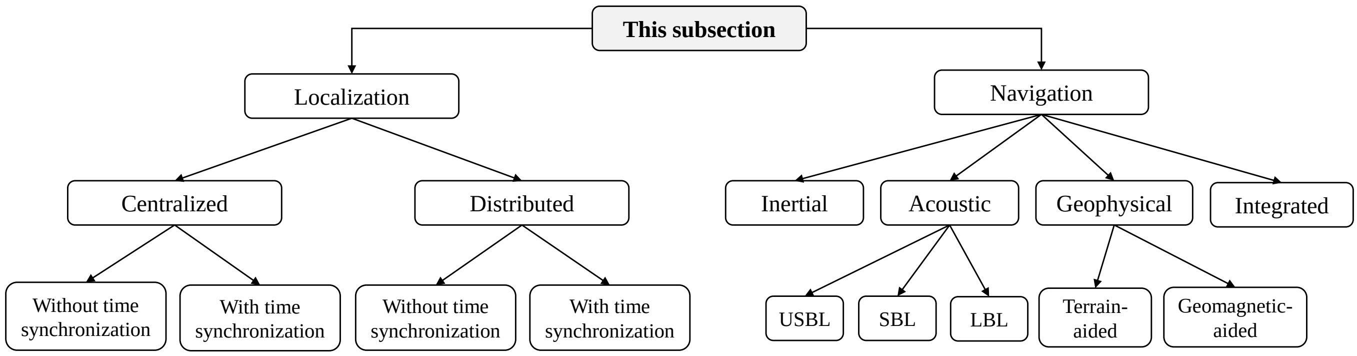

Figure 8: Survey framework and major topic organization for UWC localization and navigation.

nate the effect of asynchronous clocks, the authors established the relationship between the propagation delay and the position by adopting the ray-tracing approach without requiring it to be synchronized. In addition, the proposed localization optimization problem was formulated to minimize the measurement errors' summation. The converge conditions and CRLB were also achieved. Furthermore, Yan *et al.* [180] adopted deep reinforcement learning (DRL) to perform the localization algorithm for mobile sensor nodes in UAC networks. In this system model, surface buoys were equipped with GPS to provide self-localization and synchronization for AUVs, whereas the locations of AUVs could be estimated through their direct interaction with surface buoys. The time synchronization of AUVs, active, and passive sensor nodes was not required in real time. The proposed algorithm reduced the RMSE of positioning estimates and achieved CRLB.

We note that [174, 175, 176, 177, 178, 179] proposed localization algorithms are based on the local clock of each network node, which may no longer provide efficient solutions when UWC networks experience clock offset and clock skew phenomena [181]. To handle these problems, time synchronization has been further performed in the UWC localization systems. Specifically, an AUV-aided joint time synchronization and localization was proposed for mobile nodes in UAC networks [182], where the leveraged methods included time-of-arrival (ToA) measurement of received packets, on-board GPS receivers and inertial navigation sensors, and solving the nonlinear equations via an efficient linear algorithm. Based on the results from simulations and closed-form positioning and synchronization error analysis, the convergence of the proposed method to CRLB was demonstrated. Similar to [178], Saeed *et al.* [183] also employed a robust 3D localization algorithm based on low-rank matrix completion and outlier removal methods for UWOC networks. Nonetheless, the time synchronization problem in [183] was additionally determined based on the ranging method and the assumption that ranging information was available in the network. The simulation results have revealed that the proposed method substantially outperforms the benchmark (i.e., the iterative majorization method). Jiang *et al.* [184] designed a robust joint time synchronization and localization system for UAC networks, where the adaptive iterative local searching OMP (AILSOMP) algorithm was utilized for time synchronization and the improved three-stage weighted least squares (ITSWLS) localization algorithm using the time-difference-of-arrival (TDoA) was employed for positioning estimates. Furthermore, [185] specified the possibility of employing Doppler shift measurements for the localization of mobile UAC network nodes. With the on-board GPS and inertial sensors, the AUV could localize and synchronize itself efficiently. The high-accuracy position information of the target devices was also achieved by using a two-phase linear algorithm. In addition, the convergence between the closed-form localization error and CRLB was presented. Subsequently, the authors in [186] proposed a movement prediction location (MPL) algorithm for the mobile UAC network nodes. The proposed algorithm included two phases: mobile prediction and node location, which utilized the grey wolf optimizer, and a ToA-based ranging strategy with the time synchronization requirement. Extensive simulations have confirmed that the proposed MPL scheme achieves higher localization performance than the benchmarks (i.e., target-scale localization, scalable localization with mobility prediction, and genetic algorithm for scalable localization with mobility prediction). In [187], an accurate 3D localization technique for mobile UWOC network nodes was designed by optimizing the anchor's location for a set of smart objects, where spectral graph partitioning was utilized for valuable sensor selections. Further, the time synchronization problem between the smart objects and surface buoy was also indicated. We note that the optimization of the anchor's location for all smart objects is unnecessary, which would lead to unessential high complexity. Therefore, the proposed framework achieved significantly low computational complexity while the positioning error variance converged to CRLB. [188] proposed a localization algorithm based on synchronized UACs using an auto-regressive protocol. The algorithm initially localized the source and destination sensors to the sink node. When the permissible delay was successfully synchronized with the sensor clocks, the network initially performed the data transmission under the constraints of propagation delay and bandwidth efficiency. The auto-regressive model was subsequently applied to the transmission, synchronization, and localization loops, which were found to have better performance than the benchmark (i.e., time synchronization for high latency). Additionally, Shams *et al.* [189] studied a joint algorithm for multihop localization and time synchronization for mobile UWOC network nodes. A connection between sensors by point-to-point directed links was established and the model for synchronization was analytically formulated, whereas the localization was conducted based on the measurements of angle-of-arrival, ToA, sensor identification, and pseudocode algorithm. The experimental results in [189] have revealed that the proposed algorithm outperforms the benchmark schemes (i.e., multi-dimensional scaling–mapping, multi-stage localization, double rate localization, and no reference node) and the RMSE of the positioning estimate can converge to CRLB.

Distributed Localization. In the distributed localization schemes, sensor nodes execute localization algorithms individually to estimate their positions, based on the collected data essentially related to location estimation. In [190], the authors were concerned about the position estimation for node mobility and clock asynchronization in UAC networks, where an asynchronous localization algorithm with mobility prediction and iterative least squares estimators was designed to solve the optimization problems, which are formulated as minimizing the sum of all measurement errors. The convergence between the analysis and CRLB for localization errors were also provided. The simulation results in [190] confirmed that the proposed scheme can effectively compensate for the impact of node mobility and clock asynchronization while reducing the localization time compared to the well-established exhaustive search method. Qiao *et al.* [191] proposed a novel localization algorithm for UWC networks, namely the communication signal propagation loss localization scheme (CSPLLS). CSPLLS is a passive, cooperative, and asynchronously distributed localization method, in which the target only uses communication RSSs from anchor nodes. The benefits of the proposed framework [191] are highlighted as follows: It achieves as low as 2.2% positioning error with centroid optimization, reducing the localization time, saving the network node energy, and eliminating the asynchronization issue. Furthermore, a novel unscented transform-based localization algorithm was proposed for the UAC network nodes' localization [192], where the ray-tracing approach was adopted to characterize the stratification effect. The numerical results in [192] have shown that the proposed algorithm achieves a lower RMSE than existing works and can converge to CRLB. Subsequently, [193] investigated an energy-efficient tracking issue for mobile UAC targets, which subjected to the constraints in terms of the power restriction, asynchronous clock, and noise measurement. To solve the concerned issue, an asynchronous localization algorithm and a consensus-based Bayesian filter with a consensus fusion strategy and duty-cycle mechanism were effectively developed. Yan *et al.* [194] designed an AUV-aided localization solution for UAC networks, which subjected to the time asynchronous, stratification effect, and node mobility constraints. Based on the iterative least squares estimator, the relationship between the positioning estimation and propagation delay could be established. In addition, two asynchronous localization algorithms with active and passive sensor nodes were employed to improve the localization accuracy. The simulation and experimental results in [194] have confirmed the convergence between the error variance of the proposed scheme and CRLB. Furthermore, the mobile node localization problem in UWC systems was investigated in [195], where a modified TDoA-based localization method was proposed to handle the problem without considering the time synchronization requirement. The proposed scheme demonstrated the capability to localize passive sensor nodes with high localization robustness and low energy consumption.

Similar to the centralized localization classification, the time synchronization problem is also investigated in distributed strategies to compensate for the clock skew and clock offset phenomena. Specifically, Zhang *et al.* [196] introduced a unified framework to execute joint synchronization and localization for UWC network nodes. A ray-tracing approach was utilized to model the stratification effect, whereas the maximum likelihood estimator was leveraged based on the Gauss–Newton algorithm for non-convex optimization. In addition, CRLB was analyzed as a benchmark reference. The proposed framework [196] demonstrated superior performance in both localization accuracy and energy efficiency compared to the existing methods. The authors in [197] proposed a confidence-based localization algorithm using an ultra-short base line system for UWCs. The error characteristics of the localization methods studied in [197] were specified based on the ToA trilateration, dead reckoning utilization, and ultra-short base line system, which allowed the implementation of up to 100 tracked mobile sensor nodes. In [198], a localization framework, namely underwater localization evaluation scheme (ULES), was proposed for the UAC network's mobility nodes. Specifically, to improve the localization accuracy under beacon node drift scenes as well as to combat the inter-node time synchronization problem, the ULES algorithm utilized an analytic hierarchy process and a grey correlation method simultaneously. The superior performance of ULES was confirmed via the simulation results. [199] first introduced an anchor-AUV localization geometry in UAC networks through an isogradient sound speed profile analysis. A multivariate and nonlinear optimization problem that minimized the trace of CRLB was formulated under the angle and range constraints of anchor-AUV geometry. Although extensive simulation results in [199] validated the theoretical analysis and demonstrated the high localization accuracy of the proposed optimization framework, the considered isogradient sound speed profile may not guarantee the performance in real deployment because the speed characteristic varies nonlinearly in practical scenarios. Furthermore, Yao *et al.* [200] proposed a novel solution, based on an expectation maximization-type method, for a joint time synchronization and positioning estimation problem in UWC networks. The proposed solution yielded better localization performance than conventional schemes (i.e., least squares, weighted least squares, and generalized total least squares estimators).

Motivated by academic researches [196, 197, 198, 199, 200], scientists worldwide have recently paid more attention to proposing advanced algorithms for distributed localization with time synchronization [201, 202, 203, 204, 205, 206]. Specifically, the least square estimation-based symmetry correction was leveraged to perform the localization algorithm in UAC networks [201]. Here, the authors in [201] investigated a realistic circumstance, where (*i*) passive positioning was realized by the ToA ranging strategy, (*ii*) the actual sound speed profile was uncertain, and (*iii*) the estimated targets with mobility were considered. According to the simulation results, the good performance of the proposed framework was exhibited. [202] studied a single-leader-multi-follower Stackelberg game using an energy-efficient localization algorithm to estimate the positions of mobile UWC network nodes, where the two-way message exchange was assumed to provide time synchronization among participating nodes. The proposed framework offered an energy saving of up to 48% while providing desirable localization coverage with reasonable error and delay constraints. In addition, [203] expanded the contributions of [179] by further considered the time synchronization problem account for UWC networks, but the localization processing was conducted in a distributed manner. The surface buoys utilized an on-board GPS to acquire their locations and global time references, which would lead to self-localization and clock synchronization for sensor nodes. A consensus-based unscented Kalman filtering algorithm with feedback control and a proportional-integral estimator were designed to perform efficient networking localization. Unlike [199], a practical sound speed profile with a nonlinear variation characteristic was indicated in [204], where the positioning estimation for mobile UWC network nodes was solved via a precision-improved passive localization method. The simulation results have shown that the proposed framework [204] outperforms the localization benchmarks (i.e., those based on TDoA and ToA without ray-compensation). In [205], a joint localization and synchronization method with a duty-cycle working mode and an expectation maximization algorithm was proposed, where AUVs served as mobile anchor nodes to provide information for localizing and synchronizing the static sensor nodes. Based on the simulation experiments, the proposed framework demonstrated superior performance compared to that of the least square algorithm. Eventually, to improve the localization accuracy in the context of large-scale UACs and a limited transmission range, [206] developed a mobile-beacon-based iterative localization mechanism that realized the node hierarchically positioning of large-scale multihop UAC networks. In the system model, the mobile beacon nodes were utilized to localize adjacent static sensor nodes. The proposed mechanism not only achieved a low localization error in a short execution time but also effectively balanced the energy consumption of sensor nodes.

Some state-of-the-art UWC frameworks on localization are summarized in Table 5, where the column entitled "M" indicates whether the localization is performed for mobility network nodes or not, whereas the columns entitled "A" and "P" determine the active and passive localization strategies[1], respectively.

[1]A localization algorithm can have an active or passive communication paradigm, which is determined based on whether the participating nodes transmit during the localization process [207].

3.6.2. Navigation

Underwater navigation is regarded as the process of monitoring and controlling the movement of AUVs from one place to another, which can be divided into three main categories: inertial navigation, acoustic navigation, and geophysical navigation [208, 209, 210].

Inertial Navigation. In UWC networks, inertial navigation systems (INSs) operate based on inertial principles, where they utilize inertial measurement units (IMUs) with dead-reckoning techniques to measure and estimate both the position and velocity of mobile UWC network nodes. Dead-reckoning characterizes the process of computing the current position of a mobile vehicle (i.e., an AUV in UWC networks) by utilizing a previously determined location and orientation, and then cooperatively estimating the vehicle's velocity and acceleration [211]. INSs are self-contained (i.e., they do not exchange any external signals) and are responsible for solving the inertial navigation equations of the AUV by using data obtained from the IMU [208]. Because of the processing nature of dead-reckoning, the position and velocity estimates suffer from the drift phenomenon over time, which leads to navigation errors for long-term missions. In other words, INSs can provide short-term missions with negligible navigation errors.

In [212], Wang *et al.* proposed a novel characteristic parameter matching algorithm for gravity-aided underwater INSs, where both the gravitational field characteristic parameters of a particle filter and the gravity anomalies of each point in the fitting area were considered to increase the accuracy of matching. Based on the experimental results, the proposed scheme has demonstrated superior accuracy performance compared to the conventional vector matching algorithm. In [213], fully autonomous navigation in UWC networks was successfully achieved by utilizing parallel tracking, parallel mapping, and IMU data merged through an extended Kalman filter algorithm. The trajectory tracking was accomplished via a proportional integral derivative controller, where a pressure sensor, a magnetometer, and an extended Kalman filter provided feedback for depth control, yaw, and remaining states, respectively. Eventually, real-time experiments were conducted to validate the analytical proposal. Furthermore, Duecker *et al.* [214] integrated guidance, navigation, and control missions into an architecture with a robust, high-accuracy, and marker-based visual self-localization system in UWC networks, where the localization module consisted of a camera, an IMU, and a single-board computer. The developed concept was investigated, and it achieved small-scale submerged AUVs with reliable information on their absolute position and orientation. Therefore, the corresponding control was commanded by using only low-cost components. Subsequently, [215] developed an improved particle filter-based matching algorithm with a gravity sample vector for gravity-aided underwater INSs, which greatly reduced the latitude and longitude estimated errors. Furthermore, Xiong *et al.* [216] proposed a novel underwater gravimetry method utilizing INSs and a depth gauge under the trajectory constraint. Here, the track of gravimeters was fitted to a straight line because of the uniform motion characteristics, and the depth ob-

Table 5: Summary of state-of-the-art UWC frameworks on localization.

Classification		Ref.	Year	Network	M	A	P	CRLB	Algorithms/Remarks
Centralized localization	Without time synchronization	[174]	2018	UWOC		✓		✓	RSS-based localization
		[175]	2019	UAC	✓	✓			Compressive sensing-based self-localization using RSS indicators
		[176]	2019	UAC	✓	✓			Virtual node assisted localization, on-board GPS, RSS indicators
		[177]	2019	UWOC		✓		✓	RSS-based localization, energy-harvesting
		[178]	2019	UWOC		✓			Low-rank matrix completion and outlier removal methods
		[179]	2020	UAC			✓	✓	Consensus-based unscented Kalman filtering, ray-tracing approach
		[180]	2020	UAC	✓	✓	✓	✓	DRL-based localization, on-board GPS
	With time synchronization	[182]	2018	UAC	✓	✓		✓	On-board GPS receivers and inertial sensors, ToA-based linear algorithm
		[183]	2018	UWOC		✓			Low-rank matrix completion and outlier removal methods
		[184]	2019	UAC			✓		TDoA-based localization using AILSOMP and ITSWLS
		[185]	2020	UAC	✓	✓		✓	On-board GPS and inertial sensors, doppler-based positioning estimates using two-phase linear algorithm
		[186]	2020	UAC	✓		✓		ToA-based ranging strategy, MPL, grey wolf optimizer
		[187]	2020	UWOC	✓	✓		✓	Selected smart objects-based localization using spectral graph partitioning for sensor selections
		[188]	2020	UAC		✓			Auto-regressive protocol
		[189]	2021	UAC	✓		✓	✓	Angle-of-arrival, ToA, sensor identification, pseudocode algorithm
Distributed localization	Without time synchronization	[190]	2018	UAC	✓	✓	✓	✓	Asynchronous localization algorithm with mobility prediction, iterative least squares estimators
		[191]	2019	UAC	✓	✓	✓		CSPLLS, RSS measurements
		[192]	2019	UAC		✓		✓	Unscented transform-based localization, ray-tracing approach
		[193]	2019	UAC	✓	✓			Asynchronous localization algorithm, consensus-Based Bayesian filter with consensus fusion strategy and duty-cycle mechanism
		[194]	2020	UAC	✓	✓	✓	✓	Iterative least squares estimator, two asynchronous localization algorithms with active and passive sensor nodes
		[195]	2021	UWC	✓		✓		Modified TDoA-based localization
	With time synchronization	[196]	2017	UWC			✓	✓	Ray-tracing approach, maximum likelihood estimator, Gauss–Newton algorithm for non-convex optimization
		[197]	2018	UWC	✓		✓		Confidence-based localization, ToA trilateration, dead reckoning utilization
		[198]	2018	UAC	✓	✓			ULES using analytic hierarchy process and grey correlation method
		[199]	2018	UAC	✓	✓		✓	Isogradient sound speed profile, CRLB trace optimality
		[200]	2018	UWC	✓		✓		Expectation maximization-type method
		[201]	2019	UAC	✓		✓		ToA-based ranging strategy, least square estimation-based symmetry correction, actual sound speed profile
		[202]	2019	UWC	✓	✓			Single-leader-multi-follower Stackelberg game using energy-efficient localization algorithm, two-way message exchange
		[203]	2019	UWC	✓	✓			On-board GPS, consensus-based unscented Kalman filtering algorithm with feedback control, proportional-integral estimator
		[204]	2019	UWC	✓		✓		Precision-improved passive localization method, practical sound speed profile
		[205]	2020	UAC		✓			Duty-cycle working mode, expectation maximization algorithm
		[206]	2021	UAC			✓		Mobile-beacon-based iterative localization mechanism

servations were measured by depth gauge to correct the errors of INSs. To conclude, the proposed framework [216] attained parallel accuracy compared with the benchmark (i.e., the multi-data fusion method), which would lead to a good application for gravimetry data processing. In addition, because Doppler velocity loggers (DVLs) could be used as an additional integration along with INSs to provide high precision underwater navigation and positioning, the authors in [217] adopted a strap-down INS, a DVL, and a pressure sensor to design a tightly integrated navigation novel method for UWC networks. The simulation and experimental results confirmed that the proposed method [217] achieved 32.5% higher accuracy than that of the conventional loosely integrated method. Although the combination of DVLs and INSs can significantly improve navigation and positioning accuracy, it can also be easily affected by the external environment because DVLs are instruments based on Doppler frequency shift to measure velocity. Inspired by this, Li *et al.* [218] designed an integrated novel navigation algorithm based on deep learning model to handle DVL malfunctions in UWC networks. The proposed framework [218] was fundamentally accomplished via two phases: (*i*) In the training phase, a robust Kalman filter based on the Mahalanobis distance algorithm was applied to eliminate outliers, and then trained the nonlinear auto-regressive with exogenous input model, namely NARX, with available DVLs; (*ii*) When DVLs were interrupted, the prediction phase executed the DVL estimations as the output of the NARX model and continued integrated navigation. Experimental results in [218] have shown that the NARX–robust

Kalman filter proposal can effectively provide the high accuracy of the DVLs' prediction and outperform existing methods.

Acoustic Navigation. In UWC networks, acoustic navigation systems (ANSs) utilize a number of techniques involving the exchange of acoustic signals between a set of acoustic beacons and AUVs, thereby estimating the locations and navigate the path planning of network vehicles. In ANSs, there are three classifications, namely the ultra-short baseline (USBL), the short baseline (SBL), and the long baseline (LBL), which are determined based on the baseline term that represents the connection between primitives (i.e., receivers or transponders) in UWC networks. Specifically, (*i*) USBL has a baseline length of less than 1 m, (*ii*) SBL operates with a baseline length of 20 m to 50 m, and (*iii*) LBL has a baseline length of 100 m to 2000 m [209, Table 3]. ANSs can provide navigational aids with robust position fixing, although they usually have a low update rate, and the deployment of external devices is also required.

In [219], a LBL ANS using underwater acoustic modems was investigated through sea under-ice trials. To provide navigation missions for AUVs, the graphs of the measurement occurrence frequency distribution corresponding to the different distances between the underwater acoustic modems were plotted. Based on the experimental results, it was shown that the estimation errors obtained by using the proposal were negligible compared to the actual distance. Rypkema *et al.* [220] presented the first endeavor to implement closed-loop experiments using a miniature, a low-cost SandShark AUV, and a custom-designed and inexpensive acoustic system in UWC networks, where results were validated using an independent LBL ANS system. The experimental results revealed that closed-loop operation was the close coupling of conventional phased-array beamforming and particle filtering, which allowed for real-time configuration, a reduction in the computational complexity, an increase in partial count, and an improvement in navigational accuracy compared to the benchmark (i.e., the two-stage beamforming plus particle filtering process). Furthermore, Harris and Whitcomb [221] reported a preliminary investigation for the AUV communication and navigation utilizing a fully dynamic vehicle process model, where an USBL ANS consisted of an acoustic modem, attitude, and depth sensors, whereas an autonomous surface vehicle (ASV) was equipped with an acoustic modem and GPS. In both the simulations and the JHU Iver3 AUV for at-sea experimental trials, it was suggested that the proposed framework [221] offered a significant benefit in accuracy over the benchmark (i.e., the purely kinematic model) even without the frequency and high-accuracy velocity measurements. Subsequently, a similar preliminary study as [221] was conducted in [222], additionally considering the combined control and cooperative navigation. Anecdotal simulation results have suggested that both the control and cooperative navigation could be maintained with the low-cost implementation. Subsequently, the research group of Harris *et al.* additionally developed an USBL ANS with DVL in UWC networks [223], where a novel null-space least squares parameter identification method and preliminary evaluation were conducted for a fully nonlinear second-order six-degree-of-freedom dynamic process model. Based on the experimental and simulation results, the nonlinear model identification with six-degree-of-freedom AUV model parameters, control-surface parameters, and thruster-model parameters was first evaluated, simultaneously accomplished, and then provided the high-accuracy cooperative navigation missions. Furthermore, [224] investigated a robust leader-follower LBL ANS based on the Student's *t*-based extended Kalman filter in UWC networks to combat the outlier in the process and measurement noises. Instead of AUVs, two survey vessels were utilized, equipped with an underwater acoustic modem (i.e., S2CR 7/17 produced by Evologics). Herein, the leader vessel was equipped with a GPS to provide its own positioning information, whereas the follower vessel was equipped with a magnetic compass and a DVL to measure its own heading angle and velocity, respectively. In addition, a PHINS produced by iXBlue worked in integrated mode and was installed on the follower vessel to provide the benchmark for position, velocity, and attitude. The experimental and simulation results in [224] have revealed the efficiency and superiority of the proposed algorithm compared with the benchmark algorithm (i.e., the conventional extended Kalman filer-based ANS).

Geophysical Navigation. Geophysical navigation systems (GNSs) execute localization and navigation missions based on the physical features of the environment, which can be divided into terrain-aided geophysical navigation and geomagnetic-aided geophysical navigation [209]. The geomagnetic-aided geophysical navigation measures the related information based on magnetic sensors, which are passive sensors, whereas terrain-aided geophysical navigation utilizes sonar sensors, which are active sensors. The terrain-aided geophysical navigation compares the obtained terrain profile with a pre-stored terrain database to calculate the current positioning information, from which the positioning errors can be corrected and compensated. Similarly, geomagnetic-aided geophysical navigation performs the missions with the same operation as terrain-aided geophysical navigation, although it leverages the geomagnetic field information for a pre-stored database and real-time information collected by AUVs. GNSs are also self-contained, however the reliability of their navigation is difficult when the map database is limited.

In academic studies, Jung *et al.* [225] conducted experimental research for a geomagnetic-aided GNS in inland waters (i.e., the Jang-Seong reservoir in South Korea). In the employed system model, a magnetometer was rigidly attached to the vehicle and not towed by a cable, which significantly reduced the system size and complexity; however, it required a calibration procedure to compensate for magnetic distortion. Compared to the public magnetic field data, the proposed scheme [225] offered much higher resolution and a lower update frequency, which showed potential for refining the existing public geomagnetic field database. In [226], an adapted motion search strategy was proposed based on deep learning to solve the optimization problem for a geomagnetic-aided GNS, where the activation rule was defined to provide an interactive self-learning that minimized the cost function. The numerical results confirmed the reliability and effectiveness of the proposed algorithm. By the same analysis on a geomagnetic-aided GNS, [227] further proposed a geomagnetic gradient-assisted evolutionary algorithm with long-range navigation. The objectives of the proposed methodology were not only to optimize a navigation path based on a heading angle prediction from a geomagnetic gradient, but also to enhance the reliability and accuracy of a navigation path based on an evaluation function improvement. The efficiency of the proposed algorithm was confirmed via simulation results. Unlike [225, 226, 227], a terrain-aided GNS was investigated in [228], where a terrain-aided position confidence interval model was first proposed to compensate for the large particle filter initialization error and particle coverage interval caused by changes in an AUV operation depth. The validity of the proposed algorithm was finally validated via playback simulations, which confirmed the performance improvement in terms of convergence speed and filtering accuracy of the terrain-aided GNS. Furthermore, both types of geophysical maps (i.e., terrain and geomagnetic field strength maps) were simultaneously constructed in [229] to utilize underwater geophysical information for a GNS. The combined terrain-geomagnetic-aided GNS was investigated in an inland water environment (i.e., the Jang-Seong lake in South Korea), where the navigation algorithm utilized a terrain adaptive particle filter and the authors designed observation models for each geophysical sensor to augment geomagnetic field strength. Experimental results in [229] have validated the superior performance of the proposed framework compared with those of the INS-DVL and conventional terrain-aided GNS.

Integrated Navigation. To capture the strengths and eliminate the drawbacks of each individual navigation approach, some of the aforementioned navigation strategies can be integrated with each other [210]. Some typical state-of-the-art integrated navigation studies are described below.

Integrated navigation systems composed of INSs and GNSs can achieve high-accuracy navigation missions by compensating the cumulative error of INSs in real-time using the geophysical fields of GNSs. For example, Wang *et al.* [230] designed a multipath parallel iterated closest contour point algorithm for an INS and terrain-aided GNS integrated model. The proposed method is based on multi-beam bathymetric data acquired by a multi-beam echo-sounder (one of the main instruments of water depth measurement) and data point choices at the edge of the sounding swath data. The effectiveness and high accuracy of the proposed scheme were evaluated via simulations. Furthermore, Quintas *et al.* [231] conducted experiments on a MEDUSA AUV equipped with a towed magnetometer using a magnetic-based GNS algorithm for the integration of an INS and a geomagnetic-aided GNS. The proposed system required the configurations for inertial and body-fixed frames, the acquisition of prior magnetic maps in an area offshore of Lisbon, and the execution of data-acquisition tests with a MEDUSA AUV. A realistic assessment in real-time of the proposed methodology was shown in both simulations and experiments, confirming its superior performance. [232] described a robust integrated navigation system including both INS and GNS, where a MEDUSA ASV (equipped with a GPS), a marine magnetic explorer, a VectorNav VN-100 sensor (combined an IMU, an attitude heading reference system), and a LinkQuest NavQuest 600 Micro sensor (equipped with a DVL) were leveraged to experiment a very shallow-water lake testbed in Lisbon. The authors proposed a sequential estimation algorithm with a complementary profile correlation method to perform the high-precision navigation missions for the integrated navigation system. Recently, the research group of Quintas *et al.* developed an integrated motion planning, GNS, INS, and control system for AUVs [233], where the rapidly-exploring random tree algorithm, a sequential estimation algorithm, and a path-following controller were employed to perform the missions. Real-time performance was evaluated via hardware in the loop simulations, which claimed the realization of in-water tests of the proposed system.

For the combined models of ANSs and GNSs, [234] and [235] contributed significantly. In particular, [234] addressed the field applications of an ASV to simultaneously perform two tasks: underwater acoustic-source searching and underwater terrain-geomagnetic field data gathering. The motion was measured using a GPS compass and an attitude heading reference system. The model was programmed to gather underwater terrain and geomagnetic data. However, underwater acoustic data was utilized to validate the LBL ANS approach, terrain data and geomagnetic data were leveraged to build an underwater geophysical map for the GNS. The experimental results in [234] validated its practical application along with high-precision navigation and mapping missions. Subsequently, [235] was extended from the framework [234] by further integrating power and electrical propulsion, control, communication, and navigation devices for an ASV. In detail, an ASV platform was equipped with a multi-beam echo-sounder, a DVL, a gradiometer, a GPS compass, and an acoustic hydrophone array, along with other sensors and electronic-control units. For surface navigation, way-point tracking and obstacle avoidance were evaluated by the ASV navigation technology. For underwater navigation, acoustic-based simultaneous localization-mapping and terrain-based localization were developed. Based on the field tests conducted in an inland water environment [235], the realistic performance in terms of high-accuracy navigation was confirmed.

In integrated INS–ANS systems, ANSs can provide initial positions to be transmitted to INSs, which leads to the suppression of long-term drift of INSs. Therefore, the navigation precision of integrated INS–ANS systems is significantly improved. For instance, Kepper *et al.* [236] built an extended Kalman filter, including IMU bias estimation and coupled with a range filter, that propagated a kinematic constant acceleration model to determine the position, velocity, and acceleration of small AUVs in UWC networks. Based on a consumer-grade microelectromechanical system (MEMS) IMU and a vehicle's dynamic model velocity with a DVL, the degree of bounding positioning error of AUVs was evaluated. Subsequently, by applying a minimal navigation strap-down sensor suite and a single beacon one-way-travel-time LBL ANS, the reported navigation solution in [236] possessed the power consumption and cost degradation, allowed applicability, and accuracy threshold comparable to existing methods. In [237], a condition-adaptive gain extended Kalman filter algorithm was designed for AUVs in an USBL ANS–INS integrated navigation subject to uncertainties of UWC networks. Through [237], the long voyage of sea-trials in the South China Sea verified the superior performance of the proposed method in terms of the robustness, smoothness, practicability, and a very effective trade-off between accuracy and computational load. Furthermore, [238] introduced an interacting multiple model and unscented Kalman filter aided strap-down INS–USBL ANS. The proposed methodology was constructed via two key pillars: (*i*) the transponder position, level-arm, and misalignment angle were simultaneously estimated by using the slant range, USBL inclination angles, and depth information from the depthometer; (*ii*) an interacting multiple model and unscented Kalman filter algorithm were applied to mitigate the decreasing calibration precision caused by the single filtering parameter under complex UWCs. Simulation results in [238] indicated that the proposed methodology earned a faster convergence rate and better calibration results than other existing solutions, as well as maintained its robustness even when the observation quality varied. Wang *et al.* [239] presented a robust Student's *t*-based Kalman filter for a strap-down INS–USBL ANS integrated system. The proposed prototype system was first constructed using an IMU and an USBL acoustic array in an inverted configuration. Following that, an improved robust Student's *t*-based Kalman filter was designed with a degree-of-freedom parameter to efficiently address the acoustic outliers in the measured range and direction information. Finally, both the mathematical simulation test and field trials in [239] were performed to demonstrate the superiority and feasibility of the proposed mechanism. In [240], the authors introduced a novel scheme using the Dempster–Shafer theory augmented by least squares-support vector machines and a virtual DVL signal estimation method to perform navigation missions of an integrated system that consisted of strap-down INS and USBL ANS. The experimental results demonstrated its effectiveness in terms of long-term missions and high accuracy. Recently, Zhang *et al.* [241] reorganized Student's *t*-based Kalman filter with adaptiveness and robustness for the existing strap-down INS–USBL ANS integrated navigation systems. In the designed model, the adaptiveness was achieved by estimating the unknown measurement noise statistics via a variational Bayesian approximation, whereas the robustness was obtained by handling the Student's *t*-based measurement outliers. The superiority and feasibility of the proposed methodology were confirmed via both simulations and experiments.

In Table 6, we summarize the main algorithms and/or remarks of the state-of-the-art UWC navigation frameworks, where the columns entitled "Terr" and "Geom" determine the terrain-aided GNS and geomagnetic-aided GNS classifications, respectively.

3.7. Security and Privacy Protection

Unlike the security and privacy requirements of terrestrial and aerial wireless networks, those for UWCs are different because of the particularities and characteristics of aquatic environments and necessitate some special constraints, which mainly comprise following objectives [6]:

- *Confidentiality:* Preventing unauthorized nodes from capturing sensitive data transmitted over the network.
- *Data integrity:* To ensure that the received data is not altered or interceded by unauthorized nodes.
- *Authentication:* Authorizing users to utilize the network resources or perform the communication legitimately.
- *Non-repudiation:* To ensure that the sender cannot deny what has been sent by themselves, which provides proof of the data's origin and integrity.

The security and privacy issues of underwater networks to fulfill the aforementioned objectives can be categorized into cryptography management, trust management, localization security and privacy, and routing security.

3.7.1. Cryptography Management

Cryptography enables sensitive information to be delivered in insecure networks, which requires constructing and analyzing protocols that prevent unauthorized users from reading private data. In [242], a fully hashed Menezes–Qu–Vanstone key agreement protocol was proposed to enable secure UACs, in which two honest parties can share a common secret session key starting from an authenticated public key. The experimental results in [242] have confirmed that not only the network security but also the implementation gains in terms of computational time and energy consumption. Furthermore, Ghannadrezaii *et al.* [243] investigated the vulnerabilities of the Janus-based flooding routing protocol in a hybrid cellular/ad-hoc topology for UACs, and suggested applying a light-weight data encryption and the elliptic-curve Diffie–Hellman key agreement to enhance the communication security through its secret key and large-sized encrypted packets. In [244], a novel three-tier framework, called SenseVault, was proposed for securing data collections in UWC networks. Particularly, (*i*) a cubic cluster formation and cryptographic hash functions were leveraged to derive secret keys for the participating node authentication; (*ii*) a light-weight node revocation and the tripartite cooperation update scheme were utilized for an authentication key update; and (*iii*) a virtual phase shift deterministic quantization was utilized to secure the generation of secret keys. Subsequently, a hierarchical identity-based signcryption (HIS) technique for UWC networks was considered in [245]. In particular, HIS adopted both the signature and encryption processes in a single logical step and the private keys for the network nodes are generated based on the node's identity. This study reported that the HIS scheme outperformed elliptic-curve cryptography-certificate authority [246], group and layered key management [247], and addition of matrices [248] algorithms in terms of energy consumption and time cost while maintaining the same security functions. [249] developed a new deterministic key distribution mechanism for UAC networks, which yielded that for shared-key discovery, it broadcasted minimal or no information

Table 6: Summary of state-of-the-art UWC studies on navigation.

Ref.	Year	INS	ANS	GNS		Algorithms/Remarks
				Terr	Geom	
[212]	2019	✓				Characteristic parameter matching algorithm with particle filter and gravity anomalies
[213]	2019	✓				Extended Kalman filter algorithm with parallel tracking, parallel mapping, and IMU data
[214]	2020	✓				Guidance-navigation-control cooperative missions
[215]	2021	✓				Improved particle filter-based matching algorithm with gravity sample vector
[216]	2021	✓				Underwater gravimetry method with INSs and depth gauge under the trajectory constraint
[217]	2020	✓				Tightly integrated navigation method with strap-down INS, DVL, and pressure sensor
[218]	2021	✓				Deep learning-based integrated navigation algorithm with robust Kalman filter and NARX
[219]	2017		LBL			Measurement occurrence frequency distribution graphs
[220]	2018		LBL			Closed-loop operation with miniature, low-cost SandShark AUV, and acoustic modem
[221]	2018		USBL			Fully dynamic vehicle process model
[222]	2018		USBL			Combined control, communication, and navigation
[223]	2018		USBL			DVL, null-space least squares parameter identification method, fully nonlinear second-order six-degree-of-freedom dynamic process model
[224]	2018		LBL			Student's *t*-based extended Kalman filter, DVL, PHINS
[225]	2018				✓	Rigid magnetometer
[226]	2020				✓	Deep learning-based adapted motion search strategy
[227]	2020				✓	Geomagnetic gradient-assisted evolutionary algorithm
[228]	2020			✓		Terrain-aided position confidence interval model
[229]	2020			✓	✓	Terrain adaptive particle filter, observation models for each geophysical sensor, constructed both terrain and geomagnetic field strength maps
[230]	2018	✓		✓		Multipath parallel iterated closest contour point algorithm
[231]	2018	✓			✓	Magnetic-based GNS algorithm
[232]	2018	✓		✓	✓	Sequential estimation algorithm with complementary profile correlation method
[233]	2019	✓		✓	✓	Rapidly-exploring random tree method, sequential estimation algorithm, path-following controller
[234]	2018		LBL	✓	✓	Underwater acoustic-source searching, underwater terrain-geomagnetic field data gathering
[235]	2019		LBL	✓		Way-point tracking and obstacle avoidance algorithms for surface navigation, acoustic-based simultaneous localization-mapping, and terrain-based localization for underwater navigation
[236]	2019	✓	LBL			Extended Kalman filter, consumer-grade MEMS IMU, vehicle's dynamic model velocity with DVL, minimal navigation strap-down sensor suite, single beacon one-way-travel-time LBL ANS
[237]	2019	✓	USBL			Condition-adaptive gain extended Kalman filter algorithm
[238]	2020	✓	USBL			Interacting multiple models and unscented Kalman filter algorithm
[239]	2020	✓	USBL			Robust Student's *t*-based Kalman filter
[240]	2021	✓	USBL			Dempster–Shafer theory augmented by least squares-support vector machines, virtual DVL signal estimation method
[241]	2021	✓	USBL			Student's *t*-based Kalman filter with adaptiveness and robustness

at all, leading to enhanced network security and privacy. Furthermore, the proposed mechanism ensured that any two authorized nodes could share common key(s) with 100% probability. In addition, a secure authentication with protected data aggregation method for UWC networks was employed in [250], in which the cluster head is authenticated by the gateway to avoid compromised data, and the participating node within this cluster securely handled its data via encryption. The results of this study revealed that the proposed methodology offered security improvements while reducing delays and energy consumption.

3.7.2. Trust Management

Trust management frameworks (TMFs) are related to the development of some reliable models or technological solutions to address the insecurity and lack of privacy in UWC networks. For example, Jiang *et al.* [251] and [252] proposed a novel TMF based on cloud theory to solve the uncertainty and fuzziness of UAC networks. These studies reported that the proposed model improved the detection accuracy of malicious nodes, successful rate of networking communications, and network lifetime. Nevertheless, it required the position information of network nodes, which was a major drawback for network security. To address this issue a TMF based on multi-domain metrics and a cloud model without requiring the position information of UAC networks was proposed in [253]. A trust model defended against attacks using machine learning, whereas a cloud model addressed the uncertainty of harsh network trust. By combining two frameworks, the proposed model combated the fuzziness and randomness of uncertainties as well as greatly improved trust management. Furthermore, Han *et al.* [254] introduced a synergetic TMF based on the support vector machine to predict the accurate trust value for UAC networks. Three kinds of trust evidences and the mechanism of double cluster heads were also presented to reflect most of the malicious attacks, leading to enhanced network security and lifespan. In [255], a new anomaly and attack resilient TMF was investigated for UACs, which was referred to as ITrust. The proposed ITrust model could detect defective nodes effectively and achieved high detection accuracy by considering two phases, including (*i*) obtaining the trust metrics (i.e., data trust, communication trust, energy trust, and environment trust) and (*ii*) evaluating the derived trust dataset by utilizing the isolation forest algorithm. Subsequently, Su *et al.* [256] adopted a new TMF based on fast link quality assessment to obtain stability and accuracy for the node trust evaluation in UAC networks, which was suitable for the limited energy and computing ability scenarios. Furthermore, a TMF with the multi-armed-bandit-based hierarchical defense learning algorithm was presented in [257] to combat the intelligent attackers and protect UAC links. As reported in [257], based on the optimal spoofing scheme and a strategy that the identities of network nodes were changed periodically to hide the critical routing paths, it misled the attackers and then alleviated the potential threats from invaders.

3.7.3. Localization Security and Privacy

Location estimation is one of the crucial components in source detection and tracking applications as well as for performing network communication. Without the location information, an UWC network cannot identify the best relay node(s) to forward data or define the best route. Localization security and privacy in UWCs allow a network to determine the location of participating nodes even when malicious attacks are present. Specifically, [258] designed a modified secure localization algorithm based on the well-established gradient descent method to remove the misleading information in UWC networks. The numerical results in [258] have shown that, based on the proposed scheme, the authorized nodes can securely cooperate with each other, leading to the localization estimation error degradation, network lifetime improvement, and significant energy saving. In [259], a TMF-based adaptive neuro-fuzzy inference system was proposed to evaluate trustworthiness and improve location privacy of UWC networks. By utilizing the Markov decision process and fuzzy interference learning rules, the authorized nodes can conduct the trust behavior of forwarding subsequent nodes without leaking the location information, and then successfully eliminate malicious attacks. Furthermore, a location privacy-preserving scheme proposed in [260] has been demonstrated to provide effective protection of localization in UWC networks. With the construction of random fake paths in the directed routing phase, the proposed method can interfere with the attackers' tracking, offer high safe-time, and strengthen the location privacy protection. Wang *et al.* [261] adopted the node collaboration-based method and semantic encapsulation conception to prevent the adversary from recognizing the precise geometric locations of the users effectively in UAC networks. In [262], a novel stratification-based source location privacy strategy was employed for UACs, where fake data streams and fake source nodes were incorporated into the network cluster structure to render the adversary's estimation inaccurate. Furthermore, a privacy-preserving localization protocol utilizing DRL for estimators was further adopted for UWC networks in [263], where neural networks are trained to assist the agent(s) to obtain the global localization optimization solutions in real-time manner. The proposed scheme has been demonstrated to (*i*) effectively hide the private position information of network nodes, (*ii*) provide the optimal solution for nonsmooth and nonconvex localization problems, and (*iii*) substantially enhance the estimated location accuracy.

By considering both the location privacy and asynchronous lock problems, Meng *et al.* [165] proposed a privacy-preserving asynchronous-localization algorithm with a ray compensation strategy for UWC networks. The experimental and simulation results have revealed that the proposed scheme can not only hide the position information of network nodes but also eliminate the asynchronous clock's impact. Subsequently, in [264], privacy-preserving summation and privacy-preserving diagonal product algorithms for location estimators in conjunction with the asynchronous-localization protocol were designed for UWCs, where the outstanding performance in terms of localization tasks, position information's leakage avoidance, asynchronous clock elimination, and estimated location accuracy were confirmed. To further enhance the performance in [165] and [264], an advanced integrated model was investigated for UWC networks in [265], where a ray compensation strategy was incorporated into location estimators that utilize a RSS-based detection strategy.

3.7.4. Routing Security

In UWC networks, the participating nodes must exchange information with each other to construct the network topology, which is required to perform one of the routing protocols (i.e., reactive, proactive, and hybrid). Routing security involves secure routing protocols and secure data forwarding, where an UWC network can not only share routing information precisely but also prevent invaders from understanding, modifying, tampering, and dropping the traffic. For example, in [266], a distributed detection and mitigation approach was proposed to combat routing attacks in UWC networks, where a sliding window at each network node was utilized to store and monitor the ongoing traffic. The theoretical model provided in [266] has shown the networking security benefits of detecting malicious activities and increasing the probability of malicious node isolation. [267] investigated a novel agent-based secured routing scheme to discover wormhole resilient neighbors and lead the traffic to follow the secured path in UAC networks. By using the direction of arrival estimation and authentication at agents, the secured neighbors could be determined and the agents facilitated in providing adaptable and flexible services for secure routing. Subsequently, a security protocol suite was also developed with the pairwise key distribution to further enhance the network security. Furthermore, Saeed *et al.* [268] proposed a secure energy-efficient and cooperative routing protocol to not only maximize the network lifespan but also combat routing attacks for UWC networks. The research helps readers to realize the impact of security attacks on UWCs and further demonstrates their outstanding performance in terms of transmission loss, throughput, energy tax, latency, and number of alive nodes. Additionally, to defend against neighborship attacks (typical dominants are wormhole attacks and sybil attacks [6]), which establish fake neighbors to divert normal traffic to malicious nodes in UWC networks, the measurement frameworks have been examined in [269] and [270]. Specifically, in [269], the detection of wormhole attacks in UAC networks was efficiently evaluated through azimuth measurement and distance outliers. In [270], an integrated framework between blockchain and TMF was adopted to detect sybil nodes in UWC networks effectively, where the machine learning-based hidden Markov model was utilized to evaluate. The information about node behaviors and the obtained trust values was stored in the blocks of the blockchain. Any other network nodes could check the blockchain status and sense the trust values without re-computing. Therefore, any sybil attacks attempting to copy legitimate identification was detected.

A summary of state-of-the-art UWC contributions to security and privacy protection is presented in Table 7.

3.8. Lessons Learned

This section reviews key technological pillars for heterogeneous multi-access UWCs, where each aspect can show their individual solid lessons as follows:

- First, Section 3.1 presents existing studies, primarily focused on submarine cable support for UWC integration into 6G networks. When terminal transmissions with direct wireless links are very challenging because of the high attenuation characteristics of underwater environments, the submarine cable can be leveraged as an effective support solution to reduce the UWC distance, leading to a substantial improvement in UWC performance. Applicable network integration of cable-assisted communications and UWCs into 6G infrastructures is depicted in Fig. 10. In addition, some effective cost-saving methods and performance optimization for submarine cables have also been provided in this section.

- Second, the considerable tradeoffs among long-distance propagation, high data rates, and high communication reliability for UWC networks have been described in Sections 3.2, 3.3, and 3.4, respectively. We observed that RF UWCs and UWOCs can offer a significantly higher data rate in short-range communications, whereas UACs provide the opposite behavior (i.e., a long transmission range with low data rate and high latency). Channel properties for UAC, RF UWC, and UWOC attenuation are illustrated in Fig. 4, Fig. 5, and Fig. 6, respectively. We note that the selection of which kind of classification will be determined based on the initial purpose of communication, where Table 3 can be utilized as a reference.

- Third, Section 3.5 utilizes the formation control perspective in UWC networks to fulfill UAV tasks with better scalability, flexibility, and adaptability, where the cooperative control for AUVs to follow a predetermined trajectory is performed while maintaining a desired relative network architecture. Here, a comprehensive review of formation architectures and control strategies has been provided. We observe that the individual classification of both formation architectures and control strategies has different advantages and disadvantages, as summarized in Table 4. However, the drawbacks of each architecture are relative and can be remedied with appropriate designs, a combination of some kinds of formation control strategies is encouraged to satisfy multiple missions flexibly.

- Next, the design capability of localization and navigation strategies in UWC networks has been reviewed in Section 3.6. Specifically, localization algorithms are investigated for positioning estimation of network nodes (or even obstacles) aiming to serve underwater applications that require the sensed data with location information. We observe that when a localization algorithm is computed at a central level using globally collected information, it is referred to as a centralized classification. By contrast, a distributed localization algorithm is executed individually at each sensor node. In addition, the time synchronization problem should also be considered to eliminate the impact of clock skew and clock offset phenomena. Furthermore, underwater navigation algorithms perform the processing techniques of monitoring and controlling the AUV movement in UWC networks, which are categorized based on their own principles and features (i.e., inertial, acoustic, geophysical). Integration of some navigation strategies is also beneficial in capturing the strengths and eliminating the drawbacks of each approach. Some recent UWC frameworks on localization and navigation are summarized in Table 5 and Table 6, respectively.

- Finally, Section 3.7 describes the security and privacy protection for UWCs. As UWC networks are expected to fulfill the security and privacy objectives (e.g., confidentiality, data integrity, authentication, and non-repudiation), designing algorithms for cryptography management, trust management, localization security, and routing security deserves to be investigated. A summary of state-of-the-art UWC contributions to security and privacy protection is presented in Table 7.

4. Underwater Application Scenarios

This section presents state-of-the-art underwater application scenarios with three subcategories (i.e., military, science, and industry) in the context of utilizing autonomous vehicles and sensors for a specific application.

4.1. Military Applications

Developing military applications is an interesting but risky business. Consequently, the most novel technologies are in researches for the purpose of enhance war-fighting capabilities and defensive ability [271]. AUVs are used in a number of missions in navy forces. These devices are used to not only actively attack but also defense enemy invasions. Some AUV missions presented in this article are mine countermeasure (MCM), anti-submarine warfare, and maritime situational awareness (MSA).

Table 7: Summary of state-of-the-art UWC contributions to security and privacy protection.

Aspect	Reference	Year	Network	Algorithms/Remarks
Cryptography management	[242]	2017	UAC	Fully hashed Menezes–Qu–Vanstone key agreement protocol
	[243]	2018	UAC	Janus-based flooding routing protocol's vulnerabilities, light-weight data encryption, elliptic-curve Diffie–Hellman key agreement
	[244]	2018	UWC	SenseVault, cubic cluster formation, cryptographic hash function, light-weight node revocation, tripartite cooperation update scheme, virtual phase shift deterministic quantization
	[245]	2017	UWC	HIS algorithm
	[249]	2018	UAC	Deterministic key distribution mechanism with shared-key discovery
	[250]	2020	UWC	Secure authentication with protected data aggregation method
Trust management	[251, 252]	2017	UAC	Novel TMF based on cloud theory with uncertainty and fuzziness consideration
	[253]	2018	UAC	Novel TMF based on multi-domain metrics and cloud model without requiring position information
	[254]	2019	UAC	Synergetic TMF based on support vector machine, trust evidences, double cluster heads
	[255]	2020	UAC	ITrust model with anomaly and attack resilient TMF, isolation forest algorithm
	[256]	2020	UAC	Novel TMF based on fast link quality assessment
	[257]	2021	UAC	TMF with multi-armed-bandit-based hierarchical defense learning algorithm
Localization security and privacy	[258]	2018	UWC	Modified secure localization algorithm based on gradient descent method
	[259]	2019	UWC	TMF-based adaptive neuro-fuzzy inference system
	[260]	2019	UWC	Location privacy-preserving scheme
	[261]	2020	UAC	Node collaboration-based method, semantic encapsulation conception
	[262]	2020	UAC	Stratification-based source location privacy strategy
	[263]	2020	UWC	DRL-based privacy-preserving localization protocol
	[165]	2020	UWC	Privacy-preserving asynchronous-localization algorithm with ray compensation strategy
	[264]	2020	UWC	Location estimators based on privacy-preserving summation and privacy-preserving diagonal product algorithms, asynchronous-localization protocol
	[265]	2020	UWC	Location estimators based on ray compensation strategy, RSS-based detection strategy
Routing security	[266]	2017	UWC	Distributed detection and mitigation approach with sliding window
	[267]	2017	UAC	Agent-based secured routing scheme, direction of arrival estimation, agent authentication, security protocol suite with pairwise key distribution
	[268]	2020	UWC	Secure energy-efficient and cooperative routing protocol
	[269]	2021	UAC	Detection of wormhole attacks through azimuth measurement and distance outliers
	[270]	2021	UWC	Integrated framework between blockchain and TMF, machine learning-based hidden Markov model

4.1.1. Mine Countermeasure

MCM missions involve tasks such as ensuring the safety of national harbors and channels, as well as actively exploding sea mines before a trike.

Using sonar detection technique for unmanned surface vehicle (USV), Yang *et al.* developed an autonomous control technology of naval MCM problem [272]. Under investigating the minesweeping tasks in unfamiliar and complex sea scenarios, a designed USV's shortest path planner with real-time moving obstacle avoidance using hierarchical reinforcement learning was verified in terms of output parameters including maximized cumulative reward value and the map exploration rate.

The solution using MCM vessels in [272] is difficult to deploy for bottom mines (i.e., mines sitting on the seabed). An automatic target recognition (ATR) system using high-resolution forward-looking sonar for MCM mission deployed AUV onboard to perform detecting seafloor mine-like objects was investigated in [273]. The proposed ATR system composes of three main modules: a detector, one or more classifiers, and a probabilistic grid map. The grid map not only enhances the accuracy for the detector but also combines multiple detections into one. In addition, novel convolutional neural networks (CNNs) which required limited amount of trained sonar data were used for both detection and classification phases. According to the experimental results, the proposed ATR can relocate all targets if the relevant thresholds are aggressively set.

To handle buried mines, an effective continuous angle alignment-based solution is extending the detection range for the magnetic anomaly detection (MAD) [274]. With this solution, the false alarm rate was reduced compared to conventional magnitude-based. In case of the buried mines attached thermal sensors, a special design for unmanned underwater vehicles hull was presented in [275]. The hulls are covered by phase change materials as thermal insulation.

4.1.2. Anti-Submarine Warfare

This part focuses on methods for vehicles actively and effectively hunt and chase or destroy submarines presenting in confined waters.

An active cooperative combat system was designed to attack an underwater target on purpose using two kinds of heterogeneous vehicles [276]. In an underwater target strike mission, an unmanned aerial-aquatic vehicle (UAAV) and an AUV share a coordinated path planning. After detecting the moving underwater target, the flying UAAV dives into the water and communicates with a standby AUV to send the target's position information. Then, coordinated paths are computed by both vehicles

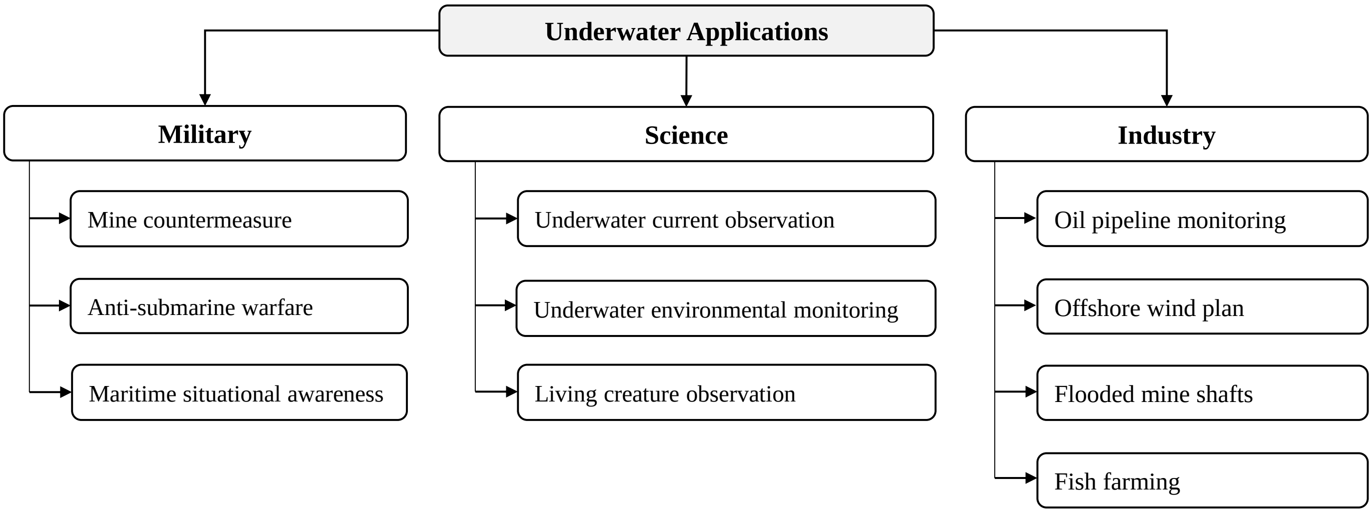

Figure 9: Schematic framework for underwater application scenarios.

to attack it simultaneously with the minimum terminal position error. This type of model provides an efficient way in reducing AUVs' time searching because of lack of global search ability.

A novel prediction planning interception method with multiple AUV deployed for harbor security protection was designed to identify and catch dynamically moving intruders [277]. This swarm of AUVs operates in two modes: surveillance and interception. In the first mode, AUVs travel in the underwater environment with static obstacles and ocean current. The second mode is turned when at least one AUV detects the intruder's presence. In particular, each AUV can independently perform the prediction the intruder's next intercept point according to its own speed and the intruder's movement trajectory. At the same time, the swarm of AUVs forms a team to complete interception task through a defined cooperative strategy. Compare to traditional tracking interception method, the proposed method has a higher interception efficiency.

A multi-channel interference based source location privacy protection scheme was proposed to conceal underwater submarine locations in an acoustic sensor network [278]. This scheme aims to protect the transmission of the source packets by exploiting the multi-channel interference, thereby resisting the eavesdropping attack as well as preventing eavesdropping. Moreover, a fake packet technology combines with the time slot control technique for reducing in the energy consumption and in packet collision. Working under this scheme, the adversary fails to track back the source packet to find the source location. The proposed scheme was assessed by metrics including safety time, energy consumption.

4.1.3. Maritime Situational Awareness

This part concerns with architectures of systems that can provide real-time information about a happening combat or site inspection (i.e., MSA), and techniques to enhance the ability of entities used for surveillance and reconnaissance.

A comprehensive system for a coastal surveillance MSA application was developed with multiple devices [279]. This system provides contextual information over a wider area by exploiting the synergy between global view. This system is a sensorized hybrid robotic network, which is comprised of an onshore camera, specific robots (i.e., Wave Gliders) equipped with passive sonars, and data fusion defined kinds of complex events. The Wave Gliders also include satellite sensors for use while working independently, instead of in cooperative mode. They emit low noise during navigation and are difficult for radar/optical sensors to detect. Their hybrid physical architecture consists of two parts (i.e., sea-surface, and submerged) attached together via a tether. The sea-surface parts act as communication relay nodes, supported by radio modules, between the underwater robots and the command and control center.

An ontology of a MSA using heterogeneous sensor network [280] addressed the information requirements of MSA use case, where different situational views supplied by sensors and platforms are combined with big data analysis, to obtain real-time information about a situation for maritime security. In this ontology, multiple classes of sensors, events, observation were defined. In addition, data collected by global ocean networks as well as observed events may be easily integrated in a MSA application through this proposed MSA network.

To ensure the security of data transmitted among entities in a underwater wireless sensor network (UWSN) for frontier surveillance in naval operations, a security mechanism based on symmetric-key cryptography was presented [281]. The entities involved in this network are bottom-sea anchored sensors, floating buoys with radio links to submarines, AUVs, ships. When detecting the presence of other devices in its sensing area, the sensor performs an authentication process or seeks help from the nearest base station (e.g., on-shore base station, off-shore base station). The proposed mechanism was tested under attacks including denial-of-Service attack, masquerade, replay, Sybil, and secret guessing attack. Moreover, the communication cost, computation cost, and the storage cost, energy consumption are calculated and compared with other security protocols; the results showed that it consumes less computational, communication, and storage overheads and can be deployed efficiently in naval operations.

Kim *et al.* proposed a novel signal processing algorithm applied electric field method used in detecting underwater moving target objects equipped acoustic stealth technology under shallow water circumstances [282]. The effectiveness of the proposed algorithm was validated in terms of signal to noise ratio and root mean square error metrics of the target response. Moreover, a real field experiment was conducted to affirm the theoretical analyses.

4.2. Science Applications

4.2.1. Underwater Current Observation

Investigating the surface properties of ocean currents including trajectory, diameter and center point is an interesting research direction. Based on the collected and processed data, marine scientists can characterize and investigate the principle of the oceanic physics to obtain accurately predictive solutions for global problems such as global climate, atmosphere, and ecological environment changes.

The study [283] contributed two methods based on oceanic glider type mobile platform with an attached current meter for ocean current observation problem. From the design perspective, these methods aim at enhancing accuracy of the measured results as well as expanding the glider based framework to broader ocean areas. In particular, the first method handles the optimal installation position of the single point current meter based on compensated inversion method, and the second solution utilizes the ocean currents' physical properties to build a reliable current velocity observation system. The theoretical proposals verified in an onsite sea trial showed that the measurement accuracy was improve by 70% by average as compared to conventional inversion method by solving the acoustic Doppler to current profiler and can be used for non-pure water environment, whereas the second method can be deployed in underwater environment with high purity.

4.2.2. Underwater Environmental Monitoring

Underwater chemical contaminants and diverse trash can be harmful for creatures living both on-land and underwater environments [284]. Therefore, detecting exactly underwater harming sources or polluted condition of the water can help to resolve the underwater pollution problem. In particular, based on the information collected from underwater monitoring systems such as types of debris materials (e.g., aluminum cans, ceramic plates, plastic bags) or leaking chemical properties of contaminants [285], or variation in plankton living in the researched environment [286], appropriate solutions for cleaning up the existing pollutants and/or preventing pollution can be applied appropriately.

A large-scale autonomous marine pollution monitoring system model consisting of mobiles AUVs, surface stations (i.e., instrumented buoys mounted in specific locations, vessels), and underwater sensor stations in fixed positions was presented in [285]. In this model, the AUVs transmit collected data and forward to surface stations for further research activities. By using optical sensing, the UAVs can classify pollutants in underwater environments, particularly in oceanic environment. To overcome the limitation of AUVs' computational resources, a collaborative algorithm is applied to the AUV network. Apparently, this model can be utilized for many general purposes on transmitting accurate information about the extent and characteristics of pollutants.

Long-term in situ detection of microplastics on the seabed can help to find out sources of microplastics in the drainage systems, and this is helpful in providing reasonable solutions for effective microplastic control as well as environmental protection projects from government. Classified into micro-sized polluters, microplastics also present in various kinds of materials, for examples, polyethylene, polypropylene, polystyrene, and polyethylene terephthalate. Therefore, the methods for searching and identifying microplastics are different for each type. Recently, some studies on microplastic detection proposed underwater imaging systems. These imaging systems are designed with progressive techniques in image processing (e.g., hyperspectral imaging [287], digital holography imaging [288] attached to appropriate classification algorithms. Many diverse classifiers are used for microplastic identification, e.g., support vector machine, neural network, least squares–support vector machine, and partial least squares–discriminant analysis [287]. Additionally, the accuracy of in situ microplastic detection is improved by applying underwater spectral image correction model. The proposed system can identify up to six types of microplastics. However, the authors conducted the laboratory experiment only with water of 0.3 m depth with a simulated tank of water.

Carbon Capture and Storage (CCS) is one of techniques to decrease CO_2 quantity in the atmosphere. In this technique, CO_2 is captured from point source emitters, compressed and then buried in geological formations in offshore storage sites. To assess the environmental impact of ocean storage of CO_2 as well as to understand the mechanisms of CO_2 leakage from seabed into turbulent seawater, numerical models were proposed in different scales (i.e., small and large scales), from meters up to kilometers. Compared to the large scale models, the small scale models and laboratory experiments, which can be relatively extrapolated to larger scale situations, are less economic and environmentally expensive [289]. A small-scale model-integrated system functioned as a 3D comprehensive solution for physicochemical detection and CO_2 leakage analysis in coasted waters was proposed in [290]. In this system, the authors combined three reciprocal models namely PLUME, FVCOM, and ERSEM. The PLUME simulates the interactions of released CO_2 bubbles with seawater, the FVCOM models the cascading hydrodynamics such as tides, currents, and turbulence. Some outputs of the combination of the PLUME and FVCOM are inputs of the ERSEM carbonate system. This model was applied by two in-situ experiments which were set on the tidally dominated north-west European continental shelf under different aims. The first experiment resolved the anomaly detection (i.e., CO_2 gas leakage) via leakage rate measurements. The input parameters include site-specific data (i.e., location, bathymetry, salinity, temperature, currents), and the release rates to the seawater, bubble sizes, and pockmark distribution map. The second experiment obtained the knowledge gained from the first experiment to provide cost-effective environmental monitoring and seepage quantification techniques. In particular, remotely operated vehicles, AUVs, optical landers were involved in mapping the investigated environment [291]. Furthermore, to measure the value changes of pH for quantifying CO_2 release the water column, novel autonomous lab-on-chip sensors were mounted on AUVs.

4.2.3. Living Creature Observation

Observation the changing of living creatures can help scientists to assess the underwater environment quality.

In [286], an onshore monitoring system about the in situ seawater mesoplankton using optical imaging technique via imagers. These imagers are placed in the water and hanged below approximately 1.5-3m under buoy-borne rafts. The imager system sends raw captured images to terrestrial remote server via 4G wireless links. Subsequently, images are post processed by a deep learning model deployed in the remote server functioning as cloud computing-based data center. To collect documentary file about the variation of the mesoplankton community structure in a coastal region, 1 545 187 images about plankton and suspending particles automatically classified up to data set of 90 categories containing 46 804 cropped regions of interest of particles, bubbles, and various plankton. The experiment showed that the data set shift is the result of the emergence of new species related to the temporal and spatial variations of the plankton.

Similarity, Mallery *et al.* [292] designed a cost-effective robotic sensor system for water quality measurement by examining water particles in size, concentration, and identification. Two main parts are composed in this system for individual purposes. Particularly, a digital in-line holographic microscope (i.e., sensor) is a set of battery, computer, laser, and camera to obtain high resolution measurements. Next, this microscope is integrated into an autonomous amphibious vehicle to enable the system to three-dimensional motion throughout a large environment of interest. This designed system was tested for its utility in real-world scenarios via an in-situ measurement of particle concentrations in South Center Lake in Chicago, Minnesota. It was deployed at a maximum depth of 5.5m, stayed there in three hours and then returned to the surface to transmit recorded and stored images via 801.11 wireless connection for further processing externally.

Understanding underwater ecosystem alteration can be attained by monitoring the size of key indicator species of fish. A cost-effective large fish species identification system based on fish size detection including underwater infrared cameras can operate in both shallow and deep waters effectively and efficiently [293]. With determined configurable minimum fish-size parameter, the recording process can be triggered to record videos for capturing the presence of large fishes over long time periods. Moreover, by applying deep learning-based solutions for object/movement detection models, the camera system connects to the cloud computing platform for post-processing. In addition, an software operating on proposed computer vision system was designed to both facilitate a minimal hardware configuration and consume low power. There are five algorithms concurrently applied in this software including (*i*) brightness scenario classifier, (*ii*) deep learning object detection, (*iii*) unsupervised object detection, (*iv*) movement detector, and (*v*) size analyzer. This system was tested in real deployment scenarios under different depth and light conditions. New finding related to food sources for giant sponge-rich benthic community found in ice-sea seamounts of Langseth Ridge within the Central Arctic was presented in [294]. In particular, Morganti *et al.* analyzed collected samples by combining advanced peculiarity techniques such as composition assessment of sponge tissue, isotope ratios of putative suspended and sedimented particulate food sources, and omics techniques. To perform such research in harsh conditions (e.g., weather, deepsea), a specialized research vessel named Polarstern can release equipment devices from its bottom. Before being launched into the sea, IXSEA POSIDONIA acoustic transponder for geo-referencing to track underwater vehicles and instrument positions is mounted to underwater devices. Devices utilized for the under-ice extreme environment exploration research include Nereid Under Ices which can be configured in both AUV mode or remotely operated vehicle mode (ROV) with an appropriate camera for each mode. In ROV configuration, the vehicle was attached with a Kraft Telerobotics 7-function electro-hydraulic manipulator arm and sampling equipment. In AUV mode, detailed and high-resolution bathymetric map of the seafloor was automatically achieved with in situ sensors mounted high on the forehead.

4.3. Industry Applications

This section describes commercial applications in which sensors and AUVs or their collected data are used to reduce the company's expenditure. In addition, some applications are aimed for increasing profit.

4.3.1. Oil Pipeline Monitoring

Marine oil pipeline system is one of economical solutions for offshore oil transportation. However, this system can be recurrently collapsed because of the corrosive effect of seawater as well as the complexity and diversity of marine environment. Therefore, underwater pipeline systems need to be protected via discovery method such as leakage location detection. To achieve this, the information of damaged positions can be collected by sensors in UANs and then it is timely forwarded to sinks for further processing. Apparently, this information can be eavesdropped by attackers who attempt to steal oil from the oil leakage. To solve this problem, a network architecture used for hiding the positions of the source sensors was presented in [295]. In particular, underwater sensors are placed randomly along with the submarine pipelines connecting oil wells (on the seabed) and oil storage vessels (on the surface). In addition, a multi-AUV system is used for transferring data collected from these sensors near the seabed whereas the sensors near the surface send data to a sink through multihop transmission. After detecting the damaged location, a sensor becomes the source and sends the incident location to the sink. To ensure the potential attackers cannot determine the source node, a cluster including fake sources with the real source node centered is formed anonymously. In this cluster, fake sources are chosen to forward fake data. The disguised AUVs are also set to stop at the fake sources. In addition, an algorithm for data delivery in aiming at reducing energy consumption was proposed. The simulation results showed that the performance of proposed system improved in terms of safety time and delay.

A solution for oil spill detection in deep water aimed at reducing the economic loss through leak position estimation was proposed in [296]. A distributed UWSN comprised of passive acoustic sensors plays a role of leak detection system that is capable of promptly detecting and positioning oil leakages in subsea production systems. The authors investigated two different methodologies for leak detection and four algorithms for leak localization. A realistic case study was conducted on Goliat floating production storage and offloading connected to one subsea production system. In this design, the data represented for leak detection is transmitted from local sensors to a fusion center to provide an estimated position of the leak source by applying localization algorithms including maximum a-posteriori estimation, minimum mean square error estimation, and two heuristic centroid-based algorithms. Next, the reliability of an upgraded spatio-temporal design of this system was analyzed in [297].

4.3.2. Offshore Wind Plan

Offshore wind energy is one kind of green forms of energy and is encouraged by governments [298, 299, 300, 301, 302]. With careful planning, the deployment of offshore wind farms (OWF) can reduce time and cost [303, 304].

A large-scale OWF balanced design for potential site implementation suitability considering both opposing and supporting factors was proposed in [303]. The integrated input parameters are considered, including economics, ecological, and societal consequences of OWF deployment. In particular, these input factors are technological properties of OWF (e.g., nameplate power rating, height, installation, commissioning, maintenance, and decommissioning costs), logistics parameters (e.g., distance to ports, and conservation areas), environmental properties (e.g., wind speed, seafloor type, water depth), ecological parameters (e.g., underwater species and habitats), and societal components (e.g., information about legislative restrictions, expected disturbance to people). Additionally, another work proposed to select the optimum locations for floating wind farm by ranking system based on expert judgments via utilizing Monte Carlo and fuzzy analytic approach [304].

For damage assessment in the operation and maintenance phase, an integrity monitoring approach for subsea power cables characterized a combination of low-frequency sensing-based technique and appropriate machine learning (ML) technique performed by AUV was presented in [305]. This approach provides a novel means for external condition monitoring of multiple types of subsea cables subject to abrasion and corrosion failure modes. Among experimental results of machine learning techniques including support vector machine, logistic regression, and CNNs, the best result in identifying cable type was provided by the third solution with over 95% accuracy.

4.3.3. Flooded Mine Shafts

A cost-effective comprehensive solution using ROV for maintenance and inspection of flooded mine shafts (e.g., coal) was proposed in [306]. This solution is an integration for several commercial elements, including an ROV (i.e., BlueROV2) housed multiple types of sensors, a RasPi camera, and can operate periodically up to 1000 m depth. For remotely inspection and intuitive teleoperation of ROV, the authors developed a graphical user interface by utilizing a commercial ROS 3D visualizer software tool named RViz. Therefore, the depth information as well as the 3D model of ROV and its pose are displayed in the scene for operator. Operating in a very harsh environment (e.g., unexpected obstacles corroded or deformed by the water break under low visibility, effect of water stratification) can provide inaccurate results in navigation and positioning. To enhance the accuracy of underwater robot's navigation, a visual navigation system based on monocular visual odometry algorithm was also developed for pose estimation that could function efficiently with the sensors and camera.

Another spherical designed robot, named UX-1 Robot, used for underwater explorer for flooded mines, was presented in [307, 308]. Its outer shape was chosen to fit with its targeted mines which are old abandoned and flooded European mines. It assigned tasks are exploration motions suitable for flooded mine shafts (e.g., vertical shafts, horizontal tunnels, underground galleries), obstacle detection less than 20m in distances by DLV sonar, resource characterization (e.g., relevant minerals). This robot was practical tested in operational mine fields including Kaatiala mine (Findland), Idrija mercury mine (Slovenia), Urgeirica mine (Portugal) [307], and Ecton copper mine (United Kingdom)[308].

4.3.4. Fish Farming

This part presents two kinds of underwater farming applications including fish farming and aquaculture farming.

A smart fish feeding system applied computer-visioned-based deep learning in determining the time for stop feeding was presented in [309]. Different from other studies that focused on image-based recognition analysis, the solution in this study is based on analyzing the size of the waves caused by fish eating. The system model consists of specific task modules: *(i)* an image sensing module composed of an image sensor (i.e., camera) and a deep learning mechanism, *(ii)* a water quality inspection model deployed by underwater sensors which can monitor multiple parameters (i.e., the oxidation-reduction ability, dissolved oxygen, and pH degree) of water quality, *(iii)* a fish feeder, *(iv)* a signal processing module with two submodules used for control feeding actions as well as further data storage and analysis via 3G/4G cellular network, and *(v)* a server computer responsible for online control. The system was installed and tested in real working conditions for three weeks at an outdoor black porgy pond, and its experimental results showed that an accuracy of up to 93.2% can be achieved.

An implant wireless sensing tag with edge computing was developed in [310]. Particularly, in biotelemetry tag, it functions as an integrated kind of sensor that allow sensing in vivo physiology, behavior, and ambient environment simultaneously. With miniaturized form, it is useful in investigating small animals with high profit value in economy. Moreover, raw data are stored in a flash memory attached to the tag and can be post-processed via acoustic communication over a distance of up to 400 meters. Under experiments for up to four weeks on three kinds of freshwater fishes (i.e., rainbow trout, walleye, and sturgeon) with the designed tag implanted, these tags did not cause severe negative effects on their natural behavior.

An aquaculture fish farm monitoring solution applies to very large farms (>400 hectares) with hundreds of ponds [311]. The authors presented a framework of a hybrid aerial/underwater robotic system in which subsystems were defined. These subsystems exist in 3D (air, underwater, and on-land) positions. On the surface, LoRa communication network connects different components. Underwater elements include submerged underwater sensors. Collected data from sensors will be transmitted to an on-land farm control center via radio links and then will be analyzed by a ML-based water quality prediction model. This model was applied in a real farm with 65 ponds for one month to validate its effectiveness.

4.4. Lessons Learned

Current research trends in wide range of fields of underwater application were investigated in three sub categories: military, research, and industry. Military applications mainly focus on completing solutions for navy forces to enhance the abilities in defense and invasion. In particular, for MCM missions, the proposed solutions are relevant to types and locations of underwater mines. To handle the reconnaissance of enemy submarines, many strategy models combining many kinds of autonomous vehicles (e.g., AUVs, UAAVs, ASVs) were investigated in harbor security protection, deep ocean. The wireless connection types in military applications are mainly acoustic (for underwater section), RF, and satellite (for upper water surface section).

Science applications surveyed in this part focus on findings about nature changes therefore suitable solutions can be adapted. These uses are applied in many academic fields and need specialized as well as interdisciplinary knowledge, e.g., oceanic physics, chemistry, biology, geoscience, bioscience, and environmental science. The mobile UWSNs play a significant role in collecting data, obtaining samples, detecting environmental anomalies (oil or CO_2 leakage, waste microplastics), measuring and quantifying specific substances (CO_2 storage), observing living creatures. Most of the models in this subsection were experimentally deployed with real data.

The industry applications can be found in wide range of fields. Contributions of surveyed papers can be used primarily for cooperations, companies with large-scale production, or exclusive companies. In particular, oil pipeline monitoring can be detected by an UWSN. The concerns of this application types include quick detection strategies, security in leakage positions and source node position, efficiency in cost, and reliability transmission. By contrast, subsea cables of offshore wind plans are High voltage current. Any damage of these cables can lead to a catastrophic disaster for ecological environment of living creatures. Moreover, building a new site of OWF requires massive expenditure. Therefore, the solutions concentrate on managing subsea power cable asset, determining the suitable places for deployment. In addition, aquaculture fish farms with precision agriculture solutions with AUVs and/or fixed underwater sensor network can increase in both the quality and quantity of products.

5. Feasible UWC-Integrated 6G Access Infrastructures

The aforementioned investigation demonstrated the potential of various technologies and developments in 6G access networks to support their envisioned applications, whereas underwater communications were neglected. Therefore, this section aims to shed light on an applicable scenario, where UWC can be integrated into the 6G infrastructure to bridge the gaps.

5.1. On-Shore Interconnections

The on-shore interconnections involve heterogeneous infrastructures at the edge of 6G networks such as terrestrial access (e.g., cables, satellite ground stations, mobile base stations–gNodeB, and long-range wireless communications at low frequencies) and aerial access (e.g., LAPs, HAPs, and satellites). These infrastructures along with their access technologies enable the Internet capability to underwater devices via sink nodes [5]. Here, the sink nodes can be an aggregate router on cable links or a gateway router on ships and buoys. Figure 10 illustrates an overview of these scenarios. Owing to the various technologies supported, the interfaces between on-shore 6G interconnections and sink nodes of UWC are typically specified as the following:

- *Cable interface* defines an aggregation point on the cable routes, which is traditionally terminated at a station on the coast to gather underwater cable links before reaching the Internet via terrestrial cable systems. This interface provides a stable, high-speed connection to underwater devices. However, cable installation under water is costly and inflexible for operation and maintenance. Therefore, this interface is suitable for fixed services and systems such as underwater transmission grids of infrastructure.

- *Cellular interface* connects UWC sink nodes to 6G gNodeBs using the NR wireless access. As the 6G gNodeB supports a broad range of frequencies from sub-6 GHz to THz bands, transmission distances, accordingly, vary from hundreds of meters to several Km. From the view of 6G terrestrial networks, the UWC sink nodes are generally considered normal UEs with data transmission requirements. This interface is appropriate for near-shore underwater services such as sub and quality-of-water sensors.

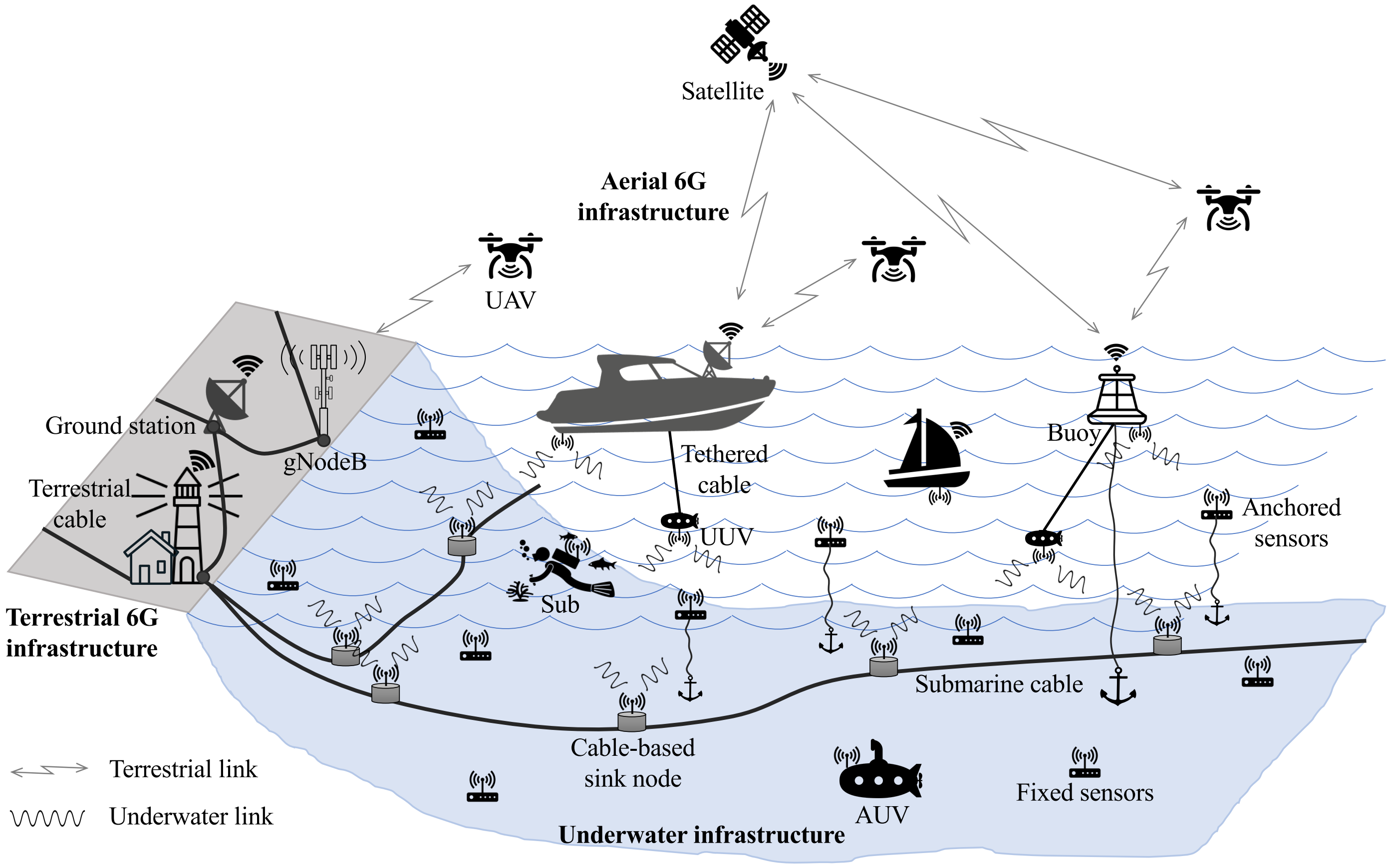

Figure 10: Applicable network integration of underwater wireless communications into 6G infrastructures.

- *Low frequency interface* specifies long-range wireless communications, where an Internet-enabled base station on the shore modulates user information on low-frequency carrier channels. Because low frequencies are utilized, the signals obtain high resistance against attenuation and therefore, achieve a high transmission distance at low data rate. This interface efficiently facilitates critical services on the sea, such as bad-weather warning notification systems and short-message communications.

- *Satellite interface* provides a direct link between an Internet-enabled satellite and a UWC sink node in the form of a two-way satellite ground station (also known as very-small-aperture terminals–VSATs) mounted on a ship or an island tower. Similar to the cellular interface's point of view, the UWC sink node is considered normal user terminal with Internet service requirements. This interface can be useful for critical services or pleasure boats.

- *Relay interface* provides an intermediate medium to either transform original interfaces such as cable, cellular, low frequency, and satellite, into supportive interfaces in a particular UWC system (e.g., cellular (gNodeB)–WiFi (UAV)–sink nodes, satellite–WiFi (VSAT/UAV)–sink nodes, and satellite–tethered cable (VSAT)–sink nodes) or extend the coverage. The relay interface is useful in heterogeneous access environments, where various Internet paths can be unified to provide a single gateway to the UWC system.

5.2. Off-Shore Access Networks

The off-shore access networks are constituted by two major components, including a grid of cable transmission links and underwater ad-hoc systems.

Connected to numerous aggregation routers on the shore, the underwater cable grid establishes a stable transmission infrastructure for UWC systems. Benefiting from the cable grid, various UWC topologies are enabled, such as chain, star, ring, and hierarchical models. Anchor points for each UWC system can be installed along the cables to serve as local gateways (sink nodes) of the system. These local gateways translate between wireless signals used in UWC systems and optical waves transmitted through the cables. Typically, the cable grids can be either extracted as special branches of the submarine cable networks [115] (e.g., deep-sea exploration vehicles) or deployed as separate cable lines dedicated to particular UWC systems (e.g., near-shore water quality measurements).

In underwater ad-hoc systems, one or several sink nodes serve as gateways to provide Internet connections to the systems. The sink nodes can be cable-based anchor points, tethered unmanned underwater vehicles (UUVs), or floating buoys on the surface. Despite being different from terrestrial/aerial ad-hoc networks in operational environments, the underwater networks inherit all the advanced techniques from these ad-hoc networks in terms of routing protocols, system organization, and relative navigation and positioning. Distinctively, wireless communications among UWC devices can be acoustic wave, microwave, RF, and visible light. Owing to different characteristics against attenuation, absorption, and scatter in underwater environments, acoustic wave provides a high transmission range of up to tens of km at a low data rate, whereas RF and laser expose high data rates but low transmission range among these technologies. Thus, the optimal design of wireless communication technologies and network structures mostly depends on the requirements of user services and aquatic conditions [312, 313, 314]. For instance, fixed and stable transceivers may utilize blue laser to obtain a high data rate at a distance of several kilometers. In a short range, RF and tethered cable may support mobile underwater devices with high throughput. Meanwhile, deep-sea exploration should utilize acoustic wave for long transmission range.

6. Open Challenges

Although existing studies have thoroughly addressed manifold aspects of UWC to improve its performance, overcoming future challenges concerning a seamless integration of the UWC as a native component into 6G networks requires further efforts.

Cross-medium communications present a critical challenge to a straightforward integration of UWC into the terrestrial mobile networks owing to water-air boundary. Initial studies [315, 316, 317] discovered that translational acoustic-RF communication (TARF) is feasible by exploiting the pressure changes caused by acoustic waves at the water-air interface and the surface displacement detection using airborne radar receivers. However, adapting these laboratory experiments to real scenarios poses several challenges such as one way transmission (i.e., from underwater acoustic transmitter to airborne radar receiver), ocean wave amplitude, short transmission distance, and misalignment. Moreover, state-of-the-art investigation exposes an achievable standard bitrate of approximately 400 bps [315], which is considered low for a number of applications. However, the cross-medium technologies are still immature, relaying surfaces and components play important roles to bridge the communications between UWC and terrestrial mobile networks.

Submarine cable infrastructure installed at an average ocean depth of 3682 m yields a prospective challenge for cable-assisted communications [318]. The *vulnerability of the cable components* can be caused by many factors, including human (e.g., fishing and anchoring), natural (e.g., tsunamis, seaquakes, and currents), and external factors (e.g., electric grid or land network outage, state failure, and operator bankruptcy). Accordingly, the maintenance of submarine cable infrastructure is more frequent, which entails a huge amount of money for such unexpected scenarios. It also faces the difficulty of replacing or upgrading the cable-assisted system. In addition, because of the wired characteristics, it is limited to serving UWC applications that require high mobility.

In an UWC system, *reliable long-range high-throughput communications* are a major triple-facet metrics needed to promote diverse underwater applications [132, 319, 320]. However, reliability, long range, and high throughput are of a Pareto front, where optimizing an individual metric leads to reductions in the others. In addition, single existing wireless technology cannot support these features simultaneously. For example, acoustic communications are highly reliable over a long transmission range; however, the technology introduces high latency and low throughput. RF transmissions offer high throughput and short-range, owing to high absorption and attenuation, whereas laser beamforming transmissions exhibit very high throughput if no physical obstacles are present and precise alignment is maintained. Although multipath techniques and heterogeneous communications have been investigated to improve the system performance [321], reliable long-range high-throughput communications will remain crucial in future research.

Regarding *formation control*, although all the mentioned works make an effort to overcome theoretical communication constraints, practical experiments receive less attention from the research community. In addition, almost all the theoretical formation control studies in UWCs are made under solid assumptions, which can be impractical. As a result, the development of UWC formation control is still in the early stages. Hence, qualified research with more realistic assumptions is needed. Besides, we also note that AUV formation control performs their work for a long time (up to several months or even several years). Unpredictable disturbances can cause the failure of AUV formation control, requiring the design of robust recovery mechanisms or adopting switching topologies.

In terms of *localization*, to our best knowledge, a low-cost positioning and time-synchronization system with high precision has not been available yet to UWC networks until now. Therefore, UWCs must rely on GPS-free localization or time synchronization. Although the time synchronization problem has been further considered for significant studies on GPS-free centralized and distributed localization to compensate for the clock skew and clock offset phenomena, perfect time synchronization is still challenging in practical UWC applications due to the sound speed variation and long propagation delay. Whilst for navigation, developing INSs with high accuracy, small dimensions, low cost, and low power consumption is, first, challenging for small AUVs. Second, when ANSs utilize techniques related to acoustic signals, they suffer from the limits of underwater acoustic characteristics. Fixed position systems can offer robust ANSs, but they are impractical. In addition, the low update rate and the requirement of external devices for ANSs also limit the usage of this single category. Third, the spatial resolution of geophysical parameters approximated by grid/spherical harmonic series in GNSs is low, which restricts reliable navigation. Consequently, integrated navigation is motivated. However, the developments in both the algorithms and technologies of integrated navigation to improve AUV navigation can expose new infeasible or impractical missions that have been previously investigated. In addition, when some nonlinear filtering algorithms that are more complicated are leveraged in integrated navigation systems, the stability of these algorithms cannot be guaranteed in practice.

Because of the peculiar particularities and constraints of UWC networks, advanced *security and privacy* solutions are difficult and costly to be directly utilized in practical applications. Although a significant number of security studies for UWCs have been investigated, the number of empirical research and experiments is relatively low, such that UWC security and privacy protection are still in an early stage. Besides that, UWC network security is a complex cross-layer issue. For the problem of employing various security technologies among these cross layers, the optimal solution to minimize extra resource consumption is non-trivial, especially for severely resource-constrained UWC networks. In addition, in an aquatic environment, the protection of each underwater node and the detection of compromised nodes are challenging. It is worth noting that the security methodologies are pre-installed on the network nodes. If any participating node is compromised and rejected from the network, more severe damage will be done. In such a scenario, periodically reconfiguring security systems is necessary, which requires a challenge in the design and realization.

The emergence of AI has resulted in manifold improvements in the performance of UWC systems. Undoubtedly, the revolution toward *intelligent communications* is one of major directions in future research. Recently, existing studies have been efficiently leveraged the power of AI to address several complex problems in UWC such as throughput maximization, energy efficiency, traffic engineering, latency minimization, formation control, and auto alignment [322, 323]. Although these efforts obtained remarkable achievements and illustrated the potentials of AI in the fields, the complexity and uncertainty of aquatic environment has been simplified within idea assumptions to reduce the dimension of state spaces for a fast-learning convergence and less resource consumption. Therefore, handling such a dynamic aquatic environment and flexibly adapting appropriate AI models in UWC systems are challenges for future research.

In terms of *network lifetime*, different from terrestrial and airborne systems, electromagnetic energy harvesting methods are considered inappropriate in the aquatic environment to wirelessly replenish energy for underwater devices. Although several existing methods are available to harvest ambient energy in the environment such as hydrokinetic turbines, piezoelectric cantilevers, and hydrophones, their conversion efficiency is limited because of the mechanical design constraints integrating into underwater devices [324, 325]. Moreover, the complex mechanical frameworks reduce the mobility of underwater devices in such an unstable aquatic environment. To overcome this issue, one feasible approach is to develop an optimal trajectory for underwater devices to find charging stations mounted on the cable systems after their battery reaches a predefined threshold. This method exposes a shortcoming as the devices must leave their positions (i.e., resulting in system formation changes) during the charging time. Nevertheless, to facilitate the UWC, wireless energy replenishment should be the focus of future research.

Underwater computing specifies the ability of temporarily or permanently providing cloud computing capability in UWC systems. Self-involving edge/cloud servers in UWC significantly improves QoS in terms of low latency, low overhead, robust execution, and locality exploitation [326, 327]. Although underwater network infrastructures are difficult to be maintained, its location benefits from low carbon emission and in close proximity to underwater devices. Moreover, local cloud computing is a key enabler to efficiently deploy modern AI algorithms to optimize the networks. Positive impacts and advantages of the underwater computing capability are undeniable. However, implementing the technology in wireless underwater systems face several challenges as networking devices in UWC are typically resource-constrained equipment and the operational environment is extremely dynamic. To achieve an efficient underwater computing platform requires high efforts in future research to overcome these problems.

Finally, the key performances in UWC thoroughly discussed in Section 3 should be continuously investigated within multiple specific application scenarios and system models to clarify any possible technical issues. In this regard, standard validation platforms are necessary to accurately measure and evaluate the performances of the proposed solution compared to state-of-the-art technologies. Moreover, as statement set of aquatic environments is sophisticated and difficult to be formularized properly, real experiments and trial implementation are strongly encouraged for validation of potential proposals in future research.

7. Concluding Remarks

This survey provided state-of-the-art knowledge and advancements of UWC with a reference to 6G development. Our findings in this investigation demonstrate that the envisioned 6G access infrastructures are insufficient to completely serve diverse underwater applications directly. To complement a comprehensive 6G access infrastructure, an integration of UWC into the system is necessary. Regarding the maturity of the technology, the achievements of a large number of related studies have significantly improved the performance of UWC. However, UWC faces several critical challenges in future research such as cross-medium barriers, reliable long-range high-throughput communications, underwater computing, and energy replenishment. Hence, the technology is considered immature yet in its current state but potential for native integration into future 6G systems. This survey is expected to enable interested engineers and researchers by updating them on current technology trends through systematical reference material.

Acknowledgment

This work was supported by the National Research Foundation of Korea (NRF) grant funded by the Korea government (MSIT) (No. 2021R1G1A1008105). Vo Nguyen Quoc Bao and Sungrae Cho are the corresponding authors.

References

[1] ITU-T FG-NET-2030, Network 2030–A blueprint of technology, applications and market drivers towards the year 2030 and beyond (2019).

[2] G. Gui, M. Liu, F. Tang, N. Kato, F. Adachi, 6G: Opening new horizons for integration of comfort, security, and intelligence, IEEE Wireless Communications 27 (5) (2020) 126–132.

[3] H. Tataria, M. Shafi, A. F. Molisch, M. Dohler, H. Sjöland, F. Tufvesson, 6G wireless systems: Vision, requirements, challenges, insights, and opportunities, Proceedings of the IEEE 109 (7) (2021) 1166–1199.

[4] Y. Li, S. Wang, C. Jin, Y. Zhang, T. Jiang, A survey of underwater magnetic induction communications: Fundamental issues, recent advances, and challenges, IEEE Communications Surveys & Tutorials 21 (3) (2019) 2466–2487.

[5] N. Saeed, A. Celik, T. Y. Al-Naffouri, M.-S. Alouini, Underwater optical wireless communications, networking, and localization: A survey, Ad Hoc Networks 94 (2019) 101935.

[6] S. Jiang, On securing underwater acoustic networks: A survey, IEEE Communications Surveys & Tutorials 21 (1) (2019) 729–752.

[7] S. Li, W. Qu, C. Liu, T. Qiu, Z. Zhao, Survey on high reliability wireless communication for underwater sensor networks, Journal of Network and Computer Applications 148 (2019) 102446.

[8] T. Islam, S.-H. Park, A comprehensive survey of the recently proposed localization protocols for underwater sensor networks, IEEE Access 8 (2020) 179224–179243.

[9] Y. Yang, Y. Xiao, T. Li, A survey of autonomous underwater vehicle formation: Performance, formation control, and communication capability, IEEE Communications Surveys & Tutorials 23 (2) (2021) 815–841.

[10] O. Gupta, N. Goyal, The evolution of data gathering static and mobility models in underwater wireless sensor networks: A survey, Journal of Ambient Intelligence and Humanized Computing (2021) 1–17.

[11] J. Luo, Y. Chen, M. Wu, Y. Yang, A survey of routing protocols for underwater wireless sensor networks, IEEE Communications Surveys & Tutorials 23 (1) (2021) 137–160.

[12] N.-N. Dao, Q.-V. Pham, N. H. Tu, T. T. Thanh, V. N. Q. Bao, D. S. Lakew, S. Cho, Survey on aerial radio access networks: Toward a comprehensive 6G access infrastructure, IEEE Communications Surveys & Tutorials 23 (2) (2021) 1193–1225.

[13] N.-N. Dao, Q.-V. Pham, D.-T. Do, S. Dustdar, The sky is the edge–Toward mobile coverage from the sky, IEEE Internet Computing 25 (2) (2021) 101–108.

[14] 3GPP TS 23.501 V16.5.0 Release 16, 5G; System architecture for the 5G system (5GS) (2020).

[15] ETSI TR 103 611 V1.1.1, Satellite Earth stations and systems (SES); Seamless integration of satellite and/or HAPS (high altitude platform station) systems into 5G and related architecture options (2020).

[16] M. Jouhari, K. Ibrahimi, H. Tembine, J. Ben-Othman, Underwater wireless sensor networks: A survey on enabling technologies, localization protocols, and internet of underwater things, IEEE Access 7 (2019) 96879–96899.

[17] X. You, C.-X. Wang, J. Huang, X. Gao, Z. Zhang, M. Wang, Y. Huang, C. Zhang, Y. Jiang, J. Wang, et al., Towards 6G wireless communication networks: Vision, enabling technologies, and new paradigm shifts, Science China Information Sciences 64 (1) (2021) 1–74.

[18] M. Vaezi, A. Azari, S. R. Khosravirad, M. Shirvanimoghaddam, M. M. Azari, D. Chasaki, P. Popovski, Cellular, wide-area, and non-terrestrial IoT: A survey on 5G advances and the road towards 6G, arXiv preprint arXiv:2107.03059 (Jul. 2021).

[19] S. Dash, C. Psomas, I. Krikidis, I. F. Akyildiz, A. Pitsillides, Active control of THz waves in wireless environments using graphene-based RIS, IEEE Transactions on Antennas and Propagation (2022) 1–1doi:10.1109/TAP.2022.3142272.

[20] S. Tarboush, H. Sarieddeen, H. Chen, M. H. Loukil, H. Jemaa, M.-S. Alouini, T. Y. Al-Naffouri, TeraMIMO: A channel simulator for wideband ultra-massive MIMO Terahertz communications, IEEE Transactions on Vehicular Technology 70 (12) (2021) 12325–12341. doi:10.1109/TVT.2021.3123131.

[21] B. Ning, Z. Chen, W. Chen, Y. Du, J. Fang, Terahertz multi-user massive MIMO with intelligent reflecting surface: Beam training and hybrid beamforming, IEEE Transactions on Vehicular Technology 70 (2) (2021) 1376–1393. doi:10.1109/TVT.2021.3052074.

[22] C. Feng, W. Shen, J. An, L. Hanzo, Joint hybrid and passive RIS-assisted beamforming for mmWave MIMO systems relying on dynamically configured subarrays, IEEE Internet of Things Journal (2022) 1–1doi:10.1109/JIOT.2022.3142932.

[23] H. Hashida, Y. Kawamoto, N. Kato, M. Iwabuchi, T. Murakami, Mobility-aware user association strategy for IRS-aided mm-wave multibeam transmission towards 6G, IEEE Journal on Selected Areas in Communications (2022) 1–1doi:10.1109/JSAC.2022.3143216.

[24] Z. Wang, Y. Liu, X. Mu, Z. Ding, O. A. Dobre, NOMA empowered integrated sensing and communication, IEEE Communications Letters (2022) 1–1doi:10.1109/LCOMM.2022.3140271.

[25] J. Chu, X. Chen, Robust design for integrated satellite–terrestrial internet of things, IEEE Internet of Things Journal 8 (11) (2021) 9072–9083. doi:10.1109/JIOT.2021.3055776.

[26] Y. Liu, S. Zhang, X. Mu, Z. Ding, R. Schober, N. Al-Dhahir, E. Hossain, X. Shen, Evolution of NOMA toward next generation multiple access (NGMA) for 6G, IEEE Journal on Selected Areas in Communications (2022) 1–1doi:10.1109/JSAC.2022.3145234.

[27] D. Xu, V. Jamali, X. Yu, D. W. K. Ng, R. Schober, Optimal resource allocation design for large IRS-assisted SWIPT systems: A scalable optimization framework, IEEE Transactions on Communications (2022) 1–1doi:10.1109/TCOMM.2022.3140467.

[28] X. Cao, B. Yang, C. Huang, G. C. Alexandropoulos, C. Yuen, Z. Han, H. Vincent Poor, L. Hanzo, Massive access of static and mobile users via reconfigurable intelligent surfaces: Protocol design and performance analysis, IEEE Journal on Selected Areas in Communications (2022) 1–1doi:10.1109/JSAC.2022.3145908.

[29] W. U. Khan, X. Li, M. Zeng, O. A. Dobre, Backscatter-enabled NOMA for future 6G systems: A new optimization framework under imperfect SIC, IEEE Communications Letters 25 (5) (2021) 1669–1672.

[30] W. U. Khan, M. A. Javed, T. N. Nguyen, S. Khan, B. M. Elhalawany, Energy-efficient resource allocation for 6G backscatter-enabled NOMA IoV networks, IEEE Transactions on Intelligent Transportation Systems (2021).

[31] K. Nallappan, H. Guerboukha, C. Nerguizian, M. Skorobogatiy, Live streaming of uncompressed HD and 4K videos using Terahertz wireless links, IEEE Access 6 (2018) 58030–58042. doi:10.1109/ACCESS.2018.2873986.

[32] V. Petrov, T. Kurner, I. Hosako, IEEE 802.15.3d: First standardization efforts for sub-Terahertz band communications toward 6G, IEEE Communications Magazine 58 (11) (2020) 28–33. doi:10.1109/MCOM.001.2000273.

[33] P. Vijayakumar, M. Azees, S. A. Kozlov, J. J. P. C. Rodrigues, An anonymous batch authentication and key exchange protocols for 6g enabled vanets, IEEE Transactions on Intelligent Transportation Systems 23 (2) (2022) 1630–1638. doi:10.1109/TITS.2021.3099488.

[34] S. Ju, Y. Xing, O. Kanhere, T. S. Rappaport, Millimeter wave and sub-Terahertz spatial statistical channel model for an indoor office building, IEEE Journal on Selected Areas in Communications 39 (6) (2021) 1561–1575. doi:10.1109/JSAC.2021.3071844.

[35] G. Berardinelli, P. Baracca, R. O. Adeogun, S. R. Khosravirad, F. Schaich, K. Upadhya, D. Li, T. Tao, H. Viswanathan, P. Mogensen, Extreme communication in 6G: Vision and challenges for 'in-X' subnetworks, IEEE Open Journal of the Communications Society 2 (2021) 2516–2535. doi:10.1109/OJCOMS.2021.3121530.

[36] E. Ndassimba, N. G. Ndassimba, G. M. Kossingou, S. Ouya, Smart Agriculture Solution Based on IoT and TVWS for Arid Regions of the Central African Republic, in: Networking, Intelligent Systems and Security, Springer, 2021, pp. 653–666.

[37] R. Singh, D. Saluja, S. Kumar, Graphical approach for V2V connectivity enhancement in clustering-based VANET, IEEE Wireless Communications Letters 10 (6) (2021) 1217–1221. doi:10.1109/LWC.2021.3062379.

[38] J. M. Eckhardt, V. Petrov, D. Moltchanov, Y. Koucheryavy, T. Kürner, Channel measurements and modeling for low-Terahertz band vehicular communications, IEEE Journal on Selected Areas in Communications 39 (6) (2021) 1590–1603. doi:10.1109/JSAC.2021.3071843.

[39] H. Yu, Z. Zhou, Optimization of iot-based artificial intelligence assisted telemedicine health analysis system, IEEE Access 9 (2021) 85034–85048. doi:10.1109/ACCESS.2021.3088262.

[40] J. Chen, W. Wang, Y. Zhou, S. H. Ahmed, W. Wei, Exploiting 5G and

Blockchain for Medical Applications of Drones, IEEE Network 35 (1) (2021) 30–36. doi:10.1109/MNET.011.2000144.

[41] G. Ye, H. Yin, T. Chen, M. Xu, Q. V. H. Nguyen, J. Song, Personalized on-device e-health analytics with decentralized block coordinate descent, IEEE Journal of Biomedical and Health Informatics (2022) 1–1doi:10.1109/JBHI.2022.3140455.

[42] F. H. Juwono, R. Reine, W. K. Wong, Z. A. Sim, L. Gopal, Envisioning 6G molecular communication for IoBNT diagnostic systems, in: 2021 International Conference on Green Energy, Computing and Sustainable Technology (GECOST), Miri, Malaysia, 2021, pp. 1–5. doi:10.1109/GECOST52368.2021.9538653.

[43] J. Chen, S. Sun, N. Bao, Z. Zhu, L.-B. Zhang, Improved reconstruction for CS-based ECG acquisition in internet of medical things, IEEE Sensors Journal 21 (22) (2021) 25222–25233. doi:10.1109/JSEN.2021.3055635.

[44] J. Simonjan, B. D. Unluturk, I. F. Akyildiz, In-body bionanosensor communication and localization for anomaly detection, in: 2021 International Balkan Conference on Communications and Networking (BalkanCom), Novi Sad, Serbia, 2021, pp. 16–20. doi:10.1109/BalkanCom53780.2021.9593231.

[45] N. Saeed, M. H. Loukil, H. Sarieddeen, T. Y. Al-Naffouri, M.-S. Alouini, Body-centric Terahertz networks: Prospects and challenges, IEEE Transactions on Molecular, Biological and Multi-Scale Communications (2021) 1–1doi:10.1109/TMBMC.2021.3135198.

[46] M. H. Kabir, S. M. R. Islam, A. P. Shrestha, F. Ali, M. A. Badsha, M. J. Piran, D.-T. Do, Electromagnetic nanocommunication networks: Principles, applications, and challenges, IEEE Access 9 (2021) 166147–166165. doi:10.1109/ACCESS.2021.3135335.

[47] S. Javaid, S. Zeadally, H. Fahim, B. He, Medical sensors and their integration in wireless body area networks for pervasive healthcare delivery: A review, IEEE Sensors Journal (2022) 1–1doi:10.1109/JSEN.2022.3141064.

[48] I. F. Akyildiz, A. Kak, S. Nie, 6G and beyond: The future of wireless communications systems, IEEE Access 8 (2020) 133995–134030. doi:10.1109/ACCESS.2020.3010896.

[49] S. Aloufi, A. E. Saddik, MMSUM digital twins: A multi-view multimodality summarization framework for sporting events, ACM Transactions on Multimedia Computing, Communications, and Applications (TOMM) 18 (1) (2022) 1–25.

[50] A. M. Elbir, K. V. Mishra, S. Chatzinotas, Terahertz-band joint ultra-massive MIMO radar-communications: Model-based and model-free hybrid beamforming, IEEE Journal of Selected Topics in Signal Processing 15 (6) (2021) 1468–1483. doi:10.1109/JSTSP.2021.3117410.

[51] L. G. de Oliveira, B. Nuss, M. B. Alabd, A. Diewald, M. Pauli, T. Zwick, Joint radar-communication systems: Modulation schemes and system design, IEEE Transactions on Microwave Theory and Techniques (2021) 1–1doi:10.1109/TMTT.2021.3126887.

[52] F.-Y. Wang, R. Qin, X. Wang, B. Hu, Metasocieties in metaverse: Metaeconomics and metamanagement for metaenterprises and metacities, IEEE Transactions on Computational Social Systems 9 (1) (2022) 2–7.

[53] P. Zhang, C. Wang, N. Kumar, L. Liu, Space-Air-Ground Integrated Multi-Domain Network Resource Orchestration Based on Virtual Network architecture: A DRL method, IEEE Transactions on Intelligent Transportation Systems (2022) 1–11doi:10.1109/TITS.2021.3099477.

[54] C. Wang, L. Liu, C. Jiang, S. Wang, P. Zhang, S. Shen, Incorporating distributed DRL into storage resource optimization of space-air-ground integrated wireless communication network, IEEE Journal of Selected Topics in Signal Processing (2021) 1–1doi:10.1109/JSTSP.2021.3136027.

[55] N. Cheng, J. He, Z. Yin, C. Zhou, H. Wu, F. Lyu, H. Zhou, X. Shen, 6G service-oriented space-air-ground integrated network: A survey, Chinese Journal of Aeronautics (Dec. 2021).

[56] F. Nait-Abdesselam, A. Alsharoa, M. Y. Selim, D. Qiao, A. E. Kamal, Towards enabling unmanned aerial vehicles as a service for heterogeneous applications, Journal of Communications and Networks 23 (3) (2021) 212–221. doi:10.23919/JCN.2021.000015.

[57] A. Al-Hourani, Session duration between handovers in dense LEO satellite networks, IEEE Wireless Communications Letters 10 (12) (2021) 2810–2814. doi:10.1109/LWC.2021.3118214.

[58] C. Suraci, S. Pizzi, A. Molinaro, G. Araniti, MEC and D2D as enabling technologies for a secure and lightweight 6G ehealth system, IEEE Internet of Things Journal (2021) 1–1doi:10.1109/JIOT.2021.3130666.

[59] R. I. Ansari, N. Ashraf, S. A. Hassan, D. G. C., H. Pervaiz, C. Politis, Spectrum on demand: A competitive open market model for spectrum sharing for UAV-assisted communications, IEEE Network 34 (6) (2020) 318–324. doi:10.1109/MNET.011.2000253.

[60] J. Angjo, I. Shayea, M. Ergen, H. Mohamad, A. Alhammadi, Y. I. Daradkeh, Handover management of drones in future mobile networks: 6G technologies, IEEE Access 9 (2021) 12803–12823. doi:10.1109/ACCESS.2021.3051097.

[61] J. Hoydis, F. A. Aoudia, A. Valcarce, H. Viswanathan, Toward a 6G AI-native air interface, IEEE Communications Magazine 59 (5) (2021) 76–81.

[62] S. Han, T. Xie, C.-L. I, L. Chai, Z. Liu, Y. Yuan, C. Cui, Artificial-Intelligence-Enabled Air Interface for 6G: Solutions, Challenges, and Standardization Impacts, IEEE Communications Magazine 58 (10) (2020) 73–79. doi:10.1109/MCOM.001.2000218.

[63] K. B. Letaief, Y. Shi, J. Lu, J. Lu, Edge artificial intelligence for 6G: Vision, enabling technologies, and applications, IEEE Journal on Selected Areas in Communications 40 (1) (2022) 5–36. doi:10.1109/JSAC.2021.3126076.

[64] X. , M. Jia, X. Gu, Q. Guo, Intelligent spectrum management based on radio map for cloud-based satellite and terrestrial spectrum shared networks, China Communications 18 (12) (2021) 108–118. doi:10.23919/JCC.2021.12.007.

[65] Z. Zhao, P. Cumino, C. Esposito, M. Xiao, D. Rosário, T. Braun, E. Cerqueira, S. Sargento, Smart unmanned aerial vehicles as base stations placement to improve the mobile network operations, Computer communications 181 (2022) 45–57.

[66] M. Vaezi, A. Azari, S. R. Khosravirad, M. Shirvanimoghaddam, M. M. Azari, D. Chasaki, P. Popovski, Cellular, wide-area, and non-terrestrial IoT: A Survey on 5G advances and the road towards 6G, IEEE Communications Surveys & Tutorials (2022).

[67] X. Fang, W. Feng, T. Wei, Y. Chen, N. Ge, C.-X. Wang, 5G embraces satellites for 6G ubiquitous IoT: Basic models for integrated satellite terrestrial networks, IEEE Internet of Things Journal 8 (18) (2021) 14399–14417. doi:10.1109/JIOT.2021.3068596.

[68] B. Ma, J. Wu, W. Liu, L. Chiaraviglio, X. Ming, Combating hard or soft disasters with privacy-preserving federated mobile buses-and-drones based networks, in: 2020 IEEE 21st International Conference on Information Reuse and Integration for Data Science (IRI), IEEE, Las Vegas, NV, USA, 2020, pp. 31–36.

[69] Z. Qadir, F. Ullah, H. S. Munawar, F. Al-Turjman, Addressing disasters in smart cities through UAVs path planning and 5G communications: A systematic review, Computer Communications 168 (2021) 114–135.

[70] X. Liu, Y. Deng, U. Challita, A. Zahemszky, et al., QoE optimization for live video streaming in UAV-to-UAV communications via deep reinforcement learning, arXiv preprint arXiv:2102.10637 (2021).

[71] D. Wang, Y. He, K. Yu, G. Srivastava, L. Nie, R. Zhang, Delay sensitive secure NOMA transmission for hierarchical HAP-LAP medical-care IoT networks, IEEE Transactions on Industrial Informatics (2021) 1–1doi:10.1109/TII.2021.3117263.

[72] N. Mehallegue, M. Djellab, K. Loukhaoukha, Efficient use of UAVs for public safety in disaster and crisis management, Wireless Personal Communications 116 (1) (2021) 369–380.

[73] T. Yang, Z. Jiang, R. Sun, N. Cheng, H. Feng, Maritime search and rescue based on group mobile computing for unmanned aerial vehicles and unmanned surface vehicles, IEEE Transactions on Industrial Informatics 16 (12) (2020) 7700–7708. doi:10.1109/TII.2020.2974047.

[74] G. Fontanesi, H. Ahmadi, A. Zhu, Over the Sea UAV Based Communication, in: 2019 European Conference on Networks and Communications (EuCNC), IEEE, Valencia, Spain, 2019, pp. 374–378. doi:10.1109/EuCNC.2019.8802019.

[75] K. Liu, P. Li, C. Liu, L. Xiao, L. Jia, UAV-aided anti-jamming maritime communications: A deep reinforcement learning approach, in: 2021 13th International Conference on Wireless Communications and Signal Processing (WCSP), Changsha, China, 2021, pp. 1–6. doi:10.1109/WCSP52459.2021.9613616.

[76] P. K. R. Maddikunta, S. Hakak, M. Alazab, S. Bhattacharya, T. R. Gadekallu, W. Z. Khan, Q.-V. Pham, Unmanned aerial vehicles in smart

agriculture: Applications, requirements, and challenges, IEEE Sensors Journal (Aug. 2021).
[77] P. Spachos, S. Gregori, Integration of wireless sensor networks and smart UAVs for precision viticulture, IEEE Internet Computing 23 (3) (2019) 8–16. doi:10.1109/MIC.2018.2890234.
[78] M. Maiouak, T. Taleb, Dynamic maps for automated driving and UAV geofencing, IEEE Wireless Communications 26 (4) (2019) 54–59.
[79] G. Avanzini, V. D. Luca, C. Pascarelli, Integrated Platform for sUAS Operations in Sensitive Areas with Improved Pilot Situation Awareness, in: 2021 IEEE Conference on Cognitive and Computational Aspects of Situation Management (CogSIMA), Tallinn, Estonia, 2021, pp. 17–24. doi:10.1109/CogSIMA51574.2021.9475927.
[80] S. Rajendran, J. Zack, Insights on strategic air taxi network infrastructure locations using an iterative constrained clustering approach, Transportation Research Part E: Logistics and Transportation Review 128 (2019) 470–505.
[81] B. Liu, Z. Su, Q. Xu, Game theoretical secure wireless communication for uav-assisted vehicular internet of things, China Communications 18 (7) (2021) 147–157. doi:10.23919/JCC.2021.07.012.
[82] K. Wang, X. Zhang, L. Duan, Cooperative Path Planning of a UAV Swarm to Meet Temporal-Spatial User Demands, in: GLOBECOM 2020 - 2020 IEEE Global Communications Conference, Taipei, Taiwan, 2020, pp. 1–6. doi:10.1109/GLOBECOM42002.2020.9322226.
[83] A. Kak, I. F. Akyildiz, Designing large-scale constellations for the internet of space things with Cubesats, IEEE Internet of Things Journal 8 (3) (2021) 1749–1768. doi:10.1109/JIOT.2020.3016889.
[84] I. F. Akyildiz, J. M. Jornet, S. Nie, A new Cubesat design with reconfigurable multi-band radios for dynamic spectrum satellite communication networks, Ad Hoc Networks 86 (2019) 166–178.
[85] S. Nie, I. F. Akyildiz, Channel modeling and analysis of inter-small-satellite links in Terahertz band space networks, IEEE Transactions on Communications 69 (12) (2021) 8585–8599. doi:10.1109/TCOMM.2021.3113942.
[86] N. Saeed, H. Almorad, H. Dahrouj, T. Y. Al-Naffouri, J. S. Shamma, M.-S. Alouini, Point-to-point communication in integrated satellite-aerial 6G networks: State-of-the-art and future challenges, IEEE Open Journal of the Communications Society 2 (2021) 1505–1525. doi:10.1109/OJCOMS.2021.3093110.
[87] F. Rinaldi, H.-L. Maattanen, J. Torsner, S. Pizzi, S. Andreev, A. Iera, Y. Koucheryavy, G. Araniti, Non-Terrestrial Networks in 5G amp; Beyond: A Survey, IEEE Access 8 (2020) 165178–165200. doi:10.1109/ACCESS.2020.3022981.
[88] Z. Jia, M. Sheng, J. Li, D. Niyato, Z. Han, LEO-satellite-assisted UAV: Joint trajectory and data collection for internet of remote things in 6G aerial access networks, IEEE Internet of Things Journal 8 (12) (2021) 9814–9826. doi:10.1109/JIOT.2020.3021255.
[89] R. Deng, B. Di, H. Zhang, L. Kuang, L. Song, Ultra-dense LEO satellite constellations: How many LEO satellites do we need?, IEEE Transactions on Wireless Communications 20 (8) (2021) 4843–4857. doi:10.1109/TWC.2021.3062658.
[90] E. Yaacoub, M.-S. Alouini, Efficient fronthaul and backhaul connectivity for iot traffic in rural areas, IEEE Internet of Things Magazine 4 (1) (2021) 60–66. doi:10.1109/IOTM.0001.1900061.
[91] K. Bhatia, Starlinked! an analysis of spacex's small satellite mega-constellation under the fourth amendment, Information & Communications Technology Law (2022) 1–22.
[92] E. Yaacoub, M.-S. Alouini, A key 6G challenge and opportunity—connecting the base of the pyramid: A survey on rural connectivity, Proceedings of the IEEE 108 (4) (2020) 533–582. doi:10.1109/JPROC.2020.2976703.
[93] H. Xie, Y. Zhan, G. Zeng, X. Pan, LEO mega-constellations for 6G global coverage: Challenges and opportunities, IEEE Access 9 (2021) 164223–164244. doi:10.1109/ACCESS.2021.3133301.
[94] C. Wang, J. Shen, P. Vijayakumar, B. B. Gupta, Attribute-based secure data aggregation for isolated IoT-enabled maritime transportation systems, IEEE Transactions on Intelligent Transportation Systems (2021) 1–10doi:10.1109/TITS.2021.3127436.
[95] T. Wei, W. Feng, Y. Chen, C.-X. Wang, N. Ge, J. Lu, Hybrid satellite-terrestrial communication networks for the maritime internet of things: Key technologies, opportunities, and challenges, IEEE Internet of Things Journal 8 (11) (2021) 8910–8934. doi:10.1109/JIOT.2021.3056091.
[96] S. Saafi, O. Vikhrova, G. Fodor, J. Hosek, S. Andreev, AI-aided integrated terrestrial and non-terrestrial 6G solutions for sustainable maritime networking, arXiv preprint arXiv:2201.06947 (2022).
[97] J. Kokkoniemi, J. M. Jornet, V. Petrov, Y. Koucheryavy, M. Juntti, Channel modeling and performance analysis of airplane-satellite Terahertz band communications, IEEE Transactions on Vehicular Technology 70 (3) (2021) 2047–2061. doi:10.1109/TVT.2021.3058581.
[98] J. Kokkoniemi, J. M. Jornet, M. Juntti, Stochastic geometry framework for THz satellite-airplane network analysis, in: 2021 IEEE International Symposium on Dynamic Spectrum Access Networks (DySPAN), Los Angeles, CA, USA, 2021, pp. 67–72. doi:10.1109/DySPAN53946.2021.9677325.
[99] S. Jeong, J. Ko, J.-M. Yeom, Predicting rice yield at pixel scale through synthetic use of crop and deep learning models with satellite data in south and North Korea, Science of the Total Environment 802 (2022) 149726.
[100] Z. Li, L. Ding, D. Xu, Exploring the potential role of environmental and multi-source satellite data in crop yield prediction across Northeast China, Science of The Total Environment (2022) 152880.
[101] S. B. Prathiba, G. Raja, S. Anbalagan, K. Dev, S. Gurumoorthy, A. P. Sankaran, Federated learning empowered computation offloading and resource management in 6G-V2X, IEEE Transactions on Network Science and Engineering (2021) 1–1doi:10.1109/TNSE.2021.3103124.
[102] S. K. Khan, N. Shiwakoti, P. Stasinopoulos, M. Warren, Security assessment in vehicle-to-everything communications with the integration of 5G and 6G networks, in: 2021 International Symposium on Computer Science and Intelligent Controls (ISCSIC), Rome, Italy, 2021, pp. 154–158. doi:10.1109/ISCSIC54682.2021.00037.
[103] G. I. Association, et al., European Vision for the 6G network ecosystem, V1. 0 (2021) 06–07.
[104] J. R. Bhat, S. A. Alqahtani, 6G ecosystem: Current status and future perspective, IEEE Access 9 (2021) 43134–43167. doi:10.1109/ACCESS.2021.3054833.
[105] I. Zhou, I. Makhdoom, N. Shariati, M. A. Raza, R. Keshavarz, J. Lipman, M. Abolhasan, A. Jamalipour, Internet of things 2.0: Concepts, applications, and future directions, IEEE Access 9 (2021) 70961–71012. doi:10.1109/ACCESS.2021.3078549.
[106] P. P. Ray, N. Kumar, M. Guizani, A vision on 6G-enabled NIB: Requirements, technologies, deployments, and prospects, IEEE Wireless Communications 28 (4) (2021) 120–127. doi:10.1109/MWC.001.2000384.
[107] S. Guan, J. Wang, C. Jiang, R. Duan, Y. Ren, T. Q. S. Quek, MagicNet: The maritime giant cellular network, IEEE Communications Magazine 59 (3) (2021) 117–123. doi:10.1109/MCOM.001.2000831.
[108] J. Du, J. Song, Y. Ren, J. Wang, Convergence of broadband and broadcast/multicast in maritime information networks, Tsinghua Science and Technology 26 (5) (2021) 592–607. doi:10.26599/TST.2021.9010002.
[109] C. Zeng, J.-B. Wang, C. Ding, H. Zhang, M. Lin, J. Cheng, Joint optimization of trajectory and communication resource allocation for unmanned surface vehicle enabled maritime wireless networks, IEEE Transactions on Communications 69 (12) (2021) 8100–8115. doi:10.1109/TCOMM.2021.3115115.
[110] Y.-c. YE, X. Jiang, G. Pan, W. Jiang, Submarine Optical Cable Engineering, Academic Press, 2018.
[111] H. Takeshita, M. Sato, Y. Inada, E. L. T. de Gabory, Y. Nakamura, Past, current and future technologies for optical submarine cables, in: 2019 IEEE/ACM Workshop on Photonics-Optics Technology Oriented Networking, Information and Computing Systems (PHOTONICS), Denver, CO, USA, 2019, pp. 36–42.
[112] S.-W. Huang, E. Chen, J. Guo, Efficient seafloor classification and submarine cable route design using an autonomous underwater vehicle, IEEE Journal of Oceanic Engineering 43 (1) (2018) 7–18.
[113] E. Mateo, K. Nakamura, T. Inoue, Y. Inada, T. Ogata, Nonlinear characterization of fiber optic submarine cables, in: 2017 European Conference on Optical Communication (ECOC), IEEE, Gothenburg, Sweden, 2017, pp. 1–3.
[114] M. M. Eid, S. El-Meadawy, A. E.-N. A. Mohammed, A. N. Z. Rashed, High data rates in optic fiber systems based on the gain optimization

techniques, Journal of Optical Communications (Apr. 2021).
[115] Submarine Cable Map, Accessed: 8 September 2021.
URL https://www.submarinecablemap.com/
[116] J. D. Downie, Maximum capacities in submarine cables with fixed power constraints for C-band, C+ L-band, and multicore fiber systems, Journal of Lightwave Technology 36 (18) (2018) 4025–4032.
[117] R. Dar, P. J. Winzer, A. Chraplyvy, S. Zsigmond, K.-Y. Huang, H. Fevrier, S. Grubb, Cost-optimized submarine cables using massive spatial parallelism, Journal of Lightwave Technology 36 (18) (2018) 3855–3865.
[118] J. Zhang, Q. Zhang, X. Xiang, Automatic inspection of subsea optical cable by an autonomous underwater vehicle, in: OCEANS 2017-Aberdeen, IEEE, Aberdeen, UK, 2017, pp. 1–6.
[119] H. Yin, Y. Li, F. Xing, B. Wu, Z. Zhou, W. Zhang, Hybrid acoustic, wireless optical and fiber-optic underwater cellular mobile communication networks, in: 2018 IEEE 18th International Conference on Communication Technology (ICCT), Chongqing, China, 2018, pp. 721–726.
[120] G. Cossu, A. Sturniolo, A. Messa, S. Grechi, D. Costa, A. Bartolini, D. Scaradozzi, A. Caiti, E. Ciaramella, Sea-trial of optical ethernet modems for underwater wireless communications, Journal of Lightwave Technology 36 (23) (2018) 5371–5380.
[121] J. Xu, B. Sun, W. Lyu, M. Kong, R. Sarwar, J. Han, W. Zhang, N. Deng, Underwater fiber–wireless communication with a passive front end, Optics Communications 402 (2017) 260–264.
[122] A. Ali, C. Zhang, S. Hassnain, W. Lyu, R. Tehseen, X. Chen, J. Xu, Underwater wireless-to-plastic optical fiber communication systems with a passive front end, in: 2019 18th International Conference on Optical Communications and Networks (ICOCN), IEEE, Huangshan, China, 2019, pp. 1–3.
[123] P.-J. Bouvet, A. Loussert, Capacity analysis of underwater acoustic MIMO communications, in: OCEANS'10 IEEE SYDNEY, IEEE, Sydney, NSW, Australia, 2010, pp. 1–8.
[124] Y. Lysanov, L. Brekhovskikh, Fundamentals of ocean acoustics, Vol. 8, Springer, 1982.
[125] Y. Zhou, A. Song, F. Tong, Underwater acoustic channel characteristics and communication performance at 85 khz, The Journal of the Acoustical Society of America 142 (4) (Oct. 2017) EL350–EL355.
[126] P.-J. Bouvet, Y. Auffret, On the achievable rate of multiple-input–multiple-output underwater acoustic communications, IEEE Journal of Oceanic Engineering 45 (3) (Jul. 2020) 1126–1137.
[127] B. M. Lee, Massive MIMO for underwater industrial Internet of things networks, IEEE Internet of Things Journal (2021).
[128] X. Zhong, F. Ji, F. Chen, Q. Guan, H. Yu, A new acoustic channel interference model for 3-D underwater acoustic sensor networks and throughput analysis, IEEE Internet of Things Journal 7 (10) (Oct. 2020) 9930–9942.
[129] D. Kari, I. Marivani, F. Khan, M. O. Sayin, S. S. Kozat, Robust adaptive algorithms for underwater acoustic channel estimation and their performance analysis, Digital Signal Processing 68 (Sep. 2017) 57–68.
[130] W. Jiang, F. Tong, S. Zheng, X. Cao, Estimation of underwater acoustic channel with hybrid sparsity via static-dynamic discriminative compressed sensing, IEEE Sensors Journal 20 (23) (Dec. 2020) 14548–14558.
[131] Y. Zhang, J. Li, Y. V. Zakharov, J. Li, Y. Li, C. Lin, X. Li, Deep learning based single carrier communications over time-varying underwater acoustic channel, IEEE access 7 (Apr. 2019) 38420–38430.
[132] J. Huang, R. Diamant, Adaptive modulation for long-range underwater acoustic communication, IEEE Transactions on Wireless Communications 19 (10) (Oct. 2020) 6844–6857.
[133] M. J. Bocus, D. Agrafiotis, A. Doufexi, Real-time video transmission using massive MIMO in an underwater acoustic channel, in: 2018 IEEE wireless communications and networking conference (WCNC), IEEE, Barcelona, Spain, 2018, pp. 1–6.
[134] A. Zoksimovski, D. Sexton, M. Stojanovic, C. Rappaport, Underwater electromagnetic communications using conduction–channel characterization, Ad Hoc Networks 34 (Nov. 2015) 42–51.
[135] P. P. Ganesh, H. Venkataraman, RF-based multihop wireless communication for shallow underwater environment, in: 2019 International Conference on Wireless Communications Signal Processing and Networking (WiSPNET), IEEE, Chennai, India, 2019, pp. 222–228.
[136] P. G. PSS, H. Venkataraman, E-CRUSE: energy-based throughput analysis for cluster-based RF shallow underwater communication, IET Communications 14 (15) (Jul. 2020) 2544–2553.
[137] C. Gabriel, M.-A. Khalighi, S. Bourennane, P. Léon, V. Rigaud, Monte-Carlo-based channel characterization for underwater optical communication systems, Journal of Optical Communications and Networking 5 (1) (2013) 1–12.
[138] C. M. Gussen, P. S. Diniz, M. Campos, W. A. Martins, F. M. Costa, J. N. Gois, A survey of underwater wireless communication technologies, Journal of Communication and Information Systems 31 (1) (2016) 242–255.
[139] M. A. Khalighi, H. Akhouayri, S. Hranilovic, Silicon-photomultiplier-based underwater wireless optical communication using pulse-amplitude modulation, IEEE Journal of Oceanic Engineering 45 (4) (Oct. 2020) 1611–1621.
[140] Y. Li, H. Yin, X. Ji, B. Wu, Design and implementation of underwater wireless optical communication system with high-speed and full-duplex using blue/green light, in: IEEE International Conference on Communication Software and Networks (ICCSN), 2018, pp. 99–103.
[141] A. Shyamalaprasanna, B. Ragavi, L. Pavithra, K. Mohanapriya, P. Santhiyadevi, Achieve high data rate by using optical modem in under water wireless communication, in: 2020 International Conference on Innovative Trends in Information Technology (ICITIIT), IEEE, Kottayam, India, 2020, pp. 1–5.
[142] L. Zhang, X. Tang, C. Sun, Z. Chen, Z. Li, H. Wang, R. Jiang, W. Shi, A. Zhang, Over 10 attenuation length gigabits per second underwater wireless optical communication using a silicon photomultiplier (SiPM) based receiver, Optics Express 28 (17) (Aug. 2020) 24968–24980.
[143] C. Zou, F. Yang, Autoencoder based underwater wireless optical communication with high data rate, Optics Letters 46 (6) (2021) 1446–1449.
[144] F. Wang, Y. Liu, F. Jiang, N. Chi, High speed underwater visible light communication system based on LED employing maximum ratio combination with multi-pin reception, Optics Communications 425 (Oct. 2018) 106–112.
[145] C. Shen, Y. Guo, X. Sun, G. Liu, K.-T. Ho, T. K. Ng, M.-S. Alouini, B. S. Ooi, Going beyond 10-meter, Gbit/s underwater optical wireless communication links based on visible lasers, in: 2017 opto-electronics and communications conference (OECC) and photonics global conference (PGC), IEEE, Singapore, 2017, pp. 1–3.
[146] X. Liu, S. Yi, X. Zhou, Z. Fang, Z.-J. Qiu, L. Hu, C. Cong, L. Zheng, R. Liu, P. Tian, 34.5 m underwater optical wireless communication with 2.70 Gbps data rate based on a green laser diode with NRZ-OOK modulation, Optics express 25 (22) (2017) 27937–27947.
[147] X. Liu, S. Yi, X. Zhou, S. Zhang, Z. Fang, Z.-J. Qiu, L. Hu, C. Cong, L. Zheng, R. Liu, et al., Laser-based white-light source for high-speed underwater wireless optical communication and high-efficiency underwater solid-state lighting, Optics express 26 (15) (2018) 19259–19274.
[148] G. N. Arvanitakis, R. Bian, J. J. McKendry, C. Cheng, E. Xie, X. He, G. Yang, M. S. Islim, A. A. Purwita, E. Gu, et al., Gb/s underwater wireless optical communications using series-connected GaN micro-LED arrays, IEEE Photonics Journal 12 (2) (2020).
[149] C. Fei, X. Hong, G. Zhang, J. Du, Y. Gong, J. Evans, S. He, 16.6 Gbps data rate for underwater wireless optical transmission with single laser diode achieved with discrete multi-tone and post nonlinear equalization, Optics Express 26 (26) (2018) 34060–34069.
[150] J. Alkhasraji, C. Tsimenidis, Coded OFDM over short range underwater optical wireless channels using LED, in: Oceans 2017-Aberdeen, IEEE, Aberdeen, UK, 2017, pp. 1–7.
[151] M. Jain, N. Sharma, A. Gupta, D. Rawal, P. Garg, Performance analysis of NOMA assisted underwater visible light communication system, IEEE Wireless Communications Letters 9 (8) (Aug. 2020) 1291–1294.
[152] C. Bai, H.-P. Ren, C. Grebogi, M. S. Baptista, Chaos-based underwater communication with arbitrary transducers and bandwidth, Applied Sciences 8 (2) (Jan. 2018) 162.
[153] S. Huang, X. Hou, W. Liu, G. Liu, Y. Dai, W. Tian, Mimicking ship-radiated noise with chaos signal for covert underwater acoustic communication, IEEE Access 8 (Oct. 2020) 180341–180351.
[154] E. Demirors, G. Sklivanitis, G. E. Santagati, T. Melodia, S. N. Batalama, A high-rate software-defined underwater acoustic modem with real-time adaptation capabilities, IEEE Access 6 (Apr. 2018) 18602–18615.
[155] P. N. Ramavath, S. A. Udupi, P. Krishnan, High-speed and reliable underwater wireless optical communication system using multiple-input

multiple-output and channel coding techniques for IoUT applications, Optics Communications 461 (Apr. 2020) 125229.

[156] F. Rehman, G. Thomas, E. Anderlini, Centralized control system design for underwater transportation using two hovering autonomous underwater vehicles (HAUVs), IFAC-PapersOnLine 52 (11) (Sep. 2019) 13–18.

[157] D. Moreno-Salinas, N. Crasta, A. Pascoal, J. Aranda, Formation control of surface marine vehicles for underwater target tracking using range information, in: 2018 13th APCA International Conference on Automatic Control and Soft Computing (CONTROLO), IEEE, Ponta Delgada, Portugal, 2018, pp. 201–206.

[158] M. T. Vu, H. N. N. Le Thanh, T.-T. Huynh, Q. Thang, T. Duc, Q.-D. Hoang, T.-H. Le, Station-keeping control of a hovering over-actuated autonomous underwater vehicle under ocean current effects and model uncertainties in horizontal plane, IEEE Access 9 (2021) 6855–6867.

[159] H. Liu, Y. Wang, F. L. Lewis, Robust distributed formation controller design for a group of unmanned underwater vehicles, IEEE Transactions on Systems, Man, and Cybernetics: Systems 51 (2) (Feb. 2021) 1215–1223.

[160] C. Yuan, S. Licht, H. He, Formation learning control of multiple autonomous underwater vehicles with heterogeneous nonlinear uncertain dynamics, IEEE Transactions on Cybernetics 48 (10) (Oct. 2018) 2920–2934.

[161] H. Haghighi, H. Heidari, S. H. Sadati, J. Karimi, A hierarchical and priority-based strategy for trajectory tracking in UAV formation flight, in: 2017 8th International Conference on Mechanical and Aerospace Engineering (ICMAE), IEEE, Prague, Czech Republic, 2017, pp. 797–800.

[162] L. Qiao, Y. Li, S. Sun, B. Sun, K. Tian, Z. Li, X. Lu, Research on task assignment based on hierarchical structure for autonomous underwater vehicle, in: 2021 IEEE/CIC International Conference on Communications in China (ICCC Workshops), IEEE, Xiamen, China, 2021, pp. 299–303.

[163] J. Li, J. Du, W.-J. Chang, Robust time-varying formation control for underactuated autonomous underwater vehicles with disturbances under input saturation, Ocean Engineering 179 (2019) 180–188.

[164] Z. Yan, Z. Yang, L. Yue, L. Wang, H. Jia, J. Zhou, Discrete-time coordinated control of leader-following multiple AUVs under switching topologies and communication delays, Ocean Engineering 172 (Jan. 2019) 361–372.

[165] Y. Meng, J. Yan, X. Yang, X. Luo, Privacy preserving localization algorithm for underwater sensor networks, in: 2020 39th Chinese Control Conference (CCC), IEEE, Shenyang, China, 2020, pp. 4481–4486.

[166] S.-k. Pang, Y.-h. Li, H. Yi, Joint formation control with obstacle avoidance of towfish and multiple autonomous underwater vehicles based on graph theory and the null-space-based method, Sensors 19 (11) (Jun. 2019) 2591.

[167] H. Wu, Z. Yang, J. Cao, L. Lai, TRiForm: formation control for underwater sensor networks with measurement errors, IEEE Transactions on Vehicular Technology 69 (7) (Jul. 2020) 7679–7691.

[168] Y. Liu, J. Gao, X. Shi, C. Jiang, Decentralization of virtual linkage in formation control of multi-agents via consensus strategies, Applied Sciences 8 (11) (Oct. 2018) 2020.

[169] L. He, P. Bai, X. Liang, J. Zhang, W. Wang, Feedback formation control of UAV swarm with multiple implicit leaders, Aerospace Science and Technology 72 (Jan. 2018) 327–334.

[170] J. Wang, C. Wang, Y. Wei, C. Zhang, Neuroadaptive sliding mode formation control of autonomous underwater vehicles with uncertain dynamics, IEEE Systems Journal 14 (3) (Sep. 2020) 3325–3333.

[171] J. Bian, J. Xiang, Three-dimensional coordination control for multiple autonomous underwater vehicles, IEEE Access 7 (May 2019) 63913–63920.

[172] Y.-L. Chen, X.-W. Ma, G.-Q. Bai, Y. Sha, J. Liu, Multi-autonomous underwater vehicle formation control and cluster search using a fusion control strategy at complex underwater environment, Ocean Engineering 216 (Nov. 2020) 108048.

[173] Z. Gao, G. Guo, Fixed-time sliding mode formation control of AUVs based on a disturbance observer, IEEE/CAA Journal of Automatica Sinica 7 (2) (Mar. 2020) 539–545.

[174] N. Saeed, A. Celik, T. Y. Al-Naffouri, M.-S. Alouini, Underwater optical sensor networks localization with limited connectivity, in: 2018 IEEE International Conference on Acoustics, Speech and Signal Processing (ICASSP), IEEE, Calgary, AB, Canada, 2018, pp. 3804–3808.

[175] Y. Lin, H. Tao, Y. Tu, T. Liu, A node self-localization algorithm with a mobile anchor node in underwater acoustic sensor networks, IEEE Access 7 (Apr. 2019) 43773–43780.

[176] C. Liu, X. Wang, H. Luo, Y. Liu, Z. Guo, VA: Virtual node assisted localization algorithm for underwater acoustic sensor networks, IEEE Access 7 (Jul. 2019) 86717–86729.

[177] N. Saeed, A. Celik, T. Y. Al-Naffouri, M.-S. Alouini, Localization of energy harvesting empowered underwater optical wireless sensor networks, IEEE Transactions on Wireless Communications 18 (5) (May 2019) 2652–2663.

[178] N. Saeed, T. Y. Al-Naffouri, M.-S. Alouini, Outlier detection and optimal anchor placement for 3-d underwater optical wireless sensor network localization, IEEE Transactions on Communications 67 (1) (Jan. 2019) 611–622.

[179] J. Yan, H. Zhao, X. Luo, Y. Wang, C. Chen, X. Guan, Asynchronous localization of underwater target using consensus-based unscented Kalman filtering, IEEE Journal of Oceanic Engineering 45 (4) (Oct. 2020) 1466–1481.

[180] J. Yan, Y. Gong, C. Chen, X. Luo, X. Guan, AUV-aided localization for internet of underwater things: A reinforcement-learning-based method, IEEE Internet of Things Journal 7 (10) (Oct. 2020) 9728–9746.

[181] G. Liu, S. Yan, L. Mao, Receiver-only-based time synchronization under exponential delays in underwater wireless sensor networks, IEEE Internet of Things Journal 7 (10) (Oct. 2020) 9995–10009.

[182] Z. Gong, C. Li, F. Jiang, AUV-aided joint localization and time synchronization for underwater acoustic sensor networks, IEEE Signal Processing Letters 25 (4) (Apr. 2018) 477–481.

[183] N. Saeed, A. Celik, T. Y. Al-Naffouri, M.-S. Alouini, Robust 3D localization of underwater optical wireless sensor networks via low rank matrix completion, in: 2018 IEEE 19th International Workshop on Signal Processing Advances in Wireless Communications (SPAWC), IEEE, Kalamata, Greece, 2018, pp. 1–5.

[184] F. Jiang, Z. Zhang, H. E. Najafabadi, Deep sea TDOA localization method based on improved OMP algorithm, IEEE Access 7 (Dec. 2019) 168151–168161.

[185] Z. Gong, C. Li, F. Jiang, J. Zheng, AUV-aided localization of underwater acoustic devices based on Doppler shift measurements, IEEE Transactions on Wireless Communications 19 (4) (Apr. 2020) 2226–2239.

[186] W. Zhang, G. Han, X. Wang, M. Guizani, K. Fan, L. Shu, A node location algorithm based on node movement prediction in underwater acoustic sensor networks, IEEE Transactions on Vehicular Technology 69 (3) (Mar. 2020) 3166–3178.

[187] N. Saeed, M.-S. Alouini, T. Y. Al-Naffouri, Accurate 3-D localization of selected smart objects in optical internet of underwater things, IEEE Internet of Things Journal 7 (2) (Feb. 2020) 937–947.

[188] J. Anand, K. Sundeep, N. D. P. Rao, Underwater sensor protocol for time synchronization and data transmissions using the prediction model, in: 2020 International Conference on Inventive Computation Technologies (ICICT), IEEE, Coimbatore, India, 2020, pp. 762–766.

[189] R. Shams, P. Otero, M. Aamir, F. H. Khan, Joint algorithm for multi-hop localization and time synchronization in underwater sensors networks using single anchor, IEEE Access 9 (Feb. 2021) 27945–27958.

[190] J. Yan, X. Zhang, X. Luo, Y. Wang, C. Chen, X. Guan, Asynchronous localization with mobility prediction for underwater acoustic sensor networks, IEEE Transactions on Vehicular Technology 67 (3) (Mar. 2018) 2543–2556.

[191] G. Qiao, C. Zhao, F. Zhou, N. Ahmed, Distributed localization based on signal propagation loss for underwater sensor networks, IEEE Access 7 (Aug. 2019) 112985–112995.

[192] J. Yan, H. Zhao, Y. Wang, X. Luo, X. Guan, Asynchronous localization for UASNs: An unscented transform-based method, IEEE Signal Processing Letters 26 (4) (Apr. 2019) 602–606.

[193] J. Yan, H. Zhao, B. Pu, X. Luo, C. Chen, X. Guan, Energy-efficient target tracking with UASNs: A consensus-based bayesian approach, IEEE Transactions on Automation Science and Engineering 17 (3) (Jul. 2020) 1361–1375.

[194] J. Yan, D. Guo, X. Luo, X. Guan, AUV-aided localization for underwater acoustic sensor networks with current field estimation, IEEE Transactions on Vehicular Technology 69 (8) (Aug. 2020) 8855–8870.

[195] F. Liu, H. Chen, L. Zhang, L. Xie, Time-difference-of-arrival-based localization methods of underwater mobile nodes using multiple surface

beacons, IEEE Access 9 (Mar. 2021) 31712–31725.
[196] B. Zhang, H. Wang, L. Zheng, J. Wu, Z. Zhuang, Joint synchronization and localization for underwater sensor networks considering stratification effect, IEEE Access 5 (Nov. 2017) 26932–26943.
[197] A. Sabra, W.-k. Fung, P. Radhakrishna, Confidence-based underwater localization scheme for large-scale mobile sensor networks, in: OCEANS 2018 MTS/IEEE Charleston, IEEE, Charleston, SC, USA, 2018, pp. 1–6.
[198] Z. Chen, Q. Hu, H. Li, R. Fan, D. Ding, ULES: Underwater localization evaluation scheme under beacon node drift scenes, IEEE Access 6 (Nov. 2018) 70615–70624.
[199] Y. Zhang, Y. Li, Y. Zhang, T. Jiang, Underwater anchor-AUV localization geometries with an isogradient sound speed profile: A CRLB-based optimality analysis, IEEE Transactions on Wireless Communications 17 (12) (Dec. 2018) 8228–8238.
[200] F. Yao, Y. Wang, X. Guan, Joint time synchronization and localization for target sensors using a single mobile anchor with position uncertainties, in: 2018 IEEE International Conference on Acoustics, Speech and Signal Processing (ICASSP), IEEE, Calgary, AB, Canada, 2018, pp. 3794–3798.
[201] S. Zhang, K. Chen, Z. Fan, E. Cheng, W. Su, The localization algorithm based on symmetry correction for underwater acoustic networks, IEEE Access 7 (Sep. 2019) 121127–121135.
[202] Y. Yuan, C. Liang, M. Kaneko, X. Chen, D. Hogrefe, Topology control for energy-efficient localization in mobile underwater sensor networks using stackelberg game, IEEE Transactions on Vehicular Technology 68 (2) (Feb. 2019) 1487–1500.
[203] J. Yan, Z. Xu, X. Luo, C. Chen, X. Guan, Feedback-based target localization in underwater sensor networks: A multisensor fusion approach, IEEE Transactions on Signal and Information Processing over Networks 5 (1) (Mar. 2019) 168–180.
[204] G. Fang, H. Chen, L. Xie, Precision-improved passive localization method in the underwater multipath environment, in: 2019 IEEE International Conference on Signal Processing, Communications and Computing (ICSPCC), IEEE, Dalian, China, 2019, pp. 1–6.
[205] W. Ma, L. Song, Y. Wang, W. Yu, G. Yang, Opportunistic localization and synchronization for underwater acoustic sensor networks, in: Global Oceans 2020: Singapore–US Gulf Coast, IEEE, Biloxi, MS, USA, 2020, pp. 1–6.
[206] Y. Su, L. Guo, Z. Jin, X. Fu, A mobile-beacon-based iterative localization mechanism in large-scale underwater acoustic sensor networks, IEEE Internet of Things Journal 8 (5) (Mar. 2021) 3653–3664.
[207] G. Deak, K. Curran, J. Condell, A survey of active and passive indoor localisation systems, Computer Communications 35 (16) (Sep. 2012) 1939–1954.
[208] G. Salavasidis, A. Munafò, C. A. Harris, T. Prampart, R. Templeton, M. Smart, D. T. Roper, M. Pebody, S. D. McPhail, E. Rogers, et al., Terrain-aided navigation for long-endurance and deep-rated autonomous underwater vehicles, Journal of Field Robotics 36 (2) (Mar. 2019) 447–474.
[209] J. Melo, A. Matos, Survey on advances on terrain based navigation for autonomous underwater vehicles, Ocean Engineering 139 (Jul. 2017) 250–264.
[210] J. Bao, D. Li, X. Qiao, T. Rauschenbach, Integrated navigation for autonomous underwater vehicles in aquaculture: A review, Information Processing in Agriculture 7 (1) (Mar. 2020) 139–151.
[211] R. Bogue, Underwater robots: A review of technologies and applications, Industrial Robot: An International Journal (May 2015).
[212] B. Wang, J. Zhu, Z. Deng, M. Fu, A characteristic parameter matching algorithm for gravity-aided navigation of underwater vehicles, IEEE Transactions on Industrial Electronics 66 (2) (Feb. 2019) 1203–1212.
[213] A. Manzanilla, S. Reyes, M. Garcia, D. Mercado, R. Lozano, Autonomous navigation for unmanned underwater vehicles: Real-time experiments using computer vision, IEEE Robotics and Automation Letters 4 (2) (Apr. 2019) 1351–1356.
[214] D. A. Duecker, N. Bauschmann, T. Hansen, E. Kreuzer, R. Seifried, Towards micro robot hydrobatics: Vision-based guidance, navigation, and control for agile underwater vehicles in confined environments, in: 2020 IEEE/RSJ International Conference on Intelligent Robots and Systems (IROS), IEEE, Las Vegas, NV, USA, 2020, pp. 1819–1826.
[215] B. Wang, J. Zhu, Z. Ma, Z. Deng, M. Fu, Improved particle filter-based matching method with gravity sample vector for underwater gravity-aided navigation, IEEE Transactions on Industrial Electronics 68 (6) (Jun. 2021) 5206–5216.
[216] Z. Xiong, M. Wu, J. Cao, Y. Liu, R. Yu, S. Cai, An underwater gravimetry method using inertial navigation system and depth gauge based on trajectory constraint, IEEE Geoscience and Remote Sensing Letters (Sep. 2021).
[217] D. Wang, X. Xu, Y. Yao, T. Zhang, Y. Zhu, A novel SINS/DVL tightly integrated navigation method for complex environment, IEEE Transactions on Instrumentation and Measurement 69 (7) (Jul. 2020) 5183–5196.
[218] D. Li, J. Xu, H. He, M. Wu, An underwater integrated navigation algorithm to deal with DVL malfunctions based on deep learning, IEEE Access (Jun. 2021).
[219] A. Y. Rodionov, F. Dubrovin, P. Unru, S. Y. Kulik, Experimental research of distance estimation accuracy using underwater acoustic modems to provide navigation of underwater objects, in: 2017 24th Saint Petersburg International Conference on Integrated Navigation Systems (ICINS), IEEE, St. Petersburg, Russia, 2017, pp. 1–4.
[220] N. R. Rypkema, E. M. Fischel, H. Schmidt, Closed-loop single-beacon passive acoustic navigation for low-cost autonomous underwater vehicles, in: 2018 IEEE/RSJ International Conference on Intelligent Robots and Systems (IROS), IEEE, Madrid, Spain, 2018, pp. 641–648.
[221] Z. J. Harris, L. L. Whitcomb, Preliminary evaluation of cooperative navigation of underwater vehicles without a DVL utilizing a dynamic process model, in: 2018 IEEE International Conference on Robotics and Automation (ICRA), IEEE, Brisbane, QLD, Australia, 2018, pp. 4897–4904.
[222] Z. J. Harris, L. L. Whitcomb, Preliminary simulation study of combined control and cooperative navigation for underwater vehicles, in: OCEANS 2018 MTS/IEEE Charleston, IEEE, Charleston, SC, USA, 2018, pp. 1–5.
[223] Z. J. Harris, T. M. Paine, L. L. Whitcomb, Preliminary evaluation of null-space dynamic process model identification with application to cooperative navigation of underwater vehicles, in: 2018 IEEE/RSJ International Conference on Intelligent Robots and Systems (IROS), IEEE, Madrid, Spain, 2018, pp. 3453–3459.
[224] Q. Li, Y. Ben, S. M. Naqvi, J. A. Neasham, J. A. Chambers, Robust student's t-based cooperative navigation for autonomous underwater vehicles, IEEE Transactions on Instrumentation and Measurement 67 (8) (Aug. 2018) 1762–1777.
[225] J. Jung, J. Park, J. Choi, H.-T. Choi, Autonomous mapping of underwater magnetic fields using a surface vehicle, IEEE Access 6 (Nov. 2018) 62552–62563.
[226] H. Li, J. Qu, Q. Wu, X. Jiang, Y. Niu, Geomagnetic perceiving navigation method for autonomous underwater vehicle using an adapted search strategy, in: 2020 39th Chinese Control Conference (CCC), IEEE, Shenyang, China, 2020, pp. 3495–3499.
[227] J. Zhang, T. Zhang, H.-S. Shin, J. Wang, C. Zhang, Geomagnetic gradient-assisted evolutionary algorithm for long-range underwater navigation, IEEE Transactions on Instrumentation and Measurement 70 (2021) 1–12.
[228] W. Rupeng, L. Ye, M. Teng, C. Zheng, G. Yusen, X. Pengfei, Improvements to terrain aided navigation accuracy in deep-sea space by high precision particle filter initialization, IEEE Access 8 (Jan. 2020) 13029–13042.
[229] J. Jung, J. Park, J. Choi, H.-T. Choi, Navigation of unmanned surface vehicles using underwater geophysical sensing, IEEE Access 8 (Nov. 2020) 208707–208717.
[230] H. Wang, X. Xu, T. Zhang, Multipath parallel ICCP underwater terrain matching algorithm based on multibeam bathymetric data, IEEE Access 6 (Sep. 2018) 48708–48715.
[231] J. Quintas, F. C. Teixeira, A. Pascoal, AUV geophysical navigation using magnetic data–The MEDUSA GN system, in: 2018 IEEE/ION Position, Location and Navigation Symposium (PLANS), Monterey, CA, 2018, pp. 1122–1130.
[232] J. Quintas, F. C. Teixeira, A. Pascoal, An integrated system for geophysical navigation of autonomous underwater vehicles., IFAC-PapersOnLine 51 (29) (2018) 293–298.
[233] J. Quintas, N. Hung, N. Crasta, F. Curado-Teixeira, P. Lima, A. Pascoal, I. Kaminer, AUV path planning, navigation, and control using geophys-

ical data, in: OCEANS 2019-Marseille, IEEE, Marseille, France, 2019, pp. 1–9.
[234] J. Park, J. Jung, Y. Lee, J. Chae, Y. Lee, J. Choi, Validation of underwater acoustic-based navigation and geophysical mapping with an autonomous surface vehicle, IFAC-PapersOnLine 51 (29) (2018) 165–170.
[235] J. Choi, J. Park, J. Jung, Y. Lee, H.-T. Choi, Validation of acoustic and geophysics based underwater localization with an autonomous surface vehicle, IFAC-PapersOnLine 52 (21) (2019) 367–371.
[236] J. H. Kepper, B. C. Claus, J. C. Kinsey, A navigation solution using a MEMS IMU, model-based dead-reckoning, and one-way-travel-time acoustic range measurements for autonomous underwater vehicles, IEEE Journal of Oceanic Engineering 44 (3) (Jul. 2019) 664–682.
[237] C. Xu, C. Xu, C. Wu, D. Qu, J. Liu, Y. Wang, G. Shao, A novel self-adapting filter based navigation algorithm for autonomous underwater vehicles, Ocean Engineering 187 (2019) 106146.
[238] Y. Yao, X. Xu, D. Yang, X. Xu, An IMM-UKF aided SINS/USBL calibration solution for underwater vehicles, IEEE Transactions on Vehicular Technology 69 (4) (Apr. 2020) 3740–3747.
[239] J. Wang, T. Zhang, B. Jin, Y. Zhu, J. Tong, Student's t-based robust Kalman filter for a SINS/USBL integration navigation strategy, IEEE Sensors Journal 20 (10) (May 2020) 5540–5553.
[240] D. Wang, X. Xu, Y. Yao, T. Zhang, Virtual DVL reconstruction method for an integrated navigation system based on DS-LSSVM algorithm, IEEE Transactions on Instrumentation and Measurement 70 (2021) 1–13.
[241] T. Zhang, J. Wang, L. Zhang, L. Guo, A student's T-based measurement uncertainty filter for SINS/USBL tightly integration navigation system, IEEE Transactions on Vehicular Technology 70 (9) (Sep. 2021) 8627–8638.
[242] A. Capossele, C. Petrioli, G. Saturni, D. Spaccini, D. Venturi, Securing underwater communications: Key agreement based on fully hashed MQV, in: Proceedings of the International Conference on Underwater Networks & Systems, Halifax, NS, Canada, 2017, pp. 1–5.
[243] H. Ghannadrezaii, J.-F. Bousquet, Securing a Janus-based flooding routing protocol for underwater acoustic networks, in: OCEANS 2018 MTS/IEEE Charleston, IEEE, Charleston, SC, USA, 2018, pp. 1–7.
[244] M. Xu, L. Liu, SenseVault: A three-tier framework for securing mobile underwater sensor networks, IEEE Transactions on Mobile Computing 17 (11) (Nov. 2018) 2632–2645.
[245] C. Yuan, W. Chen, D. Li, A hierarchical identity-based signcryption scheme in underwater wireless sensor network, in: China Conference on Wireless Sensor Networks, Springer, Singapore, 2017, pp. 44–54.
[246] P. Guo, H. Zhang, D. Fu, W. ZHOU, Hybrid and lightweight cryptography for wireless sensor network, Computer Science 39 (1) (2012) 69–72.
[247] S.-j. Deng, Y. Wang, Y. TIAN, J.-q. TANG, Grouping and layered key management strategy in WSN based on EBS, Computer Engineering 9 (39) (2013) 64–68.
[248] C. Yuan, W. Chen, Y. Zhu, D. Li, J. Tan, A low computational complexity authentication scheme in underwater wireless sensor network, in: 2015 11th International Conference on Mobile Ad-hoc and Sensor Networks (MSN), IEEE, Shenzhen, China, 2015, pp. 116–123.
[249] M. A. Hamid, M. Abdullah-Al-Wadud, M. M. Hassan, A. Almogren, A. Alamri, A. R. M. Kamal, M. Mamun-Or-Rashid, A key distribution scheme for secure communication in acoustic sensor networks, Future Generation Computer Systems 86 (Sep. 2018) 1209–1217.
[250] N. Goyal, M. Dave, A. K. Verma, SAPDA: secure authentication with protected data aggregation scheme for improving QoS in scalable and survivable UWSNs, Wireless Personal Communications (Jan. 2020) 1–15.
[251] J. Jiang, G. Han, C. Zhu, S. Chan, J. J. Rodrigues, A trust cloud model for underwater wireless sensor networks, IEEE Communications Magazine 55 (3) (Mar. 2017) 110–116.
[252] J. Jiang, G. Han, L. Shu, S. Chan, K. Wang, A trust model based on cloud theory in underwater acoustic sensor networks, IEEE Transactions on Industrial Informatics 13 (1) (Feb. 2017) 342–350.
[253] M. P. Lowney, H. Liu, E. Chabot, Trust management in underwater acoustic MANETs based on cloud theory using multi-parameter metrics, in: 2018 International Carnahan Conference on Security Technology (ICCST), IEEE, Montreal, QC, Canada, 2018, pp. 1–5.
[254] G. Han, Y. He, J. Jiang, N. Wang, M. Guizani, J. A. Ansere, A synergetic trust model based on SVM in underwater acoustic sensor networks, IEEE transactions on vehicular technology 68 (11) (Nov. 2019) 11239–11247.
[255] J. Du, G. Han, C. Lin, M. Martinez-Garcia, ITrust: An anomaly-resilient trust model based on isolation forest for underwater acoustic sensor networks, IEEE Transactions on Mobile Computing (2020).
[256] Y. Su, S. Mal, Z. Jin, X. Fu, Y. Li, X. Liu, A trust model for underwater acoustic sensor networks based on fast link quality assessment, in: Global Oceans 2020: Singapore–US Gulf Coast, IEEE, Biloxi, MS, USA, 2020, pp. 1–6.
[257] Y. Zhou, Q. Zhang, Z. Yan, C. He, MAB-learning-based hierarchical defense for secure underwater acoustic networks, in: 2021 IEEE/CIC International Conference on Communications in China (ICCC Workshops), Xiamen, China, 2021, pp. 282–287.
[258] V. Baranidharan, K. Varadharajan, Secure localization using coordinated gradient descent technique for underwater wireless sensor networks, ICTACT Journal on Communication Technology 9 (1) (Mar. 2018) 1716–1720.
[259] M. M. Arifeen, M. M. Rahman, K. A. Taher, M. M. Islam, M. S. Kaiser, et al., ANFIS based trust management model to enhance location privacy in underwater wireless sensor networks, in: 2019 International Conference on Electrical, Computer and Communication Engineering (ECCE), IEEE, Cox'sBazar, Bangladesh, 2019, pp. 1–6.
[260] X. Feng, Z. Wang, N. Han, Protection research of sink location privacy in underwater sensor networks, in: IEEE INFOCOM 2019-IEEE Conference on Computer Communications Workshops (INFOCOM WKSHPS), Paris, France, 2019, pp. 1–6.
[261] Y. Wang, Z. Tian, Y. Sun, X. Du, N. Guizani, Preserving location privacy in UASN through collaboration and semantic encapsulation, IEEE Network 34 (4) (Aug. 2020) 284–290.
[262] G. Han, H. Wang, J. A. Ansere, J. Jiang, Y. Peng, SSLP: A stratification-based source location privacy scheme in underwater acoustic sensor networks, IEEE Network 34 (4) (Aug. 2020) 188–195.
[263] J. Yan, Y. Meng, X. Yang, X. Luo, X. Guan, Privacy-preserving localization for underwater sensor networks via deep reinforcement learning, IEEE Transactions on Information Forensics and Security 16 (2020) 1880–1895.
[264] H. Zhao, J. Yan, X. Luo, X. Gua, Privacy preserving solution for the asynchronous localization of underwater sensor networks, IEEE/CAA Journal of Automatica Sinica 7 (6) (Nov. 2020) 1511–1527.
[265] J. Yan, Y. Meng, X. Luo, X. Guan, To hide private position information in localization for internet of underwater things, IEEE Internet of Things Journal (Sep. 2021).
[266] T. Dargahi, H. H. Javadi, H. Shafiei, Securing underwater sensor networks against routing attacks, Wireless Personal Communications 96 (2) (May 2017) 2585–2602.
[267] M. R. Bharamagoudra, S. S. Manvi, Agent-based secure routing for underwater acoustic sensor networks, International Journal of Communication Systems 30 (13) (Feb. 2017) e3281.
[268] K. Saeed, W. Khalil, S. Ahmed, I. Ahmad, M. N. K. Khattak, SEECR: Secure energy efficient and cooperative routing protocol for underwater wireless sensor networks, IEEE Access 8 (Jun. 2020) 107419–107433.
[269] Z. Junqing, Z. Gangqiang, L. Junkai, Wormhole attack detecting in underwater acoustic communication networks, in: 2021 OES China Ocean Acoustics (COA), IEEE, Harbin, China, 2021, pp. 647–650.
[270] M. M. Arifeen, A. Al Mamun, T. Ahmed, M. S. Kaiser, M. Mahmud, A blockchain-based scheme for sybil attack detection in underwater wireless sensor networks, in: Proceedings of International Conference on Trends in Computational and Cognitive Engineering, Springer, Singapore, 2021, pp. 467–476.
[271] W. Chen, T. Liang, V. Dinavahi, Comprehensive real-time hardware-in-the-loop transient emulation of MVDC power distribution system on nuclear submarine, IEEE Open Journal of the Industrial Electronics Society 1 (2020) 326–339. doi:10.1109/OJIES.2020.3036731.
[272] Q. Yang, Y. Yin, S. Chen, Y. Liu, Autonomous exploration and navigation of mine countermeasures USV in complex unknown environment, in: 2021 33rd Chinese Control and Decision Conference (CCDC), Kunming, China, 2021, pp. 4373–4377. doi:10.1109/CCDC52312.2021.9602457.
[273] N. Palomeras, T. Furfaro, D. P. Williams, M. Carreras, S. Dugelay, Automatic target recognition for mine countermeasure missions using forward-looking sonar data, IEEE Journal of Oceanic Engineering 47 (1)

(2022) 141–161. doi:10.1109/JOE.2021.3103269.
[274] K.-Y. Kim, E. Jeong, S. Kim, Y. Shin, Magnetic anomaly detection using continuous angle alignment of three-axis magnetic signal, IEEE Sensors Journal 19 (2) (2019) 743–750. doi:10.1109/JSEN.2018.2878890.
[275] J. F. Sánchez-Pérez, C. Mascaraque-Ramírez, J. A. M. Nicolás, E. Castro, M. Cánovas, Study of the application of PCM to thermal insulation of UUV hulls using network simulation method, Alexandria Engineering Journal 60 (5) (2021) 4627–4637.
[276] Y. Wu, Coordinated path planning for an unmanned aerial-aquatic vehicle (uaav) and an autonomous underwater vehicle (AUV) in an underwater target strike mission, Ocean Engineering 182 (2019) 162–173.
[277] X. Meng, B. Sun, D. Zhu, Harbour protection: moving invasion target interception for multi-AUV based on prediction planning interception method, Ocean Engineering 219 (2021) 108268. doi:https://doi.org/10.1016/j.oceaneng.2020.108268. URL https://www.sciencedirect.com/science/article/pii/S0029801820311872
[278] H. Wang, G. Han, Y. Hou, M. Guizani, Y. Peng, A multi-channel interference based source location privacy protection scheme in underwater acoustic sensor networks, IEEE Transactions on Vehicular Technology 71 (2) (2022) 2058–2069. doi:10.1109/TVT.2021.3135438.
[279] G. Ferri, R. Grasso, E. Camossi, A. Faggiani, K. Bereta, M. Vodas, D. Kladis, D. Zissis, K. D. LePage, Developing a robotic hybrid network for coastal surveillance: the INFORE experience, in: OCEANS 2021: San Diego – Porto, San Diego, CA, USA, 2021, pp. 1–10. doi:10.23919/OCEANS44145.2021.9705662.
[280] E. Camossi, R. Grasso, G. Ferri, A. Faggiani, K. LePage, S. Carniel, Maritime linked data for situational awareness heterogeneous sensor networks, in: OCEANS 2021: San Diego – Porto, San Diego, CA, USA, 2021, pp. 1–10. doi:10.23919/OCEANS44145.2021.9705759.
[281] U. Jain, M. Hussain, Security mechanism for maritime territory and frontier surveillance in naval operations using wireless sensor networks, Concurrency and Computation: Practice and Experience 33 (17) (2021) e6300.
[282] Y. Kim, G. Jo, H.-K. Jung, Real-time detection of electric field signal of a moving object using adjustable frequency bands and statistical discriminant for underwater defense, IEEE Transactions on Geoscience and Remote Sensing (2022) 1–1doi:10.1109/TGRS.2022.3152595.
[283] D. Song, Z. Chen, J. Fu, X. Wang, W. Jiang, J. Wu, Novel underwater glider-based absolute oceanic current observation solutions, IEEE Sensors Journal 21 (6) (2021) 8045–8054. doi:10.1109/JSEN.2020.3048136.
[284] K. Stenger, O. Wikmark, C. Bezuidenhout, L. Molale-Tom, Microplastics pollution in the ocean: Potential carrier of resistant bacteria and resistance genes, Environmental Pollution 291 (2021) 118130. doi:https://doi.org/10.1016/j.envpol.2021.118130. URL https://www.sciencedirect.com/science/article/pii/S0269749121017127
[285] H. Flores, N. H. Motlagh, A. Zuniga, M. Liyanage, M. Passananti, S. Tarkoma, M. Youssef, P. Nurmi, Toward large-scale autonomous marine pollution monitoring, IEEE Internet of Things Magazine 4 (1) (2021) 40–45. doi:10.1109/IOTM.0011.2000057.
[286] J. Li, T. Chen, Z. Yang, L. Chen, P. Liu, Y. Zhang, G. Yu, J. Chen, H. Li, X. Sun, Development of a buoy-borne underwater imaging system for in situ mesoplankton monitoring of coastal waters, IEEE Journal of Oceanic Engineering (2021) 1–23doi:10.1109/JOE.2021.3106122.
[287] H. Huang, Z. Sun, S. Liu, Y. Di, J. Xu, C. Liu, R. Xu, H. Song, S. Zhan, J. Wu, Underwater hyperspectral imaging for in situ underwater microplastic detection, Science of The Total Environment 776 (2021) 145960.
[288] V. Bianco, P. Memmolo, P. Carcagnì, F. Merola, M. Paturzo, C. Distante, P. Ferraro, Microplastic identification via holographic imaging and machine learning, Advanced Intelligent Systems 2 (2) (2020) 1900153.
[289] J. Blackford, G. Alendal, H. Avlesen, A. Brereton, P. W. Cazenave, B. Chen, M. Dewar, J. Holt, J. Phelps, Impact and detectability of hypothetical CCS offshore seep scenarios as an aid to storage assurance and risk assessment, International Journal of Greenhouse Gas Control 95 (2020) 102949.
[290] Analysis of the physicochemical detectability and impacts of offshore CO2 leakage through multi-scale modelling of in-situ experimental data using the PLUME model, International Journal of Greenhouse Gas Control 110 (2021) 103441. doi:https://doi.org/10.1016/j.ijggc.2021.103441.
[291] A. Flohr, A. Schaap, E. P. Achterberg, G. Alendal, M. Arundell, C. Berndt, J. Blackford, C. Böttner, S. M. Borisov, R. Brown, et al., Towards improved monitoring of offshore carbon storage: a real-world field experiment detecting a controlled sub-seafloor CO2 release, International Journal of Greenhouse Gas Control 106 (2021) 103237.
[292] K. Mallery, D. Canelon, J. Hong, N. Papanikolopoulos, Design and experiments with a robot-driven underwater holographic microscope for low-cost in situ particle measurements, Journal of Intelligent & Robotic Systems 102 (2) (2021) 1–11.
[293] G. Coro, M. Bjerregaard Walsh, An intelligent and cost-effective remote underwater video device for fish size monitoring, Ecological Informatics 63 (2021) 101311. doi:https://doi.org/10.1016/j.ecoinf.2021.101311. URL https://www.sciencedirect.com/science/article/pii/S1574954121001023
[294] T. M. Morganti, B. M. Slaby, A. de Kluijver, K. Busch, U. Hentschel, J. Middelburg, H. Grotheer, G. Mollenhauer, J. Dannheim, H. Rapp, et al., Giant sponge grounds of central arctic seamounts are associated with extinct seep life, Nature Communications 13 (1) (2022) 1–15.
[295] G. Han, A. Gong, H. Wang, C. Lin, M. Martinez-Garcia, Y. Peng, Anonymous cluster-based source location protection in underwater pipeline monitoring operations, IEEE Transactions on Vehicular Technology (2021) 1–1doi:10.1109/TVT.2021.3124492.
[296] G. Tabella, N. Paltrinieri, V. Cozzani, P. S. Rossi, Wireless sensor networks for detection and localization of subsea oil leakages, IEEE Sensors Journal 21 (9) (2021) 10890–10904. doi:10.1109/JSEN.2021.3060292.
[297] G. Tabella, D. Ciuonzo, N. Paltrinieri, P. S. Rossi, Spatio-temporal decision fusion for quickest fault detection within industrial plants: The oil and gas scenario, in: 2021 IEEE 24th International Conference on Information Fusion (FUSION), Sun City, South Africa, 2021, pp. 1–8.
[298] L. Murray, A buoyant future for offshore wind: Floating wind systems are on the cusp of a huge transformation as they transition from pilot projects to commercial-sized wind farms, Engineering Technology 16 (10) (2021) 1–4. doi:10.1049/et.2021.1008.
[299] X. Zhou, Z. Huang, H. Wang, G. Yin, Y. Bao, Q. Dong, Y. Liu, Site selection for hybrid offshore wind and wave power plants using a four-stage framework: A case study in hainan, china, Ocean & Coastal Management 218 (2022) 106035.
[300] J. Lloret, A. Turiel, J. Solé, E. Berdalet, A. Sabatés, A. Olivares, J. M. Gili, J. Vila-Subirós, P.-Y. Hardy, R. Sardá, Unravelling the ecological impacts of large-scale offshore wind farms in the Mediterranean Sea, Science of The Total Environment (2022) 153803.
[301] M. F. Schupp, A. Kafas, B. H. Buck, G. Krause, V. Onyango, V. Stelzenmüller, I. Davies, B. E. Scott, Fishing within offshore wind farms in the north sea: Stakeholder perspectives for multi-use from Scotland and Germany, Journal of Environmental Management 279 (2021) 111762.
[302] T. Powers, A. Sajadi, B.-M. Hodge, The current opportunities and challenges for offshore wind in the United States, The Electricity Journal (2022) 107061doi:https://doi.org/10.1016/j.tej.2021.107061. URL https://www.sciencedirect.com/science/article/pii/S1040619021001524
[303] E. A. Virtanen, J. Lappalainen, M. Nurmi, M. Viitasalo, M. Tikanmäki, J. Heinonen, E. Atlaskin, M. Kallasvuo, H. Tikkanen, A. Moilanen, Balancing profitability of energy production, societal impacts and biodiversity in offshore wind farm design, Renewable and Sustainable Energy Reviews 158 (2022) 112087.
[304] H. Díaz, A. Teixeira, C. G. Soares, Application of monte carlo and fuzzy analytic hierarchy processes for ranking floating wind farm locations, Ocean Engineering 245 (2022) 110453.
[305] W. Tang, D. Flynn, V. Robu, Sensing technologies and artificial intelligence for subsea power cable asset management, in: 2021 IEEE International Conference on Prognostics and Health Management (ICPHM), 2021, pp. 1–6. doi:10.1109/ICPHM51084.2021.9486586.
[306] O. Álvarez-Tuñón, Á. Rodríguez, A. Jardón, C. Balaguer, Underwater robot navigation for maintenance and inspection of flooded mine shafts, in: 2018 IEEE/RSJ International Conference on Intelligent Robots and

Systems (IROS), IEEE, 2018, pp. 1482–1487.
[307] R. A. S. Fernandez, Z. Milošević, S. Dominguez, C. Rossi, Motion control of underwater mine explorer robot UX-1: Field trials, IEEE Access 7 (2019) 99782–99803. doi:10.1109/ACCESS.2019.2930544.
[308] R. A. S. Fernandez, D. Grande, L. Bascetta, A. Martins, S. Dominguez, C. Rossi, Variable pitch system for the underwater explorer robot UX-1*, in: 2020 IEEE/RSJ International Conference on Intelligent Robots and Systems (IROS), Las Vegas, NV, USA, 2020, pp. 1755–1760. doi:10.1109/IROS45743.2020.9341759.
[309] W.-C. Hu, L.-B. Chen, B.-K. Huang, H.-M. Lin, A computer vision-based intelligent fish feeding system using deep learning techniques for aquaculture, IEEE Sensors Journal (2022) 1–1doi:10.1109/JSEN.2022.3151777.
[310] Y. Yang, J. Lu, B. D. Pflugrath, H. Li, J. J. Martinez, S. Regmi, B. Wu, J. Xiao, Z. D. Deng, Lab-on-a-Fish: Wireless, miniaturized, fully integrated, implantable biotelemetric tag for real-time in vivo monitoring of aquatic animals, IEEE Internet of Things Journal (Nov. 2021).
[311] B. Ouyang, P. S. Wills, Y. Tang, J. O. Hallstrom, T.-C. Su, K. Namuduri, S. Mukherjee, J. I. Rodriguez-Labra, Y. Li, C. J. Den Ouden, Initial development of the hybrid aerial underwater robotic system (HAUCS): Internet of things (IoT) for aquaculture farms, IEEE Internet of Things Journal 8 (18) (2021) 14013–14027. doi:10.1109/JIOT.2021.3068571.
[312] T.-C. Wu, Y.-C. Chi, H.-Y. Wang, C.-T. Tsai, G.-R. Lin, Blue laser diode enables underwater communication at 12.4 Gbps, Scientific reports 7 (1) (2017) 1–10.
[313] G. Schirripa Spagnolo, L. Cozzella, F. Leccese, Underwater optical wireless communications: Overview, Sensors 20 (8) (2020) 2261.
[314] Z. Wang, L. Zhang, Z. Wei, Y. Dong, G. Wei, H. Fu, Beyond 25 Gbps OFDM UOWC system based on green and blue laser diodes with wavelength and polarization multiplexing, in: 2021 9th International Conference on Communications and Broadband Networking, 2021, pp. 329–332.
[315] F. Tonolini, F. Adib, Networking across boundaries: enabling wireless communication through the water-air interface, in: Proceedings of the 2018 Conference of the ACM Special Interest Group on Data Communication, 2018, pp. 117–131.
[316] N. Huang, C. Gong, C. Fu, T. Wei, Z. Xu, Preliminary investigation of air-to-water visible light communication link under strong ambient light, in: 2021 IEEE 94th Vehicular Technology Conference (VTC2021-Fall), IEEE, 2021, pp. 1–5.
[317] F. Qu, J. Qian, J. Wang, X. Lu, M. Zhang, X. Bai, Z. Ran, X. Tu, Z. Liu, Y. Wei, Cross-medium communication combining acoustic wave and millimeter wave: Theoretical channel model and experiments, IEEE Journal of Oceanic Engineering (2021).
[318] Submarine Telecoms Forum, Submarine Telecoms Industry Report 2021/2022, Accessed: 10 Oct. 2022.
URL https://subtelforum.com/products/submarine-telecoms-industry-report/
[319] L. Liu, R. Wang, G. Xiao, D. Guo, On the throughput optimization for message dissemination in opportunistic underwater sensor networks, Computer Networks 169 (2020) 107097.
[320] I. N'doye, D. Zhang, M.-S. Alouini, T.-M. Laleg-Kirati, Establishing and maintaining a reliable optical wireless communication in underwater environment, IEEE Access 9 (2021) 62519–62531.
[321] A. S. Ghazy, S. Hranilovic, M.-A. Khalighi, Angular MIMO for underwater wireless optical communications: Link modeling and tracking, IEEE Journal of Oceanic Engineering 46 (4) (2021) 1391–1407.
[322] L. Yang, H. Wang, Y. Fan, F. Luo, W. Feng, Reinforcement learning for distributed energy efficiency optimization in underwater acoustic communication networks, Wireless Communications and Mobile Computing 2022 (2022).
[323] Y. Chen, W. Yu, X. Sun, L. Wan, Y. Tao, X. Xu, Environment-aware communication channel quality prediction for underwater acoustic transmissions: A machine learning method, Applied Acoustics 181 (2021) 108128.
[324] H. E. Erdem, H. U. Yildiz, V. C. Gungor, On the lifetime of compressive sensing based energy harvesting in underwater sensor networks, IEEE Sensors Journal 19 (12) (2019) 4680–4687.
[325] Y. Zou, P. Tan, B. Shi, H. Ouyang, D. Jiang, Z. Liu, H. Li, M. Yu, C. Wang, X. Qu, et al., A bionic stretchable nanogenerator for underwater sensing and energy harvesting, Nature Communications 10 (1) (2019) 1–10.
[326] A. M. Khasawneh, O. Kaiwartya, L. M. Abualigah, J. Lloret, et al., Green computing in underwater wireless sensor networks pressure centric energy modeling, IEEE Systems Journal 14 (4) (2020) 4735–4745.
[327] X. Su, L. Meng, J. Huang, Intelligent maritime networking with edge services and computing capability, IEEE Transactions on Vehicular Technology 69 (11) (2020) 13606–13620.